CLAY MINERALOGY AND DIAGENESIS OF K-BENTONITES OCCURRING IN THE DEVONIAN YILANLI FORMATION FROM NORTH WESTERN ANATOLIA (BARTIN-ZONGULDAK)

A THESIS SUBMITTED TO
THE GRADUATE SCHOOL OF NATURAL AND APPLIED SCIENCES
OF
MIDDLE EAST TECHNICAL UNIVERSITY

BY
ÖZGE ÜNLÜCE

IN PARTIAL FULLFILLMENT OF THE REQUIREMENTS
FOR
THE DEGREE OF MASTER OF SCIENCE
IN
GEOLOGICAL ENGINEERING

JANUARY 2013

Approval of the thesis:

CLAY MINERALOGY AND DIAGENESIS OF K-BENTONITES OCCURRING IN THE DEVONIAN YILANLI FORMATION FROM NORTH WESTERN ANATOLIA (BARTIN-ZONGULDAK)

submitted by **ÖZGE ÜNLÜCE** in partial fulfillment of the requirements for the degree of **Master of Science in Geological Engineering Department, Middle East Technical University** by,

Prof. Dr. Canan Özgen _____
Dean, Graduate School of **Natural and Applied Sciences**

Prof. Dr. Erdin Bozkurt _____
Head of Department, **Geological Engineering**

Prof. Dr. Asuman Günal Türkmenoğlu _____
Supervisor, **Geological Engineering Dept., METU**

Examining Committee Members:

Prof. Dr. M. Cemal Göncüoğlu _____
Geological Engineering Department, METU

Prof. Dr. Asuman Günal Türkmenoğlu _____
Geological Engineering Department, METU

Prof. Dr. Ömer Bozkaya _____
Geological Engineering Department, Pamukkale University

Assoc. Prof. Dr. İ. Ömer Yılmaz _____
Geological Engineering Department, METU

Assist. Prof. Dr. Zehra Karakaş _____
Geological Engineering Department, Ankara University

Date: 31/01/2013

I hereby declare that all information in this document has been obtained and presented in accordance with academic rules and ethical conduct. I also declare that, as required by these rules and conduct, I have fully cited and referenced all material and results that are not original to this work.

Name, Last Name : Özge Ünlüce

Signature:

ABSTRACT

CLAY MINERALOGY AND DIAGENESIS OF K-BENTONITES OCCURRING IN THE DEVONIAN YILANLI FORMATION FROM NORTH WESTERN ANATOLIA (BARTIN-ZONGULDAK)

Ünlüce, Özge
M. Sc., Department of Geological Engineering
Supervisor: Prof. Dr. Asuman Günal Türkmenoğlu
January 2013, 80 pages

Yellowish brown and gray-green colored K-bentonite horizons revealing thicknesses up to 60 cm are exposed within the limestone-dolomitic limestone successions (Middle Devonian-Lower Carboniferous Yılanlı formation) deposited on a shallow marine carbonate platform at Zonguldak and Bartın area in the western Black Sea region. In this study, bentonite samples collected from two different locations; Gavurpınarı quarry and Yılanlı Burnu quarry are investigated by means of optical microscopy, X-ray powder diffraction analyses (XRD), both scanning electron microscopy (SEM) and energy dispersive X-ray (EDX) analysis, high resolution transmission electron microscopy (HR-TEM) and inductively coupled plasma mass spectrometry (ICP-MS) in order to reveal their mineralogical-geochemical characteristics and understand their origin and evolution.

Illite is determined as the major phyllosilicate mineral in K-bentonites. Additionally, kaolinite and illite-smectite mixed-layer clay minerals are also detected in some samples. As non-clay minerals calcite, dolomite, quartz, gypsum, feldspar, pyrite and zircon are present in these K-bentonites.

Crystal-chemical characteristics (Kübler index-KI, intensity ratios (Ir), illite polytypes (%2M_1), (d_{060}) of illite minerals from the two different sampling locations were investigated. Their KI values (for Yılanlı Burnu sampling location varying between 0.47-0.93 (with an average of 0.71 Δ°2θ); for Gavurpınarı quarry sampling location varying between 0.69-0.77 (with an average of 0.72 Δ°2θ)); % of swelling component (smectite-max 5%) and crystallite thickness (*N*=10-20 nm) indicate that these illites were affected by high-grade diagenetic conditions. Similarly, illite polytype ratios (%2M_1/(2M_1+1M_d)) range between 20-50% (with an average of 36%) for the Yılanlı Burnu quarry samples, whereas, these ratios are between 25-45% (with an average of 37%) for the Gavurpınarı limestone quarry samples. Illite polytpe data also supports a high-grade diagenetic origin possibility of K-bentonites. Illite d_{060} values ranges between 1.491-1.503 Å, (with an average of 1.499 Å) which reflect the octahedral Mg+Fe compositions are varying between 0.27-0.51 and thus approach the ideal muscovite-phengite values close to dioctahedral muscovite composition.

Based on the data obtained from this study, volcanic ash was firstly transformed into a smectitic I/S mineral in early stages of sedimentation and burial diagenesis. This initial smectite was then be transformed into a highly illitic I/S, and finally illite by diffusion of elements into and out of the bed, during Devonian. Mineralogical-petrographical data points out that these K-bentonites evolved in a high-grade diagenetic environment (approximately 100-150 °C) from the products of volcanic eruptions having yet unknown source and distance during Middle-Late Devonian time.

Keywords: Devonian, K-bentonite, Illite, Diagenesis.

ÖZ

BATI ANADOLU'DA (BARTIN-ZONGULDAK ÇEVRESİ) DEVONİYEN YAŞLI YILANLI FORMASYONUNDA OLUŞAN K-BENTONİTLERİN KİL MİNERALOJİSİ VE EVRİMİ

Ünlüce, Özge
Yüksek Lisans, Jeoloji Mühendisliği Bölümü
Tez Yöneticisi: Prof. Dr. Asuman Günal Türkmenoğlu
Ocak 2013, 80 sayfa

Batı Karadeniz bölgesinde, Bartın ve Zonguldak çevresinde Paleozoyik yaşlı ve sığ denizel karbonat platformunda çökelmiş olan kireçtaşı-dolomitik kireçtaşı istifleri (Orta Devoniyen-Alt Karbonifer yaşlı Yılanlı formasyonu) içerisinde, kalınlıkları yer yer 60 cm'ye varan, sarımsı kahve ve gri-yeşil renkli kilce-zengin K-bentonit seviyeleri yüzeylenmektedir. Bu çalışmada Bartın-Gavurpınarı köyü ve Bartın çayı (Yılanlı Burnu) yakınındaki kireçtaşı ocaklarından alınan K-bentonitlerin optik ve taramalı elektron mikroskop ve X-ışınları kırınımı incelemeleri ile ayrıntılı mineralojik-petrografik özelliklerinin incelenerek köken ve evrimlerinin ortaya konulması amaçlanmıştır.

Bentonit seviyelerinden alınan örneklerde başlıca fillosilikat minerali illit olup, bazı örneklerde kaolinit ve illit-smektit de bulunmaktadır. Kil dışı mineraller olarak başlıca kalsit, dolomit, kuvars, daha az da jips, feldispat, götit, pirit ve zirkon mineralleri saptanmıştır. İllitlerin kristal-kimyasal karakteristikleri (Kübler indeksi-KI, politipi, d_{060}) araştırılmış ve farklı lokasyonlara göre deneştirilmiştir. İllitlerin KI verileri Yılanlı Burnu ocağı bentonitleri için 0.47-0.93 (ortalama 0.71 Δ°2θ) Bartın-Gavurpınarı ocağı için ise 0.69-0.77 (ortalama 0.72 Δ°2θ) olarak belirlenmiştir. İllitlerin KI verilerine ek olarak, genişleyebilen tabaka (% simektit) içerikleri (en çok % 5) ve kristalit kalınlıkları da (*N*:10-20 nm) bentonitlerin yüksek dereceli diyajenez koşullarına uğradığını işaret etmektedir. Benzer biçimde illit politipleri (% $2M_1/(2M_1+1M_d)$) oranları Yılanlı Burnu ocağı bentonitleri için % 20-50 (ortalama % 36), Gavurpınarı kireçtaşı ocağı bentonitlerinde ise % 25-45 arasında (ortalama % 37) değişmekte olup, yukarıdaki görüşü desteklemektedir. İllitlerin d_{060} değerleri (1.491-1.503 Å, ortalama 1.499 Å), oktahedral Mg+Fe miktarlarının 0.27-0.51 aralığında değiştiğini ve muskovit-fenjit aralığında ideal muskovite yakın bir dioktahedral bileşimi yansıttığını işaret etmektedir. Elektron mikroskop incelemeleri, illitlerin levhamsı-yapraksı morfolojiye sahip olduklarını ve otijenik olarak geliştiklerini göstermiştir.

Mineralojik-petrografik veriler K-bentonitlerin, kaynağı ve uzaklığı henüz bilinmeyen, Orta-Geç Devoniyen yaşlı, şiddetli volkanik aktiviteden türeyen ve yüksek diyajenetik koşullar altında (yaklaşık 100-150 °C) evrimleştiklerini göstermektedir.

Anahtar Kelimeler: Devoniyen, K-bentonit, İllit, Diyajenez

To my Mom and Dad

ACKNOWLEDGEMENTS

I am grateful to my supervisor Prof. Dr. Asuman Günal Türkmenoğlu for her supervision, guidance and enthutiastic approach throughout this research.

I would like to thank especially Prof. Dr. Ömer Bozkaya for his contributions in clay crystallinity interpretations in this study.

I wish to express my thanks to Prof. Dr. M. Cemal Göncüoğlu for his contributions in geochemistry chapter.

I wish to express my thanks to Assoc. Prof. Dr. İ. Ömer Yılmaz for his help and advices in sedimentalogical interpretations.

Thanks finally go to my family and my fiance for their patience and encouragements throughout the study.

This study was supported by TUBITAK Scientific Research Projects Grant No: 110Y272

TABLE OF CONTENTS

ABSTRACT ..... **v**
ÖZ ..... **vi**
DEDICATION ..... **vii**
ACKNOWLEDGEMENTS ..... **viii**
TABLE OF CONTENTS ..... **ix**
LIST OF FIGURES ..... **xi**
LIST OF TABLES ..... **xiv**
CHAPTERS
1 INTRODUCTION **1**
1.1. Purpose and Scope 1
1.2. Geographic Setting and Location of the Study Area 2
1.3. Methods of Study 2
1.3.1.Field Identification of K-bentonites and Sampling 3
1.3.2.Thin Section Preparation 10
1.3.3. X-Ray Powder Diffraction Analysis (Sample Preparation and Computer Programs Used) 10
1.3.4. Scanning Electron Microscopy Studies 11
1.3.5. High Resolution Transmission Microscopy Studies 12
1.3.6. Geochemical Analysis 12
1.4. Previous Studies 12
1.4.1. Previous Studies on Mineralogy, Chemistry and Origin of K-bentonites 12
1.4.2. Previous Studies on Clay Mineral Diagenesis with a Focus on Illitization Processes 17
1.4.3. Previous Investigations on Devonian Volcanism and K-bentonites 19
1.5. Regional Geology of the Study Area (Bartın and Zonguldak Area) 20
2 PETROGRAPHY **23**
2.1. Introduction 23
2.2. Gavurpınarı Quarry 23
2.2.1. K-bentonites 23
2.2.2. Limestones and Dolostones 23
2.3. Yılanlı Burnu Quarry 25
2.3.1. K-bentonites 25
2.3.2. Limestones and Dolostones 25
3 CLAY MINERALOGY **29**
3.1. Introduction 29
3.2. Mineralogy 29
3.2.1. Gavurpınarı Quarry K-bentonites 29
3.2.2. Yılanlı Burnu Quarry K-bentonites 33
3.3. Illite Crystallinity 35
3.3.1. Gavurpınarı Quarry K-bentonites 35
3.3.2. Yılanlı Burnu Quarry K-bentonites 36
3.4. Crystal Structure of Illites Based on HR-TEM Analyses 48
3.5. Micromorphology and Crystal Habit of Illites Based on SEM-EDX Analyses 49
4 GEOCHEMICAL CHARACTERISTICS OF K-BENTONITES **61**
4.1. Introduction 61
4.2. Major Element Composition of the Investigated K-bentonites 61
4.3. Geochemical Classification of K- bentonites 61
5 DISCUSSION AND CONCLUSION **64**
5.1. Discussion 64
5.1.1. Mineralogy of Devonian K-bentonites and Their Environment of Deposition 64
5.1.2. Illitization Process of Tephra and Degree of Diagenesis 64

5.1.3. Chemical Composition of Original Volcanic Ash and Source of Volcanism 65
5.2. Conclusions 65
REFERENCES 67
APPENDICES
A 78

LIST OF FIGURES

FIGURES

Figure 1.1. Location map of the study area and geotectonic distribution of Devonian units in Turkey (modified from Wehrmann et al., 2010). 2
Figure 1.2. Field appearance of the Gavurpınarı limestone quarry in Bartın area along the E-W direction. 3
Figure 1.3. Different levels of the Gavurpınarı limestone quarry and and vertical layering of bentonite beds along the NE-SW direction. 4
Figure 1.4. Grey coloured bentonite horizons from Gavurpınarı limestone quarry. 4
Figure 1.5. The pseudostratigraphic section along B-B' of 5. quarry level 5
Figure 1.6. The pseudostratigraphic section along C-C' of 4. quarry level 5
Figure 1.7. The pseudostratigraphic section along D-D' of 3. quarry level 5
Figure 1.8. Another view of vertically layering Gavurpınarı limestone beds along the NE-SW direction. 6
Figure 1.9. The yellowish-brown coloured bentonites and interlayering limestones in Yılanlı Burnu quarry. 6
Figure 1.10. Another interlayering bentonite sample from Yılanlı Burnu quarry. 7
Figure 1.11. Yellowish colored bentonites interlayering limestones in Yılanlı Burnu quarry successions. 7
Figure 1.12. The folding yılanlı burnu limestone layers interlayering with bentonites along the NW-SE direction. 8
Figure 1.13. The pseudostratigraphic section of the Yılanlı Burnu quarry. 9
Figure 1.14. Nine possibilities for the clay mineral formation in nature (cited in Eberl, 1984; after Esquevin, 1958 and Milot, 1970). 17
Figure 1.15. Gulf Coast sediments (well 6), Late Oligocene-Miocene. Vertical distribution of illite layers in I/S phases (<0.1 µm fraction) (A); K-feldspar percentage (2-10 µm fraction) (B); K_2O (%) (<0.1 µm fraction) (C) (from Hower et al., 1976). 19
Figure 1.16. Distribution of the Paleozoic rock units in the Istanbul and Zonguldak terranes (from Bozkaya et al., 2012). 21
Figure 1.17. Generalized lithostratigraphic section of the Zonguldak terrane (Bozkaya et al., 2012). 22
Figure 2.1. Thin section view of K-bentonite sample KRDB6 from Gavurpınarı quarry in plane-polarized light. 24
Figure 2.2. Volcanogenic mineral examples from the studied Gavurpınarı quarry K-bentonite samples 24
Figure 2.3. Sub- to anhedral and slightly rounded zircon crystals with primary feldspar phenocrysts in K-bentonite sample OC1 in plane-polarized light 25
Figure 2.4. Rhombohedral dolomite crystals in dolostone sample YBA12 from Yılanlı Burnu quarry in cross-polarized light. 26
Figure 2.5. Ostracod fossils found in clayey samples a) OCB-2B and b) OCB-2A 26
Figure 2.6. Stromatolite features bearing YBA1 dolostone sample from Yılanlı Burnu quarry 27
Figure 2.7. Thin section view of ostracod-bearing limestone sample OCCK1 from Gavurpınarı quarry (white-colored arrow indicates ostracod fossil). 28
Figure 3.1. The clay and non-clay mineral assemblage of OCB-2A sample. a) unoriented powders of whole rock (I: Illite, Q: Quartz, Cal: Calcite, D: Dolomite, F: Feldspar) b) air-dired (AD) oriented clay fraction (I: Illite), ethylene-glycolated (EG) clay fraction (I: Illite), heated clay fraction at 300 °C (I: Illite), heated clay fraction at 550 °C (I:Illite). 30
Figure 3.2. The clay and non-clay mineral assemblage of OC1(B3) sample. a) unoriented powders of whole rock (I: Illite, Kaolinite: Kao, G: Gypsum, Q: Quartz) b) air-dired (AD) oriented clay fraction (I: Illite, K: Kaolinite), ethylene-glycolated (EG) clay fraction (I: Illite, K: Kaolinite), heated clay fraction at

300 °C (I: Illite, K: Kaolinite), heated clay fraction at 550 °C (I:Illite). At 550 °C crystal structure of kaolinite collapses, thus it becomes an amourphous material. 31
Figure 3.3. The clay and non-clay mineral assemblage of OCB-2B sample. a) unoriented powders of whole rock (I: Illite, Q: Quartz, Cal: Calcite, D: Dolomite) b) air-dired (AD) oriented clay fraction (I: Illite), ethylene-glycolated (EG) clay fraction (I: Illite), heated clay fraction at 300 °C (I: Illite), heated clay fraction at 550 °C (I:Illite). 32
Figure 3.4. XRD pattern of YB1 K-bentonite. a) unoriented powders of whole rock (Q: Quartz, F: Feldspar, D: Dolomite, b) air-dired (AD) oriented clay fraction (I: Illite, I/S: Mixed-Layer Illite Smectite), ethylene-glycolated (EG) clay fraction (I: Illite), heated clay fraction at 300 °C (I: Illite), heated clay fraction at 550 °C (I:Illite). 33
Figure 3.5. XRD pattern of YBA5 K-bentonite. a) air-dired (AD) oriented clay fraction (I: Illite), ethylene-glycolated (EG) clay fraction (I: Illite, K:Kaolinite), heated clay fraction at 300 °C (I: Illite, K:Kaolinite), heated clay fraction at 550 °C (I:Illite). 34
Figure 3.6. XRD pattern of YBA-19A K-bentonite. a) air-dired (AD) oriented clay fraction (I: Illite), ethylene-glycolated (EG) clay fraction (I: Illite), heated clay fraction at 300 °C (I: Illite), heated clay fraction at 550 °C (I:Illite). 35
Figure 3.7. The KI versus Ir diagram of illites within K-bentonites collected from Yılanlı Burnu and Gavurpınarı quarries 37
Figure 3.8. Unoriented powder diffraction patterns of the illite polytypes from samples of YB4 (Yılanlı Burnu quarry) and KRDB6 (Gavurpınarı quarry). 38
Figure 3.9. Unoriented powder diffraction patterns of the illite polytypes for different sized fractions a) YBA-19A K-bentonite sample from Yılanlı Burnu quarry b) OCB-2A K-bentonite sample from Gavurpınarı quarry. 39
Figure 3.10. The polytype distribution of different sized fractions and variations in peak widths according to the increasing crystal size....41
Figure 3.11. The XRD patterns of oriented different-sized clay fractions of sample OCB-2A a) Normal, b) Ethylene-Glycolated, c) Heated. 42
Figure 3.12. The XRD patterns of oriented different-sized clay fractions of sample YBA-19A a) Normal, b) Ethylene-Glycolated, c) Heated. 45
Figure 3.13. a) HR-TEM microphotograph shows regular stacking sequence of illites (10Å) within Sample YBA-19A. b) The profile obtained perpendicularly to atomic planes. 48
Figure 3.14. a-b) The irregular platy and juxtaposed morphology of illite crystals within the sampleOCB-2A from Gavurpınarı quarry. 49
Figure 3.15. The platy habit of illites with curved flakes and surrounding calcite minerals b) The EDX pattern of sample OCB-2B (carbonate minerals result in a carbonate-rich chemical composition in EDX data)....50
Figure 3.16. Lamellar-platy morphology of illites in the OCB1G sample from Gavurpınarı quarry. 52
Figure 3.17. (a) The platy and coalesced morphology of illites within sample YBA-19A from Yılanlı Burnu quarry (b) The EDX pattern of YBA-19A presents the illitic composition (high S and Fe contents indicate pyritization). 52
Figure 3.18. Lamellar gypsum crystal seen in OCB1S sample from Gavurpınarı quarry. 54
Figure 3.19. (a) In SEM microphotograph of sample YBA-19C, rhombohedral dolomite crystals can be seen and (b) The EDX pattern of the sample reveals illite and dolomite composition. 54
Figure 3.20. The irregular distribution of platy illites and rhombohedral dolomites in sample YBA-19C. 56
Figure 3.21. (a) The SEM microphotograph displays platy and juxtaposed structure of illites and (b) EDX pattern of OC1(B3) sample indicates the illitic composition of the sample. 56
Figure 3.22. (a) The quartz and calcite crystals surrounded by thin illite flakes in sample OC1(B3) From Gavurpınarı quarry and (b) The EDX pattern of calcite and (c) quartz minerals in sample OC1(B3). 58
Figure 4.1. Geochemical characteristics of K-bentonites. a) Zr/TiO_2-Nb/Y diagram (Floyd & Winchester, 1978) (The triangles and blue squares represent K-bentonite samples from Gavurpınarı quarry, while the circles are representative of K-bentonite samples from Yılanlı Burnu quarry). 62

Figure 4.2. The chondrite-based normalized trace element diagram of K-bentonites. 63
Figure 4.3. The chondrite-based normalized REE diagram of K-bentonites..... 63

LIST OF TABLES

TABLES

Table 1. The crystal-chemical characteristics of representative K-Bentonite samples from Gavurpınarı quarry.....36
Table 2. The crystal-chemical characteristics of representative K-Bentonite samples from Yılanlı Burnu quarry.....36

CHAPTER 1

INTRODUCTION

1.1. Purpose and Scope

The products of explosive eruptions in the form of volcanic ash (tephra), after being transported for long distances, are settled and altered to bentonites (smectite-rich volcanogenic clay rocks) in early diagenesis. In late diagenesis, these bentonites are transformed into K-bentonites by chemical modification and progressive illitization, and then finally into K-metabentonites by low-grade metamorphism (Fortey et al. 1996). During diagenesis and very low grade metamorphism, due to potassium enrichment, smectite transforms to mixed-layer illite-smectite and then illite mineral in K-bentonites (Merriman and Roberts, 1990).

K-bentonites are exposed in the Devonian strata in Zonguldak-Bartın area (Türkmenoğlu, 2001; Türkmenoğlu et al., 2009). They were around 2-50 cm thick greenish-gray clay beds alternating with platform-type, shallow marine limestones and dolomitic limestones of the Yılanlı Formation. K-bentonites on the other hand have been assumed by some researchers as useful time markers of geologically instantaneous chronostratigraphic surfaces due to their sudden eruption, rapid rate of accumulation and widespread distribution. By this they have a valuable potential to make both local and regional paleogeographical, sedimentological, biogeographical, and paleoecological correlations (Huff and Morgan, 1990, Kolata et al. 1998, Min et al. 2001). Geochemistry of K-bentonites provide significant data to reveal the tectono-magmatic evolution of the source area, and also the former positions of continental plates by exhbiting the distribution patterns of wide apart ash beds (Kolata et al. 1987, Huff et al. 1992, Bergström et al. 1995). K-bentonite beds are also often datable using fission track and U/Pb dating of zircons, K/Ar, and Ar/Ar of amphibole, biotite and sanidine (Marker and Huff, 2005).

For the purpose of revealing their clay and non-clay mineralogies, texture, structure and crystal-chemical features of the K-bentonites, various analyses were performed. X-ray powder diffraction; SEM-EDX; HR-TEM; and ICP-MS analyses and thin section observations suggest that these bentonites display an illite-rich mineral composition (approximately 95% illite; 5% smectite); and are K-bentonites which were formed by alteration of tephra (volcanic ash). During Devonian time, in addition to climatic and biological changes, extensive volcanic activity associated with major tectonic processes took place. Thus, K-bentonites found in the Devonian Yılanlı Formation, in western Black Sea region may be originated in relation with a distal Devonian volcanic activity.

In the lights of the acquired data, this study firstly aims to determine the illitization process forming the illites in the Devonian K-bentonites from the Yılanlı Formation, and secondly to identify the original chemical characteristics of the source material from which those K-bentonites were derived. Additionally, crystal-chemical analyses results will also provide significant data to understand the formation conditions (temperature, pressure) and environments of the studied illites. This study is also the first masters thesis investigation based on tephra or K-bentonites in Turkey. Therefore, as an initial research of the K-bentonites from the Devonian Yılanlı Formation in north western Anatolia, this study may provide with an opening for detail studies on age of diagenesis, age of illitization, paleogeography, and tectono-magmatic evolution of the source area.

1.2. Geographic Setting and Location of the Study Area

The study area is located in the Bartın-Zonguldak area, in western Black Sea region, Turkey. Mainly two outcrops of Yılanlı Formation, between the Bartın-Zonguldak area, were investigated.

The first outcrop, the Gavurpınarı Limestone quarry, is located around Gavurpınarı village, 10 km southeast of Bartın (Figure 1.1). It is included within the coordinates of 41° 42'04.39'' N latitudes and of 32 16'41.88'' E longitudes. The second area is Yılanlı Burnu quarry which is located about 10 km southeast of Bartın. This area is located within the 41 41'05.10''N latitudes and of 32 14'49.60''E longitudes.

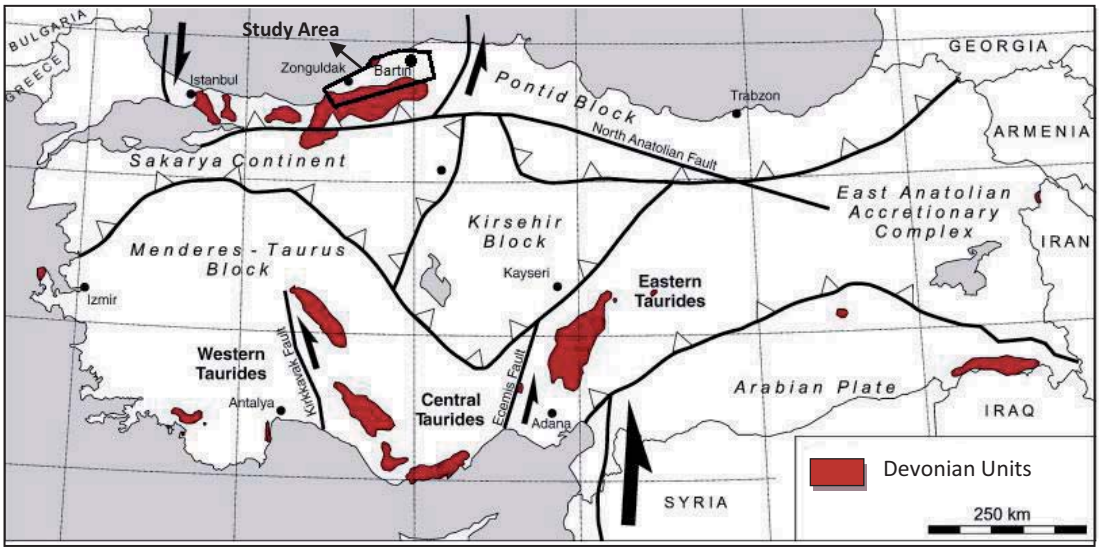


Figure 1.1. Location map of the study area and geotectonic distribution of Devonian units in Turkey (modified from Wehrmann et al., 2010).

1.3. Methods of Study

This study consists of two main stages as field and laboratory studies.

The field studies mainly consist of measuring stratigraphic sections and systematic sampling of K-bentonites and associated carbonate rocks. A total of 46 samples collected from measured stratigraphic sections, but only some selected representative K-bentonites and carbonate rocks were studied by thin sections using a polarizing microscope, by scanning electron microscopy (SEM) with energy dispersive X-ray spectrometry (EDX), by X-ray diffractometry (XRD), by high-resolution transmission electron microscopy (HR-TEM) and by chemical analyses (ICP-MS) covering major-, trace-, and rare-earth elements (REE).

During the laboratory studies, totally 44 thin sections of both bentonite and carbonate rocks were prepared for mineralogical and petrographical examinations under polarized microscope in order to reveal the relationships in terms of mineral assemblages, texture, fabric and also to compare petrographic characteristics of rock samples from different locations. XRD analyses were performed on totally 19 bentonite samples and also on some carbonate rocks to describe the clay and non-clay mineralogies.

For the geochemical identification, a total of 28 whole rock samples (including K-bentonites and carbonates) were analyzed for major, trace elements by using inductively coupled plasma-mass spectrometer (ICP-MS) in ACME Analytical Laboratories, Canada (see Appendix A for geochemical data). But, only bentonitic rocks (14 samples) were interpreted by means of their geochemistry in order to reveal the geochemistry of their tephra origin.

1.3.1. Field Identification of K-bentonites and Sampling

To recognise K-bentonites, there are several criteria which can be acquired from both field and laboratory examinations. On field, K-bentonites exhibit different colors (green, blue, red, yellow) when wet but they characteristically display yellow color due to weathering (Figure 1.2-1.4). They have a waxy, slippery texture when they are wet due to their clay-rich composition. The thickness of K-bentonites ranges between 1 mm-2 m, and their typical outcrop appearance is a fine-grained clay-rich layer (Kolata et al., 1996; Marker and Huff, 2005).

During the field work, totally 46 bentonite and carbonate rock samples were collected from both Gavurpınarı and Yılanlı Burnu quarries. In Gavurpınarı quarry, dolomitic limestone and interlayering green-brown colored K-bentonite horizons within the Yılanlı Formation (Figure 1.5-1.8) were observed and sampled along the measured stratigraphic coloumn of each quarry levels

Yılanlı Burnu quarry succession is composed of mostly dolomitic limestones. (Figure 1.8- 1.13). The warping and tilting of the limestone layers are likely due to faulting and folding. The lowest part of the sequence is represented by green-colored volcanic units.



Figure 1.2. Field appearance of the Gavurpınarı limestone quarry in Bartın area along the E-W direction.



Figure 1.3. Different levels of the Gavurpınarı limestone quarry and and vertical layering of bentonite beds along the NE-SW direction



Figure 1.4. Grey coloured bentonite horizons from Gavurpınarı limestone quarry.

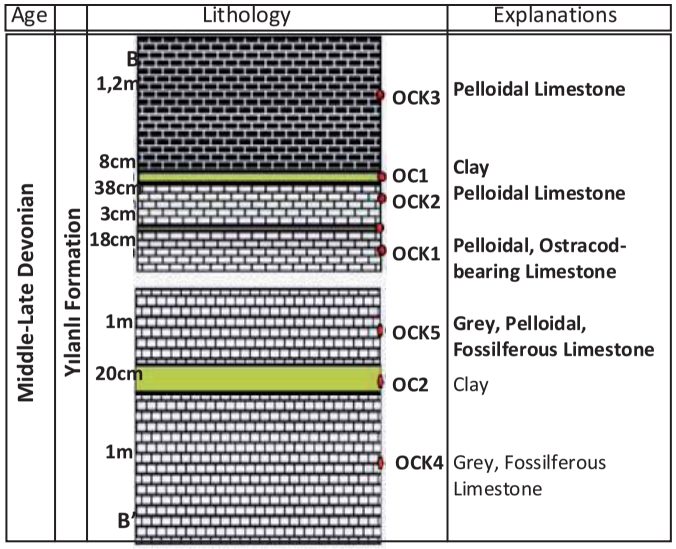


Figure 1.5. The pseudostratigraphic section along B-B' of 5. quarry level

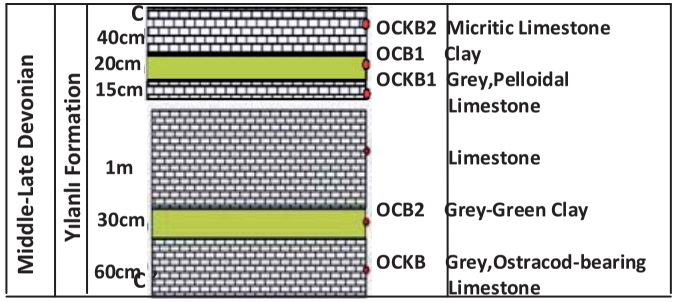


Figure 1.6. The pseudostratigraphic section along C-C' of 4. quarry level

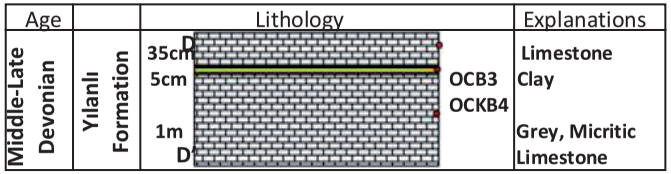


Figure 1.7. The pseudostratigraphic section along D-D' of 3. quarry level

(Not to Scale)



Figure 1.8. Another view of vertically layering Gavurpınarı limestone beds along the NE-SW direction.



Figure 1.9. The yellowish-brown coloured bentonites and interlayering limestones in Yılanlı Burnu quarry.



Figure 1.10. Another interlayering bentonite sample from Yılanlı Burnu quarry.



Figure 1.11. Yellowish colored bentonites interlayering limestones in Yılanlı Burnu quarry successions.



Figure 1.12. The folding yılanlı burnu limestone layers ınterlayering with bentonites along the NW-SE direction.

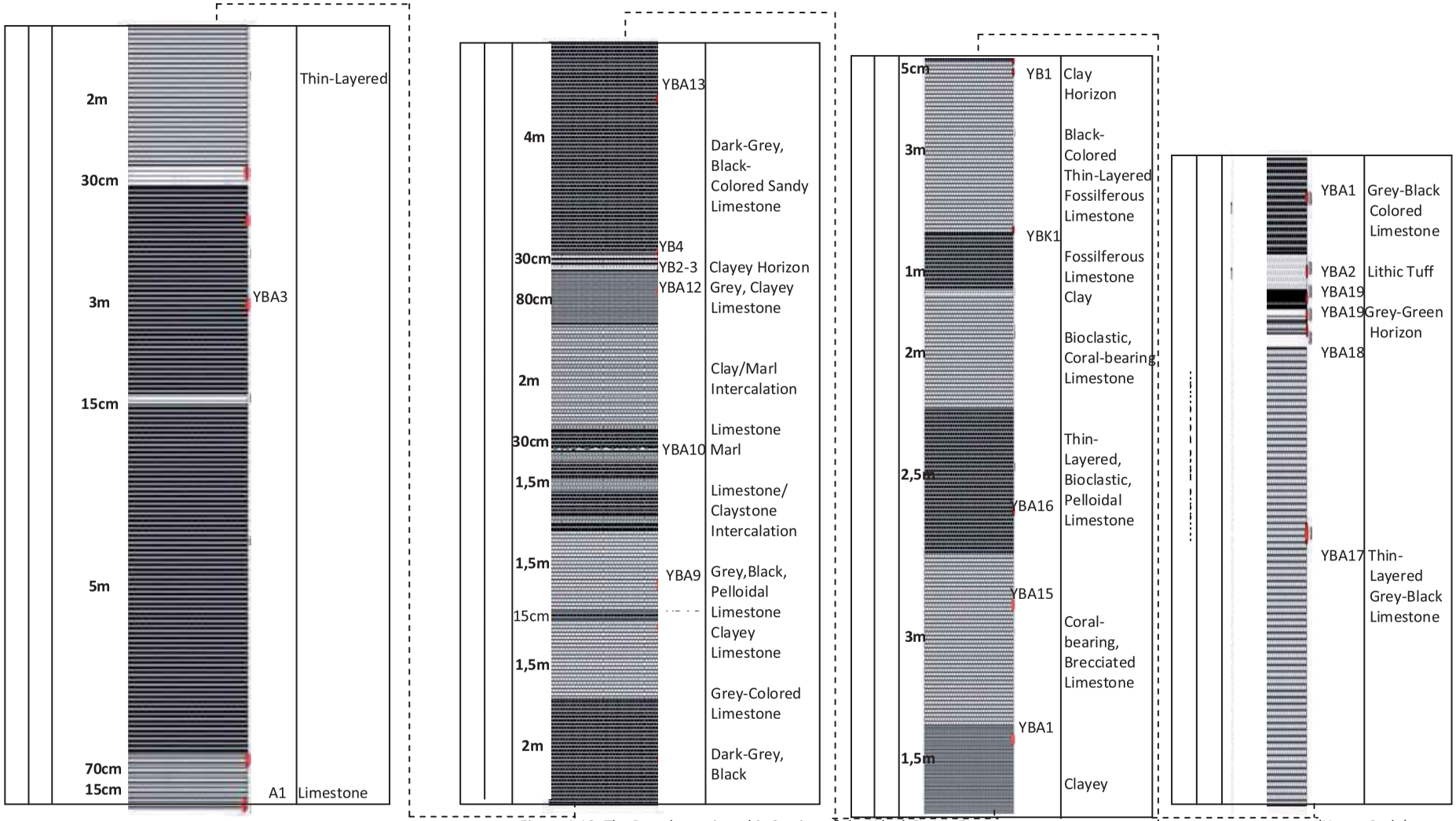


Figure 1.13. The Pseudostratigraphic Section of the Yılanlı Burnu Quarry. (Not to Scale)

1.3.2. Thin Section Preparation

The thin sections of collected rock samples were prepared in thin-section laboratory of Geological Engineering Department of METU. Textural and mineralogical features of bentonite and carbonate rock samples were examined by Swift and Nikon microscopes and photomicrographs were taken by using the Nikon camera in the Department of Geological Engineering of METU.

1.3.3. X-Ray Powder Diffraction Analysis (Sample Preparation and Computer Programs Used)

In this study, XRD analyse data of 14 selected representative bentonite samples from Gavurpınarı (OC1, OCB-2A, OCB-2B, OCB1G, OCB1S, OC1(B3), OC2, KRDB6) and Yılanlı Burnu quarries (YB1, YB2, YB4, YBA2, YBA5, YBA-19A) were interpretted in order to reveal their clay and non-clay mineralogy and illite crystallinity of studied K-bentonites.

Based on scanning of oriented slides with Cu Kα X-rays, the clay minerals were identified using diffraction patterns of basal (001) reflections. The diffraction patterns were obtained on the basis of Bragg equation ($2d \sin\theta = n\lambda$). The clay mineralogy interpretations of studied samples were done by four different types of slide preparation (air-dried, ethylene glycol-saturated, heated at 300, and 550 °C). The X-ray diffraction patterns of air-dried oriented slides provided an initiative information about clay mineralogy. To examine the presence of expandable interlayers, the ethylene-saturated (for 24 hours) slides were analyzed by X-ray diffraction; and this analysis will also allow the proportion of illite layers in mixed-layered illite/smectites to be determined. Hence, the 14 Å d-spacing of smectite will swell to a characteristic 17 Å d-spacing (Moore and Reynolds, 1997). The third and fourth type diffraction patterns were obtained by heating samples at 300 and 550 °C. The diffraction patterns of these heated slides are useful to examine the presence of smectite and kaolinite minerals. In case of smectite presence, the expanded interlayers with 17 Å d-spacing by ethylene glycol saturation will collapse to 10 Å at 300 °C. Provided that any kaolinite is present in clay fraction of sample, it will be amorphous at 550 °C (cited in Whittington 2010).

On the basis of steps mentioned above, samples weighing about 10 g were crushed slightly before clay separation to prevent clastic mineral addition into the clay-sized fraction. Then, the crushed samples passing through a 170 mesh sieve were separated in order to carry out sedimentation process. The dispersed < 2 µm size clay fraction was extracted using Stokes Law by sedimentation after acid removal treatment. Subsequent to sedimentation process for 4-8 hours, a 5 cm deep clay suspension was vacuumed into centrifuge tubes using a glass pipette. Then, samples were centrifuged at 6000 rpm for 10 min to complete sedimentation process.

Afterwards, the slides were examined to reveal mineralogical compositions of the clay fractions by X-ray diffraction using a Rigaku Miniflex II diffractometer in the Department of Geological Engineering of METU (Ankara, Turkey) for air-dried, vapor-saturated with ethylene glycol for 24 hours at 60°C, heated at 300 °C and at 550 °C samples. Slides were scanned at 2° 2θ / min. using Cu K_α radiation with a graphite monochromator, at 35 kV and 15mA for random powder diffractions, whereas the clay mineral diffractograms and illite crystallinity analyses were performed at 1° 2θ/min. (Kisch, 1991; Histon et al., 2007). Based on data from Moore and Reynolds (1997) and Hoffman and Hower (1979), the X-ray patterns were interpreted in order to determine clay mineralogy.

In this study, to determine illite crystallinity "Kübler Crystallinity Index" (KI) and Srodon's Intensity Ratio (peak-height intensity ratio) (Ir) were used. The Kübler indices (Illite "crystallinity" indices) (KI: Kübler, 1968; Guggenheim et al., 2002), were determined by measuring the width at half height of the (001) illite reflection of air-dried and ethylene glycolated samples. The calibration of KI values was done on the basis of the CIS scale proposed by Warr & Rice (1994). For KI calibration, the lineer equation of "IC_{CIS}=1.18 x $IC_{ODTÜ}$ - 0.015, R2 = 0.999" was obtained and used. Narrowing of the peak width suggests an increase in illite crystallinity due to decrease of the scattering domain of illite by collapse of interlayers and conversion of smectite to illite under increasing temperature and

pressure conditions. A broad peak indicates interstratification of expandable clays, interlayer hydration and small crystal size (Weaver, 1961; Kübler, 1968). Kübler (1968) suggested that the (I001) peak sharpness is related with increasing metamorphic conditions, and diagenesis equates to a sharpness >0.42° 2θ. By using the intensity ratio of Srodon (1984), relative abundances of expandable layers found in minerals were quantified.

The intensity ratio of Srodon is defined as the ratio between the (001) to (003) illite peaks for air dried samples versus the same ratio for ethylene glycol solvated samples. Illite crystallinity increases with the decreasing intensity ratio. This measurement allows to measure small amounts of expandable layers (<10% smectite layers) in mixed layer illite/smectite minerals. In case of quartz presence, the overlapping of the quartz (101) reflection with the illite (003) reflection could result in measurement errors. The Intensity Ratio is defined as follows Środoń 1984:

Intensity Ratio = (I001)/(I003) Air Dried / (I001)/(I003) Ethylene Glycol

The b_0 values of illite, by taking the (211) peak of quartz (2θ=59,970°, d=1,541Å) as a reference, were identified with d_{060} peak in order to estimate probable pressure conditions during illite formation; and also the octahedral composition (Mg+Fe) data of illite was acquired (Hunziker et al., 1986). Illite-crystallite size (domain size) values were determined by WINFIT computer program (Krumm, 1996).

For Mg+Fe content determinations, illite (060) reflections and also $(I_{002})/(I_{001})$ ratios were used. The Mg+Fe contents of clay minerals were determined by analyzing the intensity ratio of the 5Å (I_{002}) and 10Å (I_{001}) diffraction peaks. By this analysis, it is possible to estimate the presence of dioctahedral Al rich illite versus trioctahedral Fe and/or Mg rich illite (Esquevin, 1969). The relationship between Al content of illite and crystallinity has been discussed by Esquevin (1969). He examined the increase in illite crystallinity associated with high Al / (Mg+Fe) ratios in the octahedral layers of illites during anchi- or epimetamorphism on the basis of the ratio of intensities of the (002) diffraction peak at 5Å and the (001) diffraction peak at 10Å as an index of the Al / (Mg+Fe) ratio in the octahedral layer. He suggested that when the intensity ratio $I_{002(5Å)}/I_{001(10Å)}$ is above 0.3, indicating a high Al / (Mg+Fe) ratio, the 10 peak width can be used as a reliable indicator of the grade of metamorphism. The $I_{002(5Å)}/I_{001(10Å)}$ below 0.3 represents a high Mg+Fe content and a trioctahedral illite (Larsen and Chilingar 1983). On the other hand, the illite (060) reflection-based determination of dioctahedral versus trioctahedral illite, by scanning the randomly oriented slides for count times of >4 sec., is more accurate method (Moore and Reynolds, 1997). The deconvolution of XRD patterns were performed using WINFIT computer program (by Prof. Dr. Ömer Bozkaya).

The clay fractions were analyzed to establish the percentage of the $2M_1$ (% $2M_1$) illite polytype present in the clay fractions of the Yılanlı Burnu and Gavurpınarı K-bentonites on the base of Maxwell and Hower (1967). For illite polytype analyses, random powder mounts of each sample were prepared and scanned from 28° to 36° 2θ with a count time of forty five seconds per step. To eliminate overlapping reflections of dolomite and calcite, random powder samples were exposed to carbonate removal treatment before analysis. Illite polytypes were identified at characteristic peaks (2θ = 16-36°) for non-oriented preparations (Bailey, 1988). I(2.80) / I(2.58) and I(3.07) / I(2.58) peak area ratios, proposed by Grathoff & Moore (1996), were used in order to describe $2M_1$, $1M$ and $1M_d$ polytype ratios (% $2M_1/(2M_1+1M_d)$). The illite ratios of I/S mixed-layers were calculated based on "% illite = 183.41 x ln (Δ°2θ) - 297.48 (R2=0.9896)" equation of Moore and Reynolds (1997).

1.3.4. Scanning Electron Microscopy Studies

The SEM analyses in combination with EDX (Energy Dispersive X-ray spectroscopy), were performed by SEM with Quanta 400F Field Emission instrument at METU Central Laboratory, (Ankara, Turkey), in order to determine the particle morphologies and textural relationships of the selected 11 K-bentonite and carbonate rock samples outcropped at both Gavurpınarı and Yılanlı Burnu quarries, in Bartın-Zonguldak area. But only SEM-EDX analyses results of some representative samples are presented here. Operating conditions were 32 s counting time and 20 kV accelerating voltage.

Additionally, the chemical composition data for studied samples were obtained by energy dispersive X-ray analyses (EDX).

1.3.5. High Resolution Transmission Microscopy Studies

Besides of XRD analyses, transmission electron microscopy is the other useful method to measure the expandability of clay minerals. On the basis of this fact, separated < 0.1 μm clay fractions were seperated by high-speed centrifuge and then examined with a high-resolution transmission electron microscope (HR-TEM) using a JEOL JEM 2100F operating at 80-200 kV on samples precipitated from a dilute suspension onto a carbon coated grid at METU Central Laboratories (Ankara, Turkey), in order to examine lattice images and thickness distribution of illites; and presence of expandable (I/S) layers.

1.3.6. Geochemical Analysis

Totally, the selected 14 whole rock samples of bentonites collected from both Gavurpınarı (OC1, OCB-2A, OCB-2B, OCB1G, OCB1S, OCB3, OC2, KRDB6, KRDB7) and Yılanlı Burnu (YB1, YB2, YB4, YBA5, YBA-19A) quarries were chemically analyzed. Additionally, some carbonate whole rock samples (limestones and dolomitic limestones) from the study area were also analysed by ICP-MS. The chemical compositions of these clay fractions were determined using inductively coupled mass spectrometry in ACME Analytical Laboratories (Vancouver) Ltd. (Vancouver, Canada). Samples were prepared and analyzed in a batch system for major, trace elements, and rare elements.

1.4. Previous Studies

1.4.1. Previous Studies on Mineralogy, Chemistry and Origin of K-bentonites

In this chapter, a review of previous studies of K-bentonites from different locations will be summarized in historical order.

Nelson (1921, 1922) is the one who originally denoted the pyroclastic nature of Paleozoic rock system in the eastern part of the United States. In several stratigraphic units of the Paleozoic rock system, except the Cambrian, altered volcanic ash material was documented. Following Nelson's original remark, a number of researchers quoted the volcanic origin of these Paleozoic age altered volcanic ashes. Allen (1932) called an attention to the crescent-shaped shard structures, the entity of sanidine, apatite and euhedral zircon crystals in the Ordovician ash bed as evidence for the volcanic origin of those deposits. Rosenkrans (1934) and Kay (1944) firstly use bentonites on stratigraphic correlations (Lounsbury and Melhorn 1964).

The term K-bentonite was firstly used by Weaver and Bates (1952) to define Ordovician bentonites separating from Cretaceous bentonites with their high potassium content. Weaver (1953) stated that original smectite transforms into mixed layer illite/smectite during diagenesis and low-grade metamorphism along with disappearance of the characteristic swelling property of younger clays, as a consequence of the potassium bounding to the smectite structure. He suggested that the montmorillonite, originally resulting from glass alteration, adsorbed K^+ ions from sea water to produce non-expanding illite (about 80 per cellt of the mixed-clay layers), and this appears consistent with the observed proportions of illite and montmorillonite in the altered ash.

Weaver (1956) described the mineralogy of Middle Devonian Tioga K-bentonite from Pennsylvania, and the published paper includes an X-ray diffraction diagram for this material. He pointed out the presence of biotite, euhedral zircon and apatite in the heavy mineral suite, which are indicators of volcanic origin. Nelson (1959) made a study of an after-discovered bentonite zone from Pennsylvanian rocks of south-western Virginia, by means of its clay mineralogy and petrography. Grim (1962, p.895) shortly emphasized in his work the significance of volcanic ash effect on the characterization of terrigenous sedimentation in Paleozoic shales over wide geographic areas and comprehensive stratigraphic intervals. Lounsbury and Melhorn (1964) investigated K-bentonite

seams from midwestern and eastern Paleozoic rocks of the eastern United States. They submitted the euhedral volcanic minerals and volcanic structures in these Paleozoic rocks as the evidence for the volcanic origin of the thin seams of K-bentonite. They pointed out a volcanic origin for those K-bentonites.

Huff and Türkmenoglu (1981) studied the mixed-layer illite/smectite characterization and origin of Ordovician K-bentonites along the Cincinnati arch. They performed chemical analysis of K-bentonites for both whole-rock samples and < 0.1 μm size fractions to reveal their compositions. Based upon the chemical analyses results, they stated that there is a clear gain of K and Mg and a clear loss of Si, Fe, Ca, and Na in composition during post-depositional alteration. They stated relatively high contents of K and Mg by both seawater and parent material composition at the time of formation. By account of K-fixation, they also deduced that the interstratification developed from a montmorillonite precursor.

Jeans et al. (1982) examined the mineralogy, petrology and trace element geochemistry of volcanogenic clays in the Cretaceous of Southern England and Northern Ireland. In their study, they remarked the development process and distribution patterns of these volcanogenic clays. They suggested that the effective process is the argillization of predominantly acid or alkaline ash during early diagenesis in development of the smectite-rich clays in southern England. They described the clays as seperated deposits such as; primary, secondary and bentonitic. Primary and secondary bentonites were defined respectively as thin ash-falls deposited in quiet, brackish and marine waters (Speeton Clay, Ryazanian; Weald Clay, Barremian), and as local accumulations of ash transported into the Cretaceous seas by rivers draining ash-blanketed, local land areas (London Platform, Portsdown Axis). Bentonitic clays and marls were described as widespread accumulations of argillized ash. They suggested that the ash originated from penecontemporaneous, subaerial volcanism located in the southern part of the North Sea. They explained the distribution pattern of these smectite-rich clays in southern England by the changing palaeogeography of the area in Cretaceous times.

Knox (1983) investigated the stratigraphical significance of volcanic ash in the Oldhaven Beds of southeast England. He revealed the presence of significant proportions of volcanic ash grains, indicating probable correlation with the ash-bearing Harwich Member (London Clay Formation) of East Anglia and with the North Sea 'Ash Marker' by performing the thin section studies of the Oldhaven Beds of the London Basin.

Elliot and Aronson (1987) analysed the Alleghanian episode of K-bentonite illitization in the southern Appalachian Basin. They denoted that the mixed-layer illite-smectite (I/S) from Middle Ordovician K-bentonites are uniformly illitic. They proposed that the illitization was a short-lived episode (between 272 and 303 Ma-Late Pennsylvanian to Early Permian) and prompted by the Alleghanian orogeny. They concluded that the illitization was caused by flushing of hot saline fluids to the basin edges from deeply buried part of the foreland basin during the orogeny.

Batchelor and Weir (1988) investigated mineralogy and geochemisty of Llandovery metabentonite beds associated with the black mudrocks from the Moffat Shale Group. They found out a volcanic origin for these metabentonites based on their geochemical and mineralogical analyses.

Merriman and Roberts (1990) examined the tectonic setting of the Moffat Shale Group from the Southern Uplands of Scotland by means of investigations on the geochemistry of metabentonites occured extensively in those shales. They indicated a volcanic origin for these metabentonites with regard to relatively high concentrations of trace elements, including Ba, Cs, Hf, Nb, Rb, Ta, Th, U, Y, Zr and REEs. Their immobile trace element data point out silicic ash compositions ranging from subalkaline to mildly peralkaline. They stated that the volcanic ashes derive from the magmas, produced in an insialic arc transitional to a back-arc setting.

Huff et al. (1991) studied on clay mineralogy, geochemistry, and isotope geochemistry of bentonites from the Central Belt of the Southern Uplands Terrane, both Scotland and Ireland. They stated that the bentonites were composed of mixed-layer illite/smectite (I/S) containing 90–95% illite. They also

mentioned that the illitization arose during low-grade metamorphism. They assigned age range of 379 ± 10 to 406 ± 10 Ma for bentonites by K-Ar age determination method. They explained the differences in Rb and other trace elements between the K–bentonite beds by means of differences in original ash composition, and remarked these differences as a useful criteria to group the beds within biostratigraphically-defined boundaries.

Bergström et al. (1992) correlated the pre-Pridolian Silurian successions from Balto-scandia and the British Isles with seven Silurian K-bentonite beds from this stratigraphic interval in eastern North America. In this study, researchers emphasized the event-stratigraphic potential of some beds from Baltoscandia and the British Isles due to their concentration in certain graptolite zones. And, they also stated that few K-bentonite beds from the Silurian of North America had occured at approximately the same stratigraphic levels as some widespread K-bentonite beds in northwestern Europe. By geochemical analyses, they presented the difference in the trace element compositions of the Wenlockian K-bentonites and the Llandoverian and Ludlovian beds in Europe. Based on immobile trace element geochemistry, they expressed the calc-alkaline source for the Silurian K-bentonite beds in the Iapetus Region, and also volcanoes in a destructive plate margin tectonic setting which these beds derived from. Even if the geographic location of the source volcanoes remained enigmatic, they suggested that the Silurian K-bentonite beds in the Iapetus Region are different from that of the numerous Ordovician K-bentonites in northwestern Europe and eastern North America.

Batchelor and Clarkson (1993) searched out a horizon of rapid faunal change with a rich assemblage below and an empoverished assemblage above in metabentonite horizon within the Upper Llandovery and early Wenlock succession of the North Esk Inlier of the Pentland Hills, Scotland. Constituent apatite crystals of metabentonite, on the basis of rare earth and other trace elements, allowed the researchers to correlate two separate outcrops locally, and also widely with similar occurrences elsewhere in northern Europe and identify the source magma type.

In their study, Bergström et al. (1995) investigated on K-bentonite beds from the Middle Ordovician of Baltoscandia. Short-lived volcanic eruptions generating laterally extensive ash beds make the ash layers useful time markers for stratigraphic correlation. In this study, workers mentioned that biostratigraphic character and situation, chemical fingerprinting, and lithologies (e.g. relative thikness) of K-bentonite beds are also significant tools to correlate different beds over large areas. Researchers originally analyzed these beds throughout their overall distribution in Baltoscandia, also named K-bentonite beds and traced the Grefsen, Sinsen, Kinnekulle, and Grimstorp K-bentonites from Norway to Ingria in westernmost Russia. They designated the biostratigraphic position of each unit by standard conodont, graptolite, and chitinozoan zonal units, and separated the beds by trace element study of K-bentonite samples.

In another tephra-based study, Cronin et al. (1996) made correlations of andesitic tephras from the eastern ring plain of Ruapehu volcano, North Island, New Zealand. In their investigation, they used mineral compositions, ferromagnesian mineral assemblages and outcomes of fieldwork as tools for geological mapping and correlation. In mineralogy-based identification of tephra units, hornblende and olivine were used as indicator minerals. In addition to hornblende and olivine, titanomagnetite crystals, available in all tephra samples, were also used. According to the analyses performed in this study, the researchers suggested a strong relationship between ferromagnesian and titanomagnetite mineral chemistries which indicates the same melt composition or the same melt conditions that ferromagnesians formed from before eruption of each tephra.

In the study of late Caledonian volcanic origin of Silurian and late Ordovician K-bentonites from the British Isles, Fortey et al. (1996) performed mineralogic, chronostratigraphic and geochemical analyses on samples collected from their study area to reveal possible volcanic origin of K-bentonites. Hence, it was thougt that prolonged volcanism with the closure of the Iapetus and Tornquist Oceans originated Silurian and late Ordovician K-bentonites of the British Isles. According to the data they attained from geochemical analyses, more than one possible continental margin

arcs being geochemically and geographically different from each other were proposed which generated the volcanic ashes.

Another possible volcanic origin research on K-bentonites was done by Bergström (1997) et al. for Silurian K-bentonite beds at Arisaig, Nova Scotia, eastern Canada. They used new graptolite collections as significant biostratigraphic indicators to establish biostratigraphic position of K-bentonite deposits in the Ross Brook Formation. By their geochemical data, they suggest calc-alkaline composition for the Arisaig ash beds. When researchers evaluated stratigraphic distribution differences of Arisaig K-bentonites, with paleogeographic assesments, it is understood that location of the source volcanoes of the Silurian K-bentonite beds at Arisaig is much further to the south in the Iapetus than the British–Baltoscandian Llandoverian K-bentonites.

The Lower Silurian Osmundsberg K-bentonite's mineralogical and chemical features allowed researchers (Huff et al. 1998) to correlate these K-bentonite beds regionally with other sections in Sweden, and also in Norway, Estonia, Denmark and Great Britain. They stated that K-bentonites include the minerals mixed-layer illite/smectite and kaolinite, on the basis of mineralogical analyses on clay fractions. They suggested minimal burial temperatures associated with the presence of kaolinite and high amounts of smectite. To identify probable tectonic setting of the source volcanoes and composition of original magma, they made investigation of melt inclusions. With biostratigraphic, lithostratigraphic and geochemical data, they defined the Osmundsberg K-bentonite, originated probably from the west of Baltica, as one of the most extensive ash fall beds in the early Phanerozoic.

Bergström et al. (1998) discovered new K-bentonite beds (Middle Llandoverian age) at five localities in Georgia, Tennessee, and Virginia, in the southern Appalachian thrust belts, eastern USA. They defined the clay minerals comprised in K-bentonites as mixed layer illite/smectite, chlorite/smectite and kaolinite, on the other hand the non-clay ones are quartz, biotite, zircon, and apatite. They revealed that K-bentonites originated from subalkaline silicic magmas which were dacitic in composition. They mentioned that the volcanoes generated these K-bentonites present a different geographic position from those of Llandoverian K-bentonites in Europe.

Clay-rich beds in Turonian–Coniacian chalks from the Anglo-Paris Basin, northwest Europe were studied by Wray (1999). He classified the studied beds as 'bentonites' and 'detritals' on the grounds of their rare-earth element (REE) and mineralogical composition. In his discription, bentonites were represented by their negative Eu anomaly and elevated smectite content; whereas detrital beds characterized by a minimal or absent Eu anomaly and a greater proportion of illite. His correlations provided enough information to understand that bentonites from the Anglo-Paris Basin indicate the same tephro-event with others from eastern England and northern Germany.

Huff et al. (2000) presented the possible volcanic origin of K-bentonites from the Silurian section of the Dnestr Basin of Podolia, Ukraine. They performed several geochemical, mineralogical and biostratigraphical analyses to propound diagnostic characteristics of these beds. Due to its well-documented macro- and microfaunal assemblages, the Silurian section of the Dnestr Basin is represented as a standart for both regional and widespread correlations by the researchers in this study. Discrimination diagrams relying on immobile trace elements and rare earth element data analyses presented that K-bentonites had a volcanic origin in a collision margin setting related to subduction in this study. They also emphasised the possibility of estimating the prevailing wind circulation for the designated paleolatitudes at a time in the geologic past by examining volcanic ashes. Hence the preserved volcanic ash falls in sediments should represent several deposition process effects, it is possible to use them as tracers for studying sedimentological characteristics (Thompson et al., 1986).

In this context, Berkley and Baird (2002) studied geochemical and petrographical characteristics of cemented series of altered ash beds in Trenton Group and Utica Shale of New York State. On the basis of well-developed glass shard textures in beds, they suggested that cementation took place before clay mineral alteration of glass. They also stated that calcareous ash beds indicate a felsic-

intermediate composition with their REE patterns showing enrichments in light REE and moderate to distinct Eu anomalies.

Ver Straeten (2004) stated that there are some important cases controlling the preservation potentials of volcanic ashes in marine environments. In some cases, K-bentonites could record more than one eruptions. When he evaluated the degree of preservation potentials of volcanic ashes in Lower to Middle Devonian marine strata in the Appalachian foreland basin, he also considered paleontological findings, authegenic minerals, multilayered beds and distribution manner of these K-bentonites. He also revealed that post-depositional sedimentological events may induce modifications in preservation potentials of ash beds. Hence, to describe the preservation potential of Lower to Middle Devonian K-bentonites in Appalachian foreland basin, he represented a model. He combined associated physical, biological, and chemical processes active in epicontinental seas and marine foreland basins peripherally by this model. He concluded on the basis of his model that the volcanism generating these Early to Middle Devonian ancient volcanic ashes is related with the Acadian orogen.

Benedict (2005) also studied Devonian K-bentonites of the Appalachian foreland basin. He presented similar conclusions to Ver Straeten's (2004). He reported that geochemical and physical examinations on these K-bentonites indicate two or more source eruptions. He supported his idea with incongruities in geochemistry of apatite phenocrystals from multiple and individual K-bentonite beds in the study area. He emphasized different bedding manners. He also stated post-depositional events such as redeposition of materials on the sea floor by changing turbulence (biological activity).

Leslies et al. (2006) documented the Mohawkian Deicke and Millbrig K-bentonites from the Appalachians to the Upper Mississippi Valley and from Alabama to Ontario as useful marker horizons for both local and widespread correlations.

Histon et al. (2007) aimed to identify volcanic ash horizons and define the geochemical characteristics of Lower Palaeozoic K-bentonites from the Carnic Alps, Austria so as to search out their stratigraphical potential for regional correlation. They revealed biotite, apatite and zircon (showing magmatic resorption) crystals as an evidence of volcanic origin of these K-bentonites. With widespread correlations between K-bentonites in Carnic Alps and those in the British Isles, Sweden, Canada and North America, researchers suggested the closing of the Iapetus Ocean and northward drifting of microplates derived from the northern margin of Gondwana as a possible source volcanic activity which also generated these K-bentonites in Carnic Alps. They pointed out that K-bentonite is a bentonite in which the smectite has converted to K-rich, mixed-layer illite-smectite (I/S) as a reflection of both diagenesis and time.

Inanlı et al. (2009) studied the correlation potantial of Osmundsberg K-bentonite by performing different analyses. Several samples, consisting both known and suspected Osmundsberg K-bentonites, were examined on the basis of major and trace element compositions. The chemical results showed that diagnosable chemical characteristics of these bentonites allowed researchers to use them as event-stratigraphic markers for both local and regional correlations.

Kiipli et al. (2010b) correlated relations between altered volcanic ash layers (K-bentonites) and Telychian chitinozoans by using K-bentonite-based chemostratigraphy, and also biostratigraphy (graptolite, conodont, chitinozoan) for East Baltic sections, in Estonia and Latvia. Related to the different K-bentonite thicknesses, they also suggested that the probable source volcano was to the west-northwest.

Sell et al. (2011a) made a study based on the apatite trace-element chemistry of tephras to constitute geochemical correlations. Due to the heavily alteration of original glass, they applied another method in their research by using apatite crystals as tephra indicators due to their trace element concentrations. They analyzed apatite crystals from several unaltered Quaternary and Paleogene rocks with an electron microprobe. Despite differences in trace-element compositions of analyzed apatite phenocrystals, researchers stated that the apatite trace-element data could be used

as unique bed indicators. Related with their conclusions, researchers suggested this method establishes a fingerprint for a particular eruption, and presents also a useful information about the source magma.

1.4.2. Previous Studies on Clay Mineral Diagenesis with a Focus on Illitization Processes

Illite/smectite (I/S) can be described as a common, interstratified clay mineral which is composed of arranged illite and smectite layers in stacking sequences along the crystallographic c axis (Weaver, 1956-1959; Reynolds, 1980; Bethke et al., 1986). And, illite clay mineral can be formed by three different ways of "smectite to illite transformation": (1) burial diagenesis, (2) hydrothermal alteration, and (3) contact metamorphism (Nadeau et al., 1985; Inoue, 1986; Inoue and Kitagawa, 1994). Illites can be found as a common clay mineral in various rock types such as; bentonites, K-bentonites, shales. Shales may contain both detrital and diagenetic illites, while bentonites and especially K-bentonites consist of only diagenetic illites (Bailey et al., 1962; Moore and Reynolds, 1997). This makes K-bentonites a significant tool for illite-based studies in sedimentary basins.

Researches on smectite to illite transformation mechanism began in the late 1950's. Velde and Hower (1963) and also Hower and Mowatt (1966) originally propounded the mineralogical difference of mixed layer illite/smectite and illite in their studies. Several studies based on smectite to illite transition, determination of illite amounts in diagenetic illites, development of crystal growth models, and also various geological applications of sedimentary basins have been carried out extensively for more than four decades (Powers, 1959-1967; Hower et al., 1963; Burst, 1969; Hower et al., 1976; Boles and Franks, 1979; Nadeue et al., 1985; Inoue et al., 1986; Ahn and Peacor, 1986-1989; Freed and Peacor, 1989; Inoue et al., 1990; Buatier et al., 1992; Peacor, 1992a; Inoue and Kitagawa, 1994; Moore and Reynolds, 1997; Pevear, 1999; Bozkaya and Yalçın, 2004). These studies suggest an increasing proportion of illite within mixed-layer illite/smectite with increasing depth or temperature (Perry and Hower 1970; Hoffman and Hower 1979; Pytte and Reynolds 1989; Price and McDowell 1993).

In several studies based on clay mineral formation, three different mechanisms: (i) inheritance (detrital), (ii) neoformation, and (iii) transformation (positive and negative transformation or aggredation and degradation) (Millot, 1970; Bozkaya and Yalçın, 2009) were suggested. Origin by inheritance represents that a detrital clay mineral formed in another area during a previous stage; and that the clay mineral is stable in their previous location due to slow reaction rates or chemical equilibrium. Thus, inherited clay minerals provide information about the provenance history of sedimentary basin and also paleoenvironment of there. Origin by neoformation presents that the clay formed by either precipitation from solution or reaction of amourphous silicate material; and neoformed clay precipitated in return for in situ conditions. The transformed clays originated by modification of inherited clays by way of either ion exchange (exchange of loosely bound ions with those of the environment) or layer transformation (modification of firmly bound octahedral, tetrahedral or fixed interlayer cations). Transformed clays carry information on the chemical conditions of the environment under which they formed (Eberl, 1984; Bozkaya and Yalçın, 2009).

The environments of clay formation are: (i) the weathering environment, (ii) the sedimentary environment, and (iii) the diagenetic-hydrothermal environment (Figure 1.14) (Esquevin, 1958; Milot, 1970; cited in Eberl, 1984). In the sedimentary environments, both detrital and neoformed clays can be found. The transformed clay minerals form in diagenetic or hydrothermal environments as a result of higher temperature conditions (Eberl, 1984).

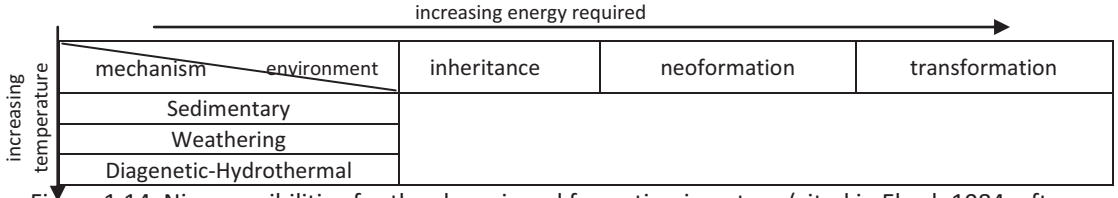


Figure 1.14. Nine possibilities for the clay mineral formation in nature (cited in Eberl, 1984; after Esquevin, 1958 and Milot, 1970).

With increasing diagenetic or metamorphic conditions, dioctahedral clay minerals present a progressive transformation as: smectite → mixed-layer I/S → illite → muscovite. These transformations are related with increase in crystal arrangement; and can be determined by crystal size and illite crystallinity. In other words, the crystal size (or crystal degree) increases with this progressive transformation, whereas crystal disorder decreases. And, due to decrease in interlayering, the microtextural relationships become more ordered (Peacor, 1992a; Pevear, 1999; Bozkaya and Yalçın, 2009).

There are two reaction series for clay mineral transformations: (i) dioctahedral (smectite-I/S-illite-muscovite), and (ii) trioctahedral (smectite-mixed-layer chlorite/smectite (C/S)-chlorite). These sequences representing subsidence sedimentary basins associated with lithostatic pressure usually display early to late diagenesis or low-anchizone conditions dominantly. Detrital or volcanic glass-originated smectite transforms into illite at about 3000 m depth and 90 °C temperature (Hower et al.,1976).

The I/S reaction serie for four different mineral zones can be described as: (i) Early Diagenetic Zone: R=0 (20-25 % I), R=1 (50-85% I), and R > 1 (> 85% I); (ii) The Early Stages of Late Diagenesis: R=1 (50-85% I), R=0 and R>1 (> 85% I); (iii) Late Diagenetic Zone: illite-bearing R>1 (85-90% I), R=1 and R>1 (> 90% I); (iv) Anchizone: R>1 (> 90% I) and illite (Wang et al., 1996). During illitization, the interlayer stratifications transforms from random (R0) to short-range ordered (R1), and then to long-range ordered (R3), here *R* represents the Reichweite parameter. In shallow depths, smectites exhibit R0-type (disordered) I/S layers and consist of 25% illite layers. Conjuction with increasing depth (> 3000 m), the increasing illite layer ratio reaches up to 80% at 3700 m. (Weaver and Back, 1971; Hower et al., 1976; Bethke et al., 1986). Ach and Peacor (1986) was stated that the illite content of I/S layers reaches up to 80% and the crystallite thickness comes at 50-100 Å with transition to the late-diagenetic zone, and also the a-b crystallographic planes are orientated parallel or subparallel to layering based on TEM data (cited in Bozkaya and Yalçın, 2009). In addition to TEM observations, polytype studies may provide significant information about ilitization mechanisms and they can be also used as indicators of thermal histories of sedimentary basins. For instance, Hower et al. (1963) studied polytypes of illite material in Paleozoic rocks on the basis of XRD analysis. They defined three natural polytypes of illite reflecting “temperature stabilities” as: 1Md, 1M and 2M1. On the basis of several researches, this polytype evolution was described as a transformation from turbostratic stacking of smectite-rich I/S to 1Md or 1M of illite-rich I/S, and then to 2M1 of pure illite during illitization (Inoue et al., 1987; Bethke et al., 1986; Reynolds, 1993). Hower et al. (1963) concluded that 1Md and 1M polytypes present low-temperature formations (< 200-350 °C); while 2M represents high-temperature formations (> 200-350 °C). They also stated that the investigation of illite polytypes allow researchers to explain the origin(s) of illite material. They determined only 1Md and 2M polytypes in Paleozoic rocks that they investigated (Pevear 1999).

In the study of smectite illitization of the Tertiary sediments in the Gulf Coast of United States (Hower et al., 1976), it was stated that illite layers in I/S increased as a function of Gulf Coast burial diagenesis. And, Hower et al. (1976) also mentioned that the conversion of smectite to illite could be explained by increased temperature associated with increasing burial depth (Figure 1.15). They described the conversion process on the basis of cation substitution in original smectite layers during a continous solid-state transformation. They suggested that the illitization process was formed as a result of Si, Na and H_2O loss, but K and Al gain. In another research, Eslinger and Pevear (1962) also noted that the illite layers in I/S mixed-layer mineral increase associated with increasing depth, temperature and with geologic age. In Hower (1981), this directly proportional relationship between illitization and increasing temperature (depth) were suggested as evidences for a progressive transformation of smectite to illite (cited in Pevear, 1999). Bethke et al. (1986) made a similar assumption that the conversion of smectite in mixed-layer I/S to illite is directly proportionate to increased burial depths in sedimentary basins. Compton et al. (1999) studied the volcanic ash layers from Miocene Monterey Formation by means of their isotope geochemistry, and also XRD, and SEM analyses. They concluded that the progressive burial diagenesis resulted in bentonite and metabentonite transition of volcanic ash layers.

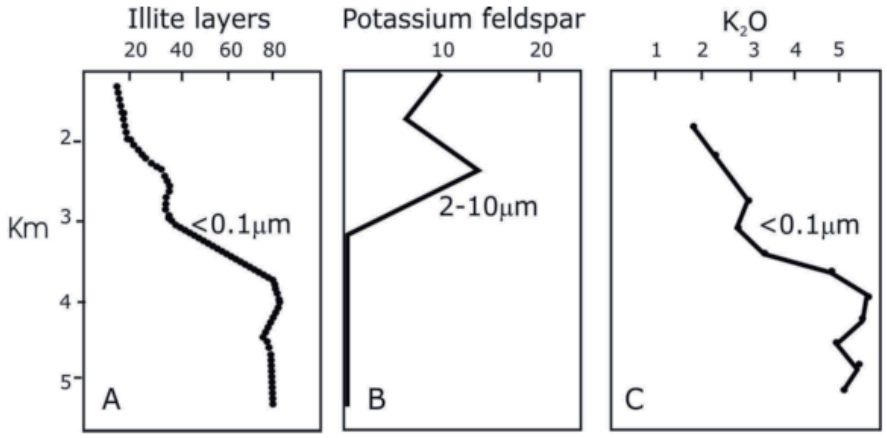


Figure 1.15. Gulf Coast sediments (well 6), Late Oligocene-Miocene. Vertical distribution of ıllite layers in I/S phases (<0.1 μm fraction) (A); K-feldspar percentage (2-10 μm fraction) (B); K2O (%) (<0.1 μm fraction) (C) (from Hower et al., 1976).

In brief, the illitization mechanism (neoformation or transformation) of illite minerals in sedimentary rocks (shales, bentonites, K-bentonites) will provide significant information about the sedimentary basin (e.g. thermal history of basin). By interpretation of the expandable layer content (I/S%), the stacking order (R), the polytype ratios (2M1%) and also TEM images of illites, it is possible to determine the mechanism which form illite.

1.4.3 Previous Investigations on Devonian Volcanism and K- bentonites

In the Devonian, there are four accepted extinction events: the mid-Givetian Taghanic event, the two Frasnian upper and lower Kellwasser events, and the late Famennian Hangenberg event. Hallam and Wignall (1997) and also Racki (1999a) examined these events, and they described the Kellwasser events, causing decimation of all pelagic and most benthic groups, and including the sudden crash of the stromatoporoid coral reefs, as the most serious biotic crises. In the study of mass-extinction causality scenarios (Keller, 2005), it was stated that pelagic and benthic faunas, and reef ecosystems were decimated as a consequence of climatic, sea level and oxygenation changes (Buggisch 1991; Copper 1986, 1998, 2002; Walliser 1996a; Racki et al. 2002; Tribovillard et al. 2004), and eutrophication (Murphy et al. 2000), nutrient-driven bioerosion (Peterhansel & Pratt 2001). In Keller (2005) it was cited that Late Devonian biotic crises are thought to be basically associated with probable magmatic extrusions due to tectonic rifting (Wilson & Lyashkevich 1996; Racki 1999a, b; Ma & Bai 2002; Sandberg et al. 2002; House et al. 2000; Racki et al. 2002).

There are several studies performed on Devonian K-bentonites. In one of those, Benedict et al. (2004) presented geochemical, physical and petrologic characteristics of Lower-Middle Devonian K-bentonites, in the Appalachian Basin, North America. He observed microscopic features within K-bentonites, indicating variations in depositional environments. Nevertheless, redoposited bentonites presented fossil layers which represent marine fauna. The researchers suggested that inconsistencies in results of geochemical analyses reveal multi eruptions generating those Devonian K-bentonite beds. In this study, it was also stated that as K-bentonites represent a single eruption, they also bear the traces of two or more eruptive events. The different trace-element compositions of phenocrystals in K-bentonites and/or distinct physical features of K-bentonite layers in the same bed were submitted as supporting evidences of two or more source eruptions.

Trapp et al. (2004) stated that 1 cm. thick metabentonites (tuff horizons) within the Hasselbachtel sequence (Sauerland, Germany) presented an age of 360.5 Ma on the basis of U/Pb radiometric dating of zircons. They also suggested that the volcanic origin of these metabentonites should be related with the volcanism at Devonian-Carboniferous boundary. They mentioned that the

geochemical characteristics of these wide-distributed metabentonites indicate a rhyolitic-rhyodacitic volcanic origin.

In the study of modelling the Late Devonian and Permian-Triassic extinction conditions, McGhee (2005) aimed to reconsider hypotheses which were previously suggested for those extinctions. One of the projected hypotheses propounded that the end-Frasnian biological diversity crisis arises from the global-cooling effects. To clarify those biodiversity crises, two different models were suggested by researchers; large igneous volcanism or astreoid/comet impact. A single impact model can be ignored, because possible effects of such a disaster run short to explain the Late Frasnian extinction impacts on biological diversity. Both the catastrophic volcanism and multi impact models would produce such a global cooling effect. Alternatively, it was stated that a global greenhouse-induced temperature raise could be suggested as a result of volcanism and multiple impacts, whether that is not compatible with their empirical data. In this study, it was also mentioned that to choose among suggested models, an exact Frasnian/Faminian (F/F) age and accurate Late Devonian global temperature data are required. On the basis of researches, it was suggested that the impact related extinction models are improbable, owing to discordant radiometric age data between F/F boundary (376 Ma) and known impact craters (McGhee, 2005).

Chalot-Plat (2007) also discussed Late Devonian and Early-to-Late Triassic basaltic volcanism in the Donbas and Fore-Caucasus regions, in the Eastern European Platform. It was also suggested that volcanic stacks probably generated by continental rifting processes about 600 km away from anticipated active oceanic subduction zones. The researcher stated that the southern margin of the Eastern European Platform includes two main units such as the Sarmatia segment of the East European Craton and the Scythian Platform which were structurally seperated. In his research, the investigations of basaltic rocks showed that higher alkali-silica ratios, higher TiO2, K2O, P2O5, FeO contents, higher trace element contents, a higher degree of fractionation between the most and the least incompatible elements, and the absence of Ta-Nb negative anomalies differentiated the Late Devonian alkaline basic rocks from the calc-alkaline Triassic basic rocks. Those variations could be explained by mantle source effects by means of partial melting and fractional crystallization. The kimberlite occurences in the eastern Siberian platform were also suggested as possible residues of Devonian basaltic flows indicating Devonian volcanism in (Keller, 2005). And, Ver Straeten (2007) suggested Early and Middle Devonian volcanic eruptions originated K-bentonites in Appalachian basin. Artyushkova ve Maslov (2008) studied the Early and Late Devonian (Emsian-Eifelian) rift basalts and island-arc type explusive eruptions in South Urals, Russia.

1.5. Regional Geology of the Study Area (Bartın and Zonguldak Area)

The orogenic frame of Turkey is formed by several Alpine “terranes” (Göncüoğlu et al., 1997) containing active and passive continental margins, arc and suture complexes, rifts which were formed by opening and closure of various Neotethyan oceanic branches. However, rocks being products of Pan-African/Cadomian, Variscan and Cimmerian orogenic events, are included in metamorphic units within the basement of Alpine tectonic units (Göncüoğlu, 2010). From north to south the Alpine tectonic units can be classified based on Yılmaz end Şengör (1981) such as: Istıranca Terrane, Istanbul-Zonguldak Terrane, Intra-Pontide Ophiolite Belt, Sakarya Composite Terrane, Izmir-Ankara-Erzincan Ophiolite Belt, Tauride-Anatolide Composite Terrane, SE Anatolian Belt, and the Arabian Plate.

In northwest Anatolia, the Istanbul and Zonguldak terranes (Figure 1.16) consist of two Variscan units having an associate Cadomian (Ustaömer and Roger, 1999; Chen et al., 2002) basement, and also an associate Alpine overstep sequence (Göncüoğlu, 2010; Bozkaya et al., 2012). Okay et al. (1994) suggested that this composite terrane was located further north between the Moesian platform and Crimea as part of the Odessa shelf previous to Albian; and during the Albian to Early Eocene it migrated southward along two major transform faults by the opening of the Western Black Sea basin. This area is also so-called as Rhodope-Pontide fragment (Şengör and Yılmaz, 1981), the Istanbul Zone (1989), Istanbul and Zonguldak Terranes (Göncüoğlu, 1997). The Cadomian basement being exposed in Bolu area also represents a tectono-stratigraphic similarity to that of western

Europe (Ustaömer, 1999) and consists of amphibolites, paragneisses, and oceanic mafic rocks intruded by granotoids (Ustaömer and Rogers, 1999).

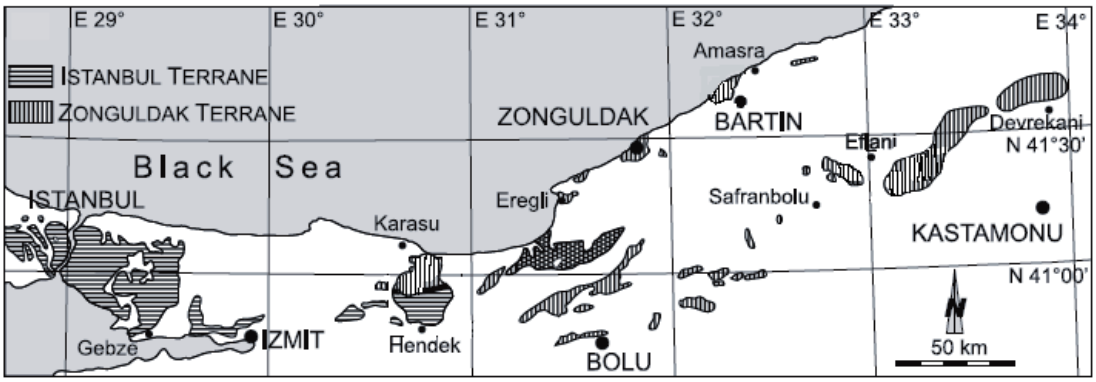


Figure 1.16. Distribution of the Paleozoic rock units in the Istanbul and Zonguldak terranes (from Bozkaya et al., 2012).

In the Zonguldak terrane, the basement rocks are similar to those of the Istanbul terrane, and are composed of a crystalline serie covering continental crust-originated gneisses, an oceanic set of gabbros, basalts, and ultramafics, and an island-arc complex of pyroclastics, granites, and felsic-volcanites. The Cadomian basement is overlain by Ordovician units comprising greenish grey siltstones and mudstones (Bakacak Formation) , dark-red conglomerates and sandstones (Kurtköy and Aydos Formations) (Figure 1.17) unconformably (Dean et al., 2000; Lakova et al., 2006), dark-grey mudstones and siltstones consisting Middle Ordovician fossils. The Ordovician Aydos Formation sequence is reported as similar to that in Istanbul area (Dean et al. 1997, 2000; Göncüoğlu 1997; Kozur and Göncüoğlu 1998; Gedik and Önalan 2001). Succeeding thick pack of Upper Ordovician limestones, the Early-Middle Silurian era is represented by the Fındıklı Formation including graptolitic black and gray shales and siltstones which characterizes the deposition variation in the Zonguldak terrane from shelf-type to coastal-lagoonal sediments of the Istanbul terrane. The Fındıklı Formation was deposited on a shallow mixed (clastic-carbonate) shelf during Early Devonian; and its deposition also becomes shallower upwards and represented by cross-bedded sandstones. The Fındıklı Formation is overlain by the Ferizli Formation consisting of red, grey, fine-to-medium-bedded siltstones, shales and reddish, greenish, well and thick-bedded, fine-grained, cross-bedded sandstones of the Ferizli Formation; and upwards with thick-bedded calcareous siltstones and sparitic, iron-rich algal limestones (Late Lower Devonian conglomeratic sandstones and quartzites of the Ferizli Formation) overlain Silurian and earliest Devonian units by an angular unconformity (Boncheva et al. 2009). Late Early Devonian (Emsian)- Late Early Carboniferous (Sephukovian) Yılanlı Formation including shallow-marine dolomites and limestones (Figure 1.17) succeed those Ferizli Formation conglomerates (Yalçın and Yılmaz, 2010; Bozkaya et al., 2012). The Yılanlı Formation is composed of grey, dark grey, black, medium to thick bedded limestones, dolomitic limestones and dolomites alternating with thin-bedded, black, calcareous shales. The approximate thickness of the Yılanlı Formation is 800 m. The boundaries of Yılanlı Formation with the lower Ferizli Formation and the upper Madendere Formation are reported as transitional by Gedik et al. (2005). The fossil observations (Aydın et al. 1987) indicate Efelian-Visean age (Middle Devonian-Early Carboniferous) for the Yılanlı Formation; however the Yılanlı Formation is overlain by Namurian Alacaağzı Formation. The eroded upper parts of Yılanlı Formation in the Çamdağ-Zonguldak area is overlain either by the Permo-Triassic or younger units with an angular unconformity to the west and south of Zonguldak. The deposition of the Yılanlı Formation continued from Middle Devonian to Early Carboniferous in a marine carbonate platform/shelf (Yalçın and Yılmaz 2010).

In this study, the investigated K-bentonite sequences are located within the Yılanlı Formation, lying within the Middle-Late Devonian sedimentary successions of the Pontide tectonic belt, in Zonguldak terrane.

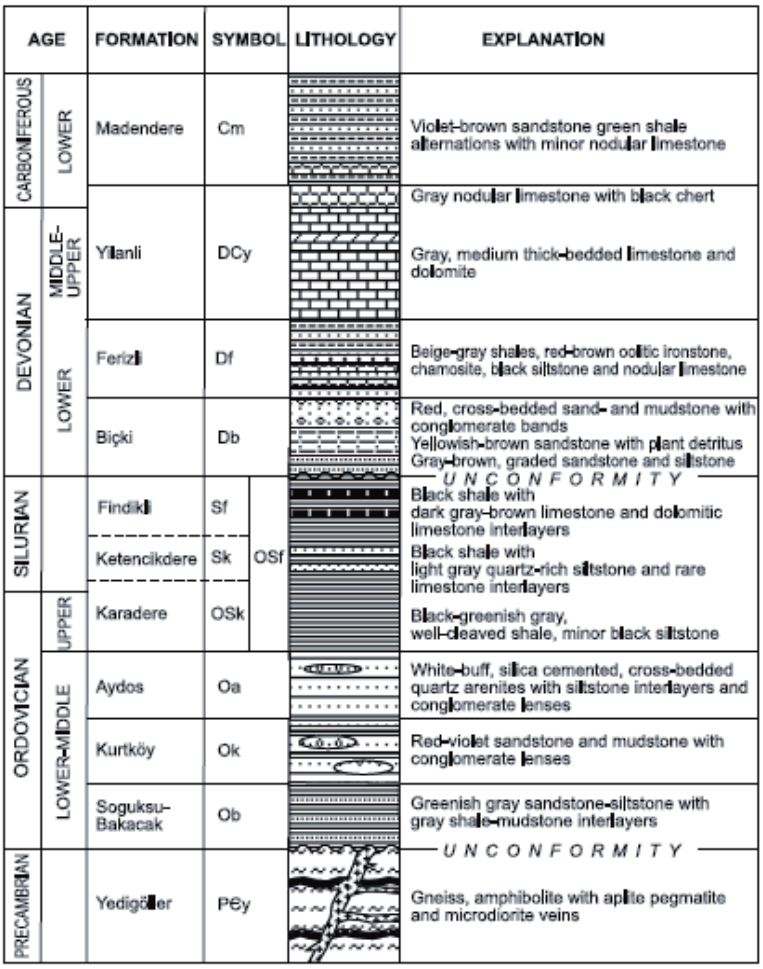


Figure 1.17. Generalized lithostratigraphic section of the Zonguldak terrane (Bozkaya et al., 2012).

CHAPTER 2

PETROGRAPHY

2.1. Introduction

For petrographical purposes, a total of 44 rock samples from two localities (Gavurpınarı and Yılanlı Burnu quarries) were examined under polarizing microscope. 26 samples are from Gavurpınarı quarry (Bartın area) and 18 samples are from Yılanlı Burnu quarry (Bartın-Zonguldak area). These samples involve both clastic and non-clastic sedimentary rocks. The clastic ones are composed of K-bentonites and shales, while non-clastic ones consist of limestones, dolomitic limestones and dolostones. It must be noted that limestones and dolostones were examined for only paleontological age and sedimentary environment interpretation and they were included briefly in this chapter. The mineralogical and textural features of K-bentonites were studied on the basis of visual estimation.

2.2. Gavurpınarı Quarry

2.2.1. K-bentonites

On the basis of laboratory examinations of some representative samples (OCB2-B, OCB2-A, OCB1-G, OCB1-S, OC1, OCB3, OC2, KRDB6), K-bentonites in Gavurpınarı quarry reveal similar mineralogical and petrographical features. The primary minerals characterizing the volcanic origin of those K-bentonites are biotite, zircon, quartz, feldspar, amphibole and apatite. Biotite and zircon crystals display euhedral to anhedral crystal forms (Figure 2.2 and 2.3). The presence of sharp euhedral zircon and biotite crystals indicates a possible volcanic origin for K-bentonites (tephras) (Figure 2.2). However, in the sample OC1 zircon crystals are sub- to anhedral and represent a slightly rounded crystal form (Figure 2.3). On the basis of Larsen and Poldervaart (1957), this feature can be explained by magmatic resorption rather than mechanical abrasion (Histon et al., 2007). On the other hand in Clayton et al. (1995), the rounded form of zircons within the Oakhill Lower Carboniferous K-bentonites were interpreted by reworking and sorting due to storm conditions. In this study, the crystal size of zircons is about 100 µm. This crystal size can be interpreted as a possible distal volcanic origin for K-bentonites.

In thin section examinations, pyrite, dolomite and calcite minerals were also observed as diagenetic minerals. And, pyrites are mostly oxidized which resulted in yellowish-brown colors of K-bentonites on field. It was reported that samples OCB-2A and OCB-2B contain ostracod fossils (Figure 2.5).

2.2.2. Limestones and Dolostones

Gavurpınarı quarry non-clastic sedimentary rocks consist of stromatolitic dolomitic limestones; ostracod-bearing peloidal micritic limestones; ostracod-bearing clayey limestones; ostracod- and intraclast-bearing peloidal micritic limestones; poligenic calcereous breccia; and clayey limestone/marn.

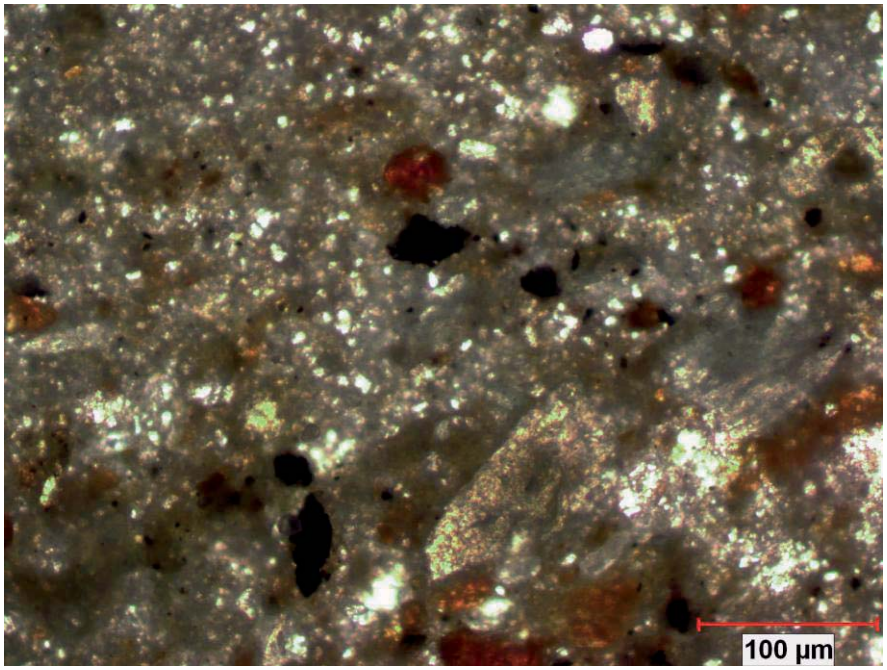


Figure 2.1. Thin section view of K-bentonite sample KRDB6 from Gavurpınarı quarry in plane-polarized light.



Figure 2.2. Volcanogenic mineral examples from the studied Gavurpınarı quarry K-bentonite samples (Türkmenoğlu et al., 2009).

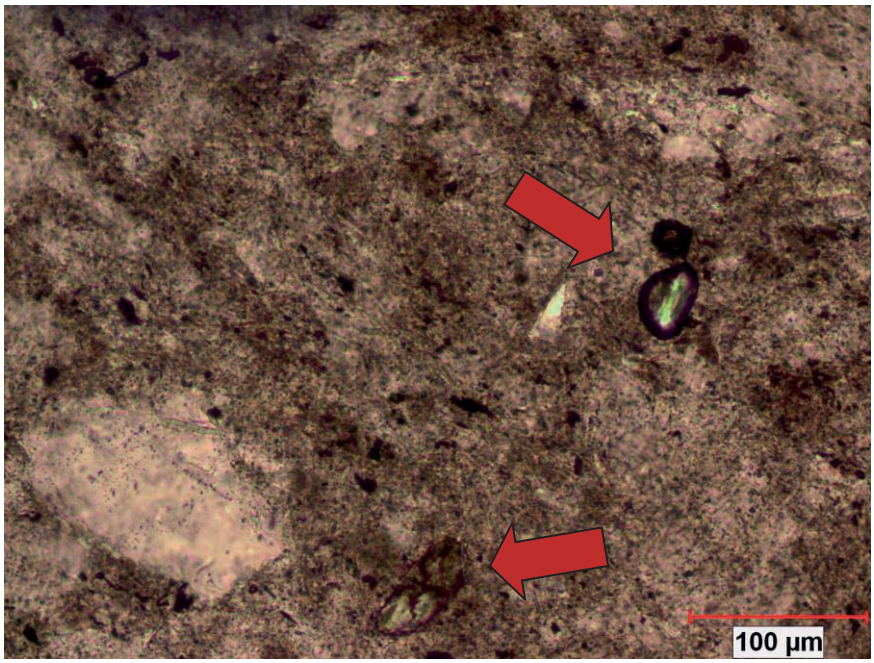


Figure 2.3. Sub- to anhedral and slightly rounded zircon crystals with primary feldspar phenocrysts in K-bentonite sample OC1 in plane-polarized light (red-colored arrows point out zircon crystals).

2.3. Yılanlı Burnu Quarry

2.3.1. K-bentonites

Yılanlı Burnu quarry K-bentonites (YB1, YB2, YB4, YB5, YBA-19A) exhibit similar petrographical and mineralogical features to Gavurpınarı quarry samples. Zircon, quartz, feldspar, and apatite crystals were observed. Dolomite, calcite, pyrite, and gypsum minerals were identified as non-clay diagenetic minerals. Similar to Gavurpınarı K-bentonites, thin section observations also present that pyrites are oxidized; and due to this oxidation, bentonites display yellowish-brownish colors, being used as a significant tool to recognize bentonites during the field work. Together with other sharp euhedral zircons in Yılanlı K-bentonites, the rounded and tiny zircon crystals were identified too.

2.3.2. Limestones and Dolostones

According to thin section observations, the carbonate rock samples collected from the Yılanlı Burnu quarry are composed of limestones or dolostones. Rhombohedral dolomite crystals can be observed in their prepared thin sections as a result of dolomite replacement of calcite during early marine diagenesis (Figure 2.4). Dolomitized stromatolite (Figure 2.6), bivalve-bearing dolostone, peloidal dolostone, organic dolostone, ostracod-bearing clayey limestone/marn facies (Figure 2.7) are common in Yılanlı Burnu facies.

On the basis of both field and microfacies observations, the abundance of stromatolite- and ostracod-bearing facies; but the absence of any pelagic and/or sedimentary structures indicating a high-energy environment points out a shallow intra-platform sedimentation environment. Additionally, the presence of microbreccia, but the absence of coral /crinoid/echinid/foraminifera/algae fossils support this interpretation. And, also the intercalation of marn and mudstone; and limestone and dolostone indicates that the sedimentation environment should be an 'epieric' platform (by Assoc. Prof. İ. Ömer Yılmaz, associated with the TUBITAK Research Project grant no: 110Y272).

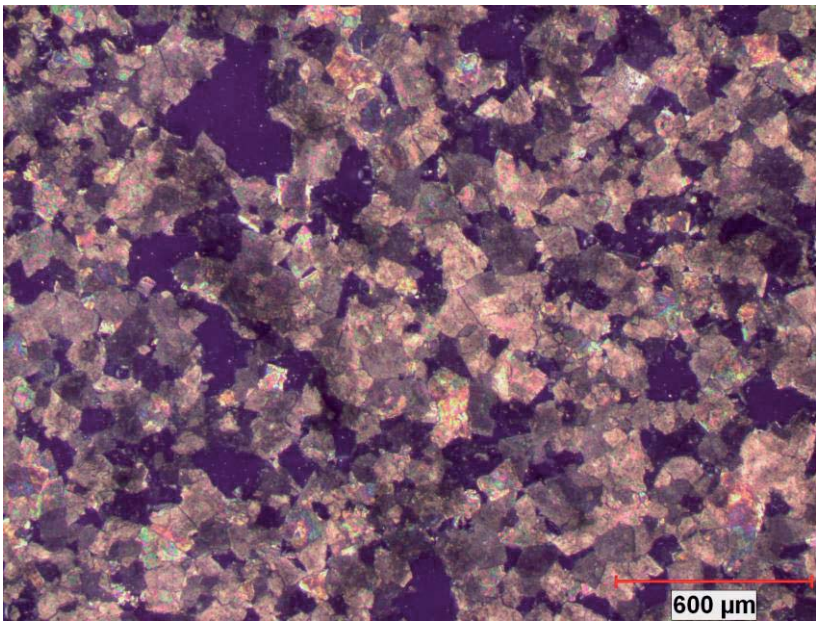


Figure 2.4. Rhombohedral dolomite crystals in dolostone sample YBA12 from Yılanlı Burnu quarry in cross-polarized light.

a)

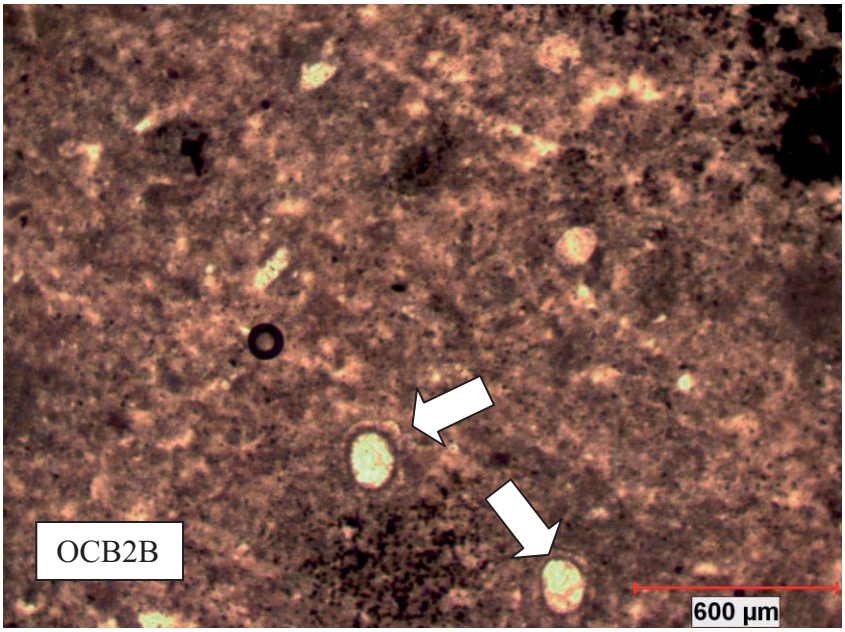


Figure 2.5. Ostracod fossils found in clayey samples a) OCB-2B and b) OCB-2A (white-colored arrows indicate ostracods).

b)

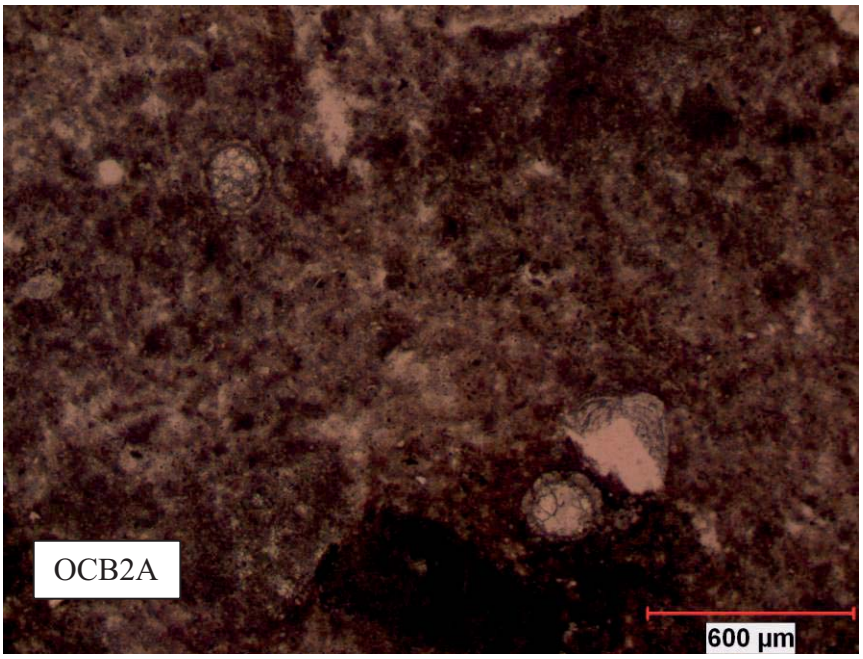


Figure 2.5. Ostracod fossils found in clayey samples a) OCB-2B and b) OCB-2A (continued).

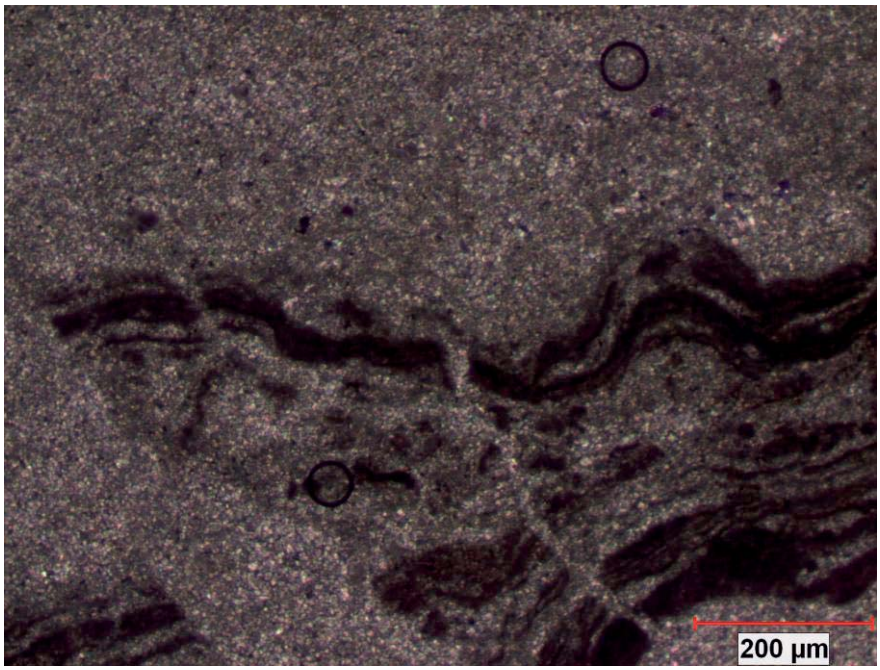


Figure 2.6. Stromatolite features bearing YBA1 dolostone sample from Yılanlı Burnu quarry.

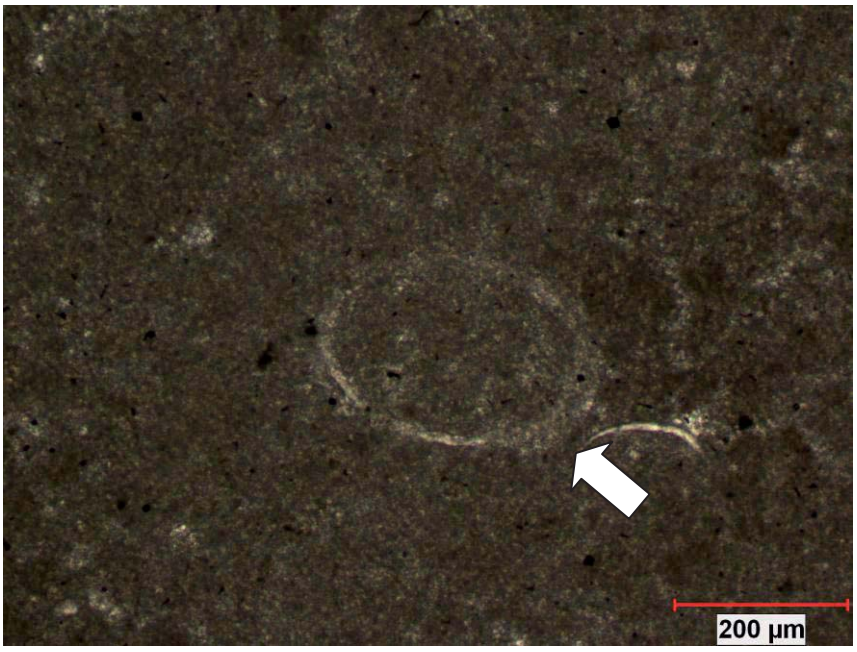


Figure 2.7. Thin section view of ostracod-bearing limestone sample OCCK1 from Gavurpınarı quarry (white-colored arrow indicates ostracod fossil).

.

CHAPTER 3

CLAY MINERALOGY

3.1. Introduction

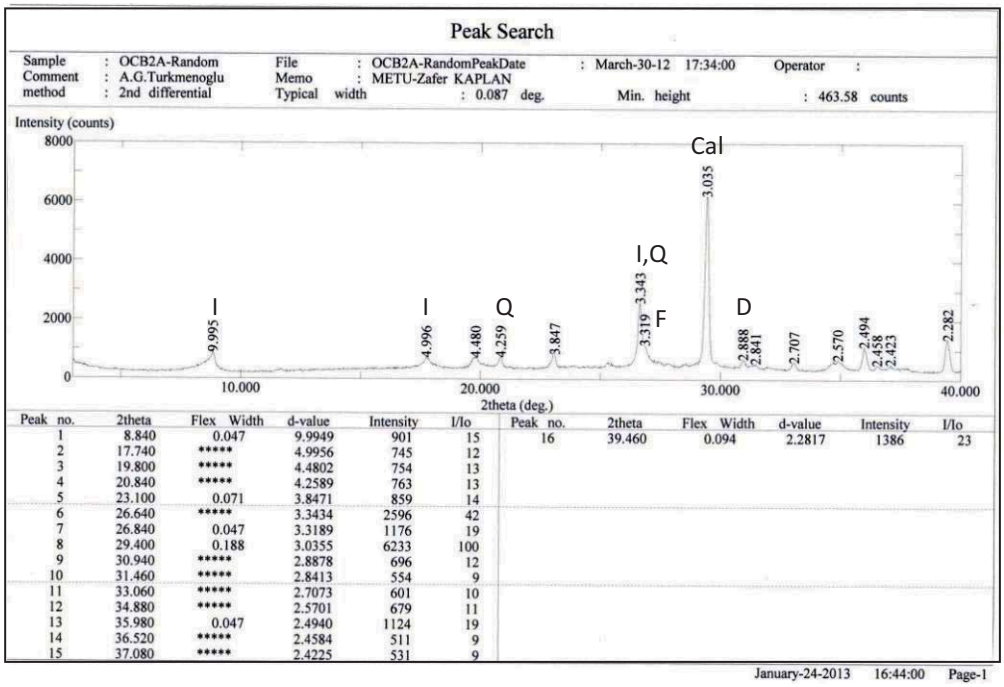
On the basis of the performed XRD-based analyses, the mineralogical and crystal-chemical characteristics of K-bentonites within the Yılanlı Formation successions in Bartın-Zonguldak area were determined for 3 samples from Gavurpınarı quarry (OCB-2A, OCB-2B, OC1(B3) and for 6 samples from Yılanlı Burnu quarry (YB1, YB2, YBA5, YBA8, YBA10, YBA-19A). Four different types of slide were prepared (air-dried, ethylene glycol-saturated, heated at 300, and 550 °C) for mineral identification. In addition to mineralogical identification, proportion of expandable layers (I/S %), illite crystallinity (KI and I_r), illite polytype ratios ($2M_1$%), and Mg+Fe content of illite (I_{002}/I_{001} and d_{060} values) were determined for crystal-chemical interpretations, and b_0 values of the studied illites were acquired to understand occurrence conditions (pressure/temperature). Data obtained from those XRD-based analyses could be used in order to interpret the illitization mechanism of illites within those K-bentonites.

3.2. Mineralogy

3.2.1. Gavurpınarı Quarry K-bentonites

XRD patterns of the studied K-bentonites collected from different steps of Gavurpınarı quarry reveal mainly illite as clay mineral, with kaolinite in some samples. On the basis of XRD analyses of sample OCB-2A, calcite, dolomite, quartz and feldspars are determined as non-clays in unoriented sample; whereas illite as the dominant clay mineral in the analyses of oriented slides (Figure 3.1). The XRD analysis performed for unoriented bulk sample of OC1(B3) reveals gypsum and quartz as non-clays. The oriented clay-fraction analyses of the same sample present mixed-layer illite/smectite, illite and kaolinite (Figure 3.2). In sample of OCB-2B the main clay mineral is illite (Figure 3.3).

a)



Peak no.	2theta	Flex Width	d-value	Intensity	I/Io	Peak no.	2theta	Flex Width	d-value	Intensity	I/Io
1	8.840	0.047	9.9949	901	15	16	39.460	0.094	2.2817	1386	23
2	17.740	*****	4.9956	745	12						
3	19.800	*****	4.4802	754	13						
4	20.840	*****	4.2589	763	13						
5	23.100	0.071	3.8471	859	14						
6	26.640	*****	3.3434	2596	42						
7	26.840	0.047	3.3189	1176	19						
8	29.400	0.188	3.0355	6233	100						
9	30.940	*****	2.8878	696	12						
10	31.460	*****	2.8413	554	9						
11	33.060	*****	2.7073	601	10						
12	34.880	*****	2.5701	679	11						
13	35.980	0.047	2.4940	1124	19						
14	36.520	*****	2.4584	511	9						
15	37.080	*****	2.4225	531	9						

b)

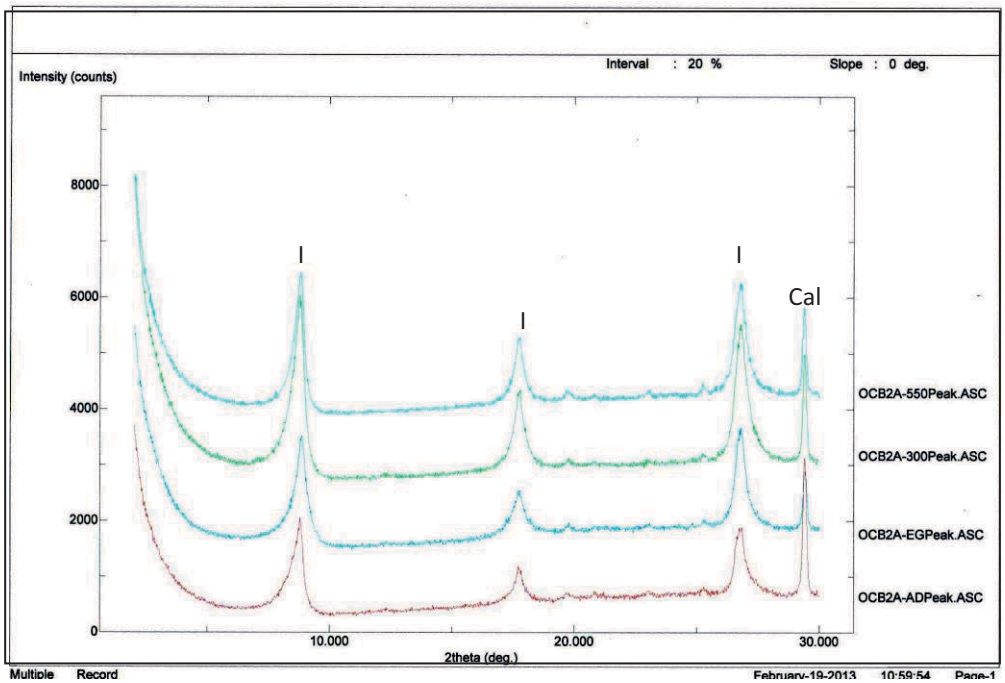
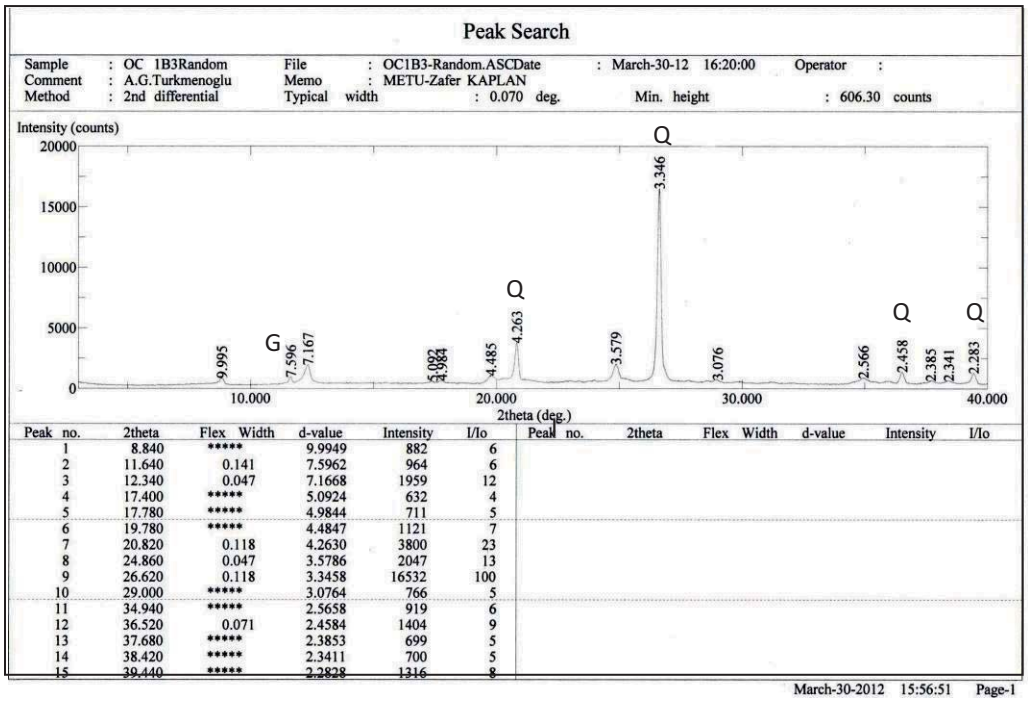


Figure 3.1. The clay and non-clay mineral assemblage of OCB-2A sample. a) unoriented powders of whole rock (I: Illite, Q: Quartz, Cal: Calcite, D: Dolomite, F: Feldspar) b) air-dired (AD) oriented clay fraction (I: Illite), ethylene-glycolated (EG) clay fraction (I: Illite), heated clay fraction at 300 °C (I: Illite), heated clay fraction at 550 °C (I:Illite).

a)



Peak no.	2theta	Flex	Width	d-value	Intensity	I/Io
1	8.840	*****		9.9949	882	6
2	11.640		0.141	7.5962	964	6
3	12.340		0.047	7.1668	1959	12
4	17.400	*****		5.0924	632	4
5	17.780	*****		4.9844	711	5
6	19.780	*****		4.4847	1121	7
7	20.820		0.118	4.2630	3800	23
8	24.860		0.047	3.5786	2047	13
9	26.620		0.118	3.3458	16532	100
10	29.000	*****		3.0764	766	5
11	34.940	*****		2.5658	919	6
12	36.520		0.071	2.4584	1404	9
13	37.680	*****		2.3853	699	5
14	38.420	*****		2.3411	700	5
15	39.440	*****		2.2828	1316	8

b)

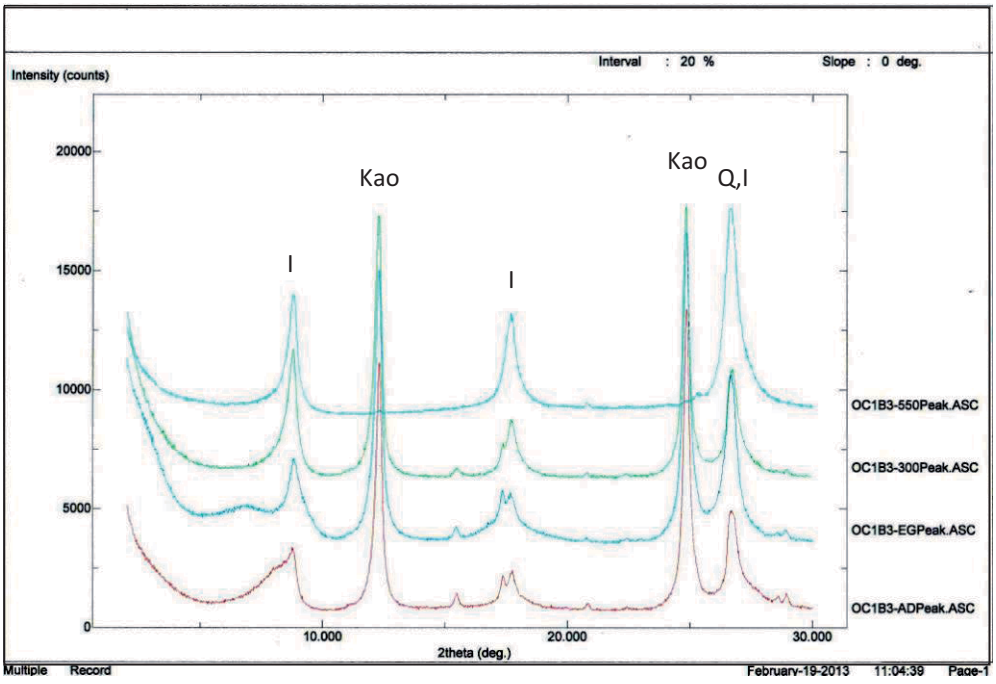
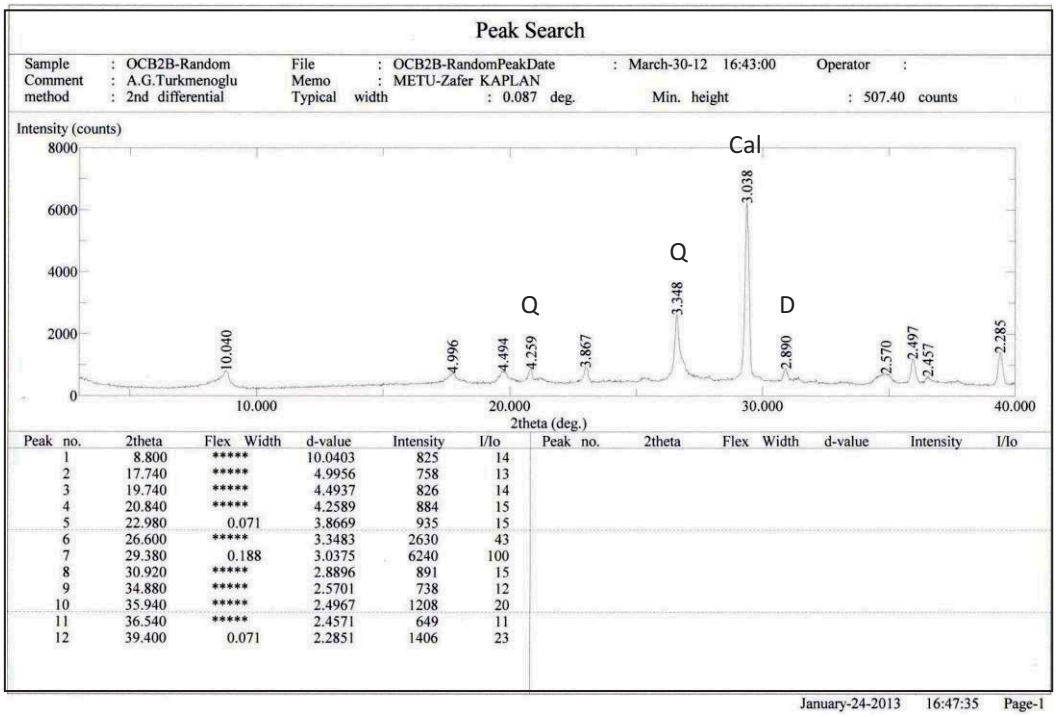


Figure 3.2. The clay and non-clay mineral assemblage of OC1(B3) sample. a) unoriented powders of whole rock (I: Illite, Kaolinite: Kao, G: Gypsum, Q: Quartz) b) air-dired (AD) oriented clay fraction (I: Illite, K: Kaolinite), ethylene-glycolated (EG) clay fraction (I: Illite, K: Kaolinite), heated clay fraction at 300 °C (I: Illite, K: Kaolinite), heated clay fraction at 550 °C (I:Illite). At 550 °C crystal structure of kaolinite collapses, thus it becomes an amourphous material.

a)



b)

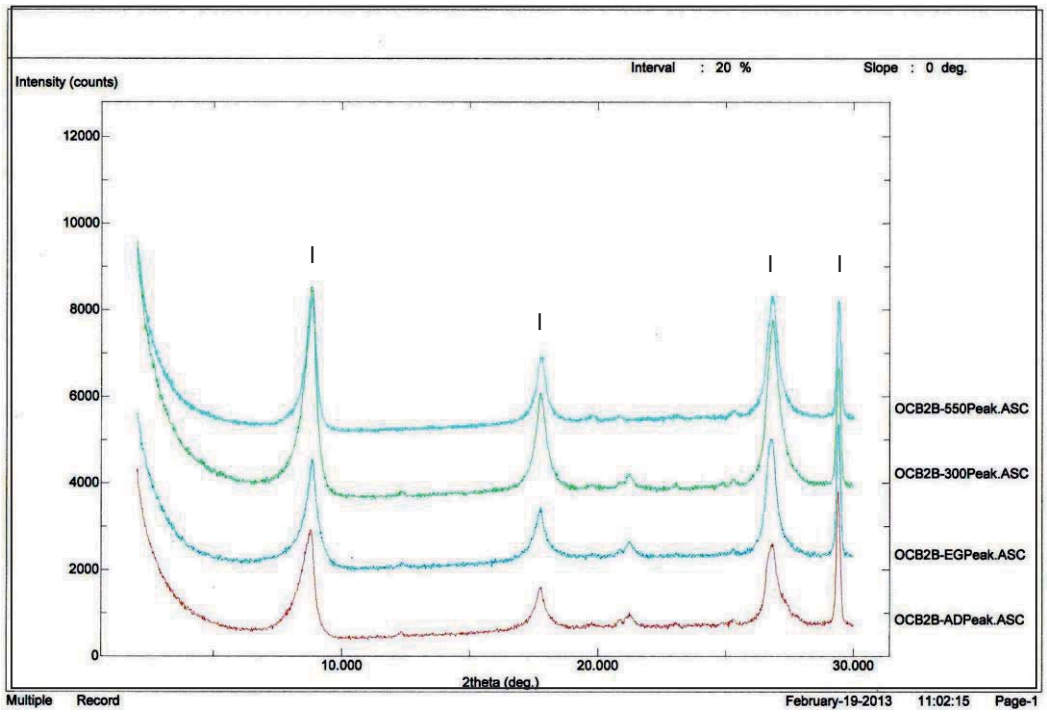


Figure 3.3. The clay and non-clay mineral assemblage of OCB-2B sample. a) unoriented powders of whole rock (I: Illite, Q: Quartz, Cal: Calcite, D: Dolomite) b) air-dired (AD) oriented clay fraction (I: Illite), ethylene-glycolated (EG) clay fraction (I: Illite), heated clay fraction at 300 °C (I: Illite), heated clay fraction at 550 °C (I:Illite).

3.2.2. Yılanlı Burnu Quarry K-bentonites

Yılanlı Burnu quarry samples present illite-rich clay mineralogies on the basis of XRD analyses. The non-clay minerals in unoriented slide of sample YB1 are quartz, feldspar and dolomite. And, illite is found in the oriented slides as the main clay mineral (Figure 3.4). In clay mineral assamblage of sample YBA5, kaolinite is present with higher amounts of illite (Figure 3.5). In sample YBA-19A, the clay mineral assamblage is composed of illite (Figure 3.6).

On the basis of XRD analysis, K-bentonites reveal an illite-rich mineralogical composition. However, they might contain kaolinite in some samples and some mixed-layer I/S. The presence of kaolinite can be represented by chemical weathering of feldspars within K-bentonites (tephras). Higher amounts of illite in K-bentonites could be explained by progressive smectite to illite transformation process during burial diagenesis (Histon et al., 2007).

a)

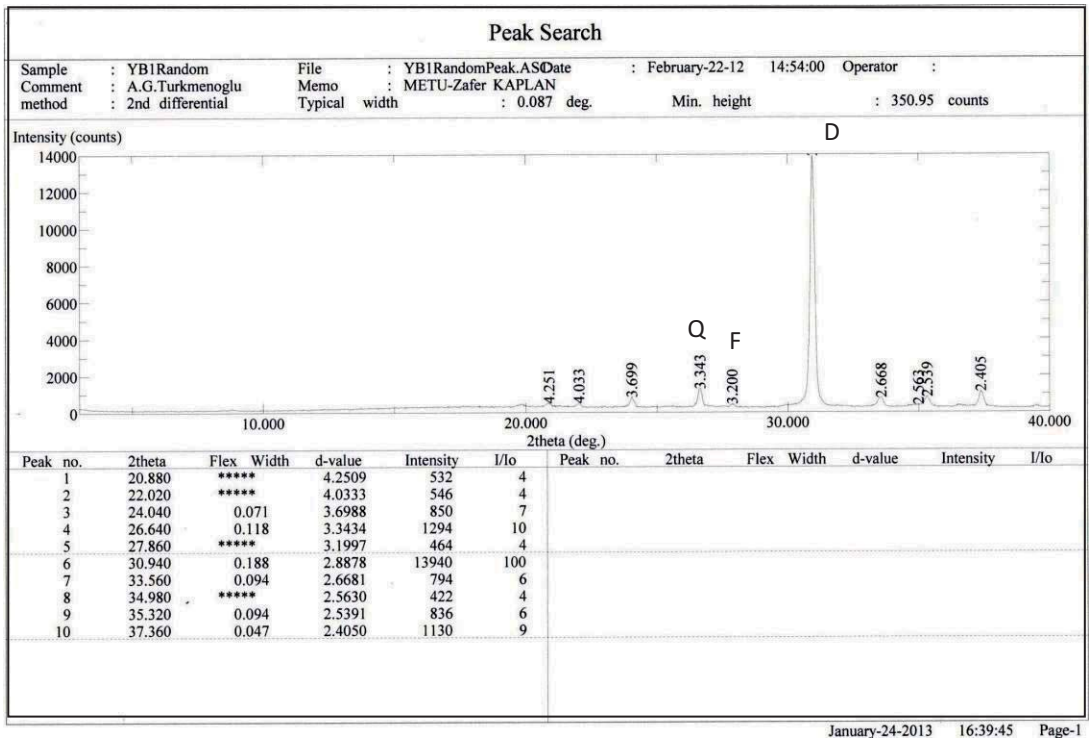


Figure 3.4. XRD pattern of YB1 K-bentonite. a) unoriented powders of whole rock (Q: Quartz, F: Feldspar, D: Dolomite, b) air-dired (AD) oriented clay fraction (I: Illite, I/S: Mixed-Layer Illite Smectite), ethylene-glycolated (EG) clay fraction (I: Illite), heated clay fraction at 300 °C (I: Illite), heated clay fraction at 550 °C (I:Illite).

b)

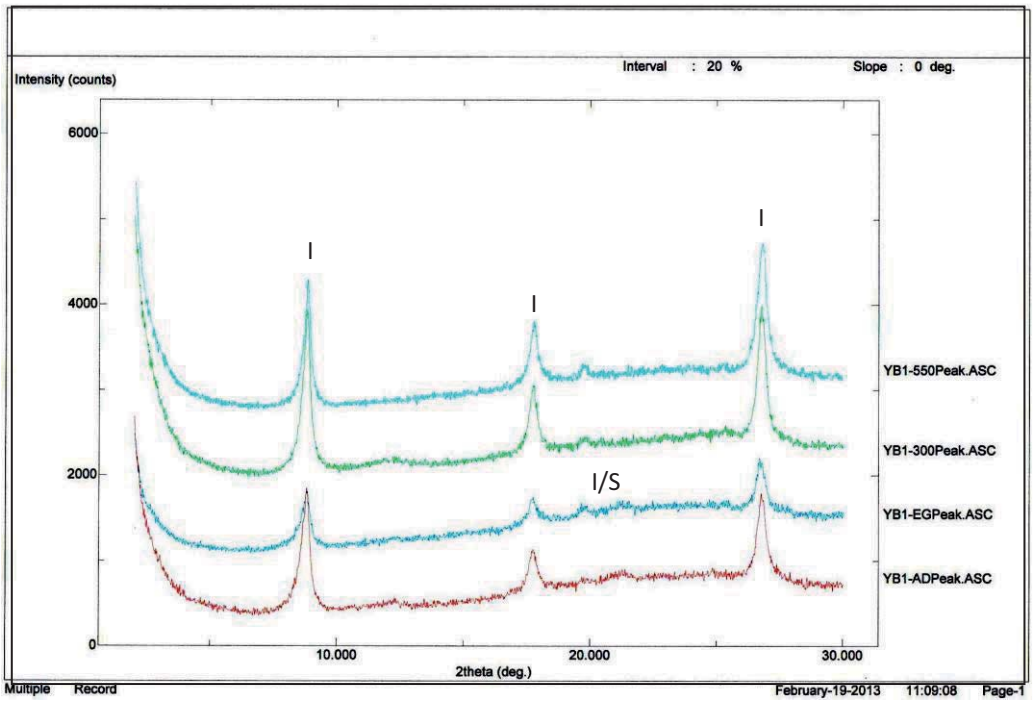


Figure 3.4. XRD pattern of YB1 K-bentonite. a) unoriented powders of whole rock (Q: Quartz, F: Feldspar, D: Dolomite, b) air-dired (AD) oriented clay fraction (I: Illite, I/S: Mixed-Layer Illite Smectite), ethylene-glycolated (EG) clay fraction (I: Illite), heated clay fraction at 300 °C (I: Illite), heated clay fraction at 550 °C (I:Illite) (continued).

a)

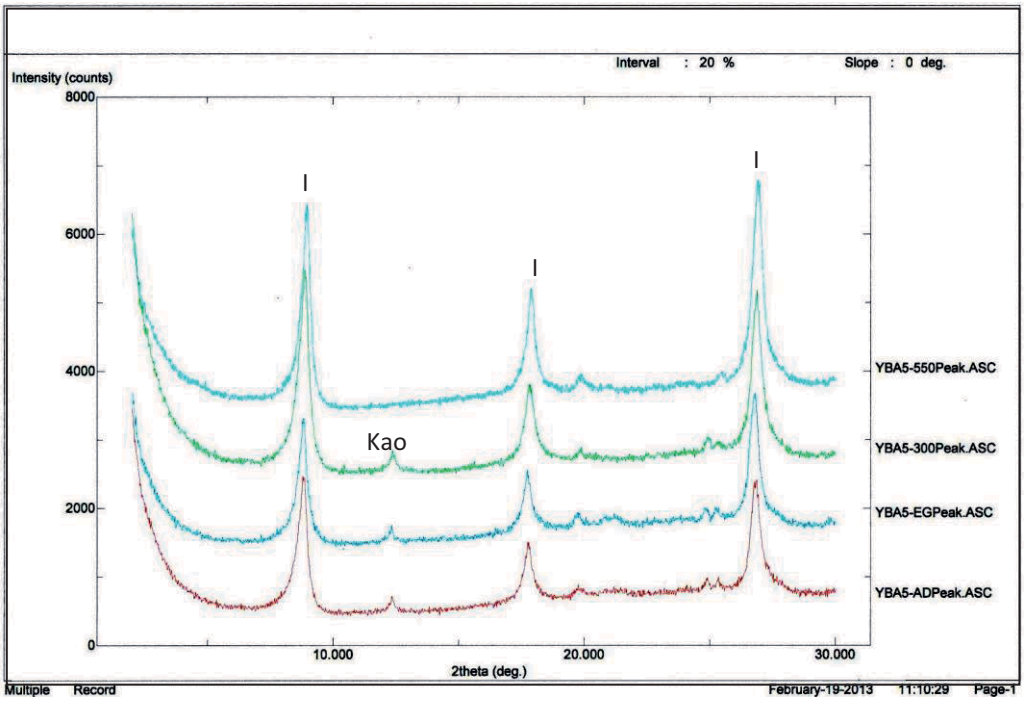


Figure 3.5. XRD pattern of YBA5 K-bentonite. a) air-dired (AD) oriented clay fraction (I: Illite), ethylene-glycolated (EG) clay fraction (I: Illite, K:Kaolinite), heated clay fraction at 300 °C (I: Illite, K:Kaolinite), heated clay fraction at 550 °C (I:Illite).

a)

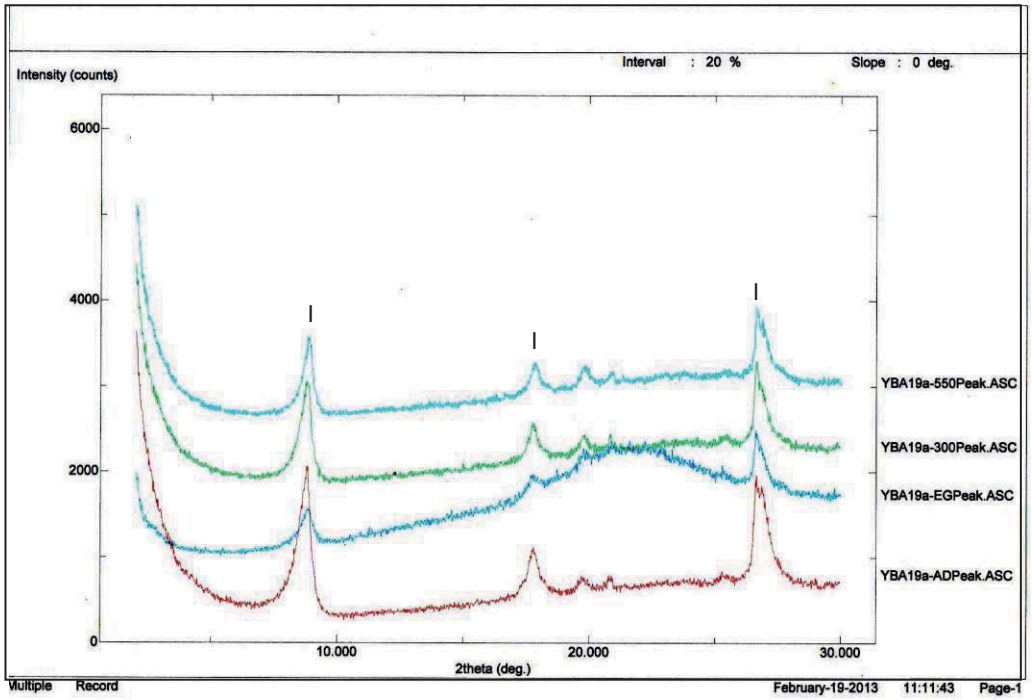


Figure 3.6. XRD pattern of YBA-19A K-bentonite. a) air-dired (AD) oriented clay fraction (I: Illite), ethylene-glycolated (EG) clay fraction (I: Illite), heated clay fraction at 300 °C (I: Illite), heated clay fraction at 550 °C (I:Illite).

3.3. Illite Crystallinity

Illite crystallinity is controlled by the parameters such as disorder in crystal structure, crystal thickness, crystal size, expandable mineral presence, precurser volcanic glass composition (Altaner and Ylagan 1997) and stage of diagenesis during illitization (cited in Whittington, 2010). In order to determine the crystallinity degree of illites KI and Ir of the studied K-bentonites, and from the Gavurpınarı and Yılanlı quarries were presented (Table1 and Table 2). The (060) reflections and also $(I_{002})/(I_{001})$ ratios of illites were used for Mg+Fe content determinations. $2M_1$, $1M$ and $1M_d$ polytype ratios (% $2M_1/(2M_1+1M_d)$ were obtained using I(2.80) / I(2.58) and I(3.07) / I(2.58) peak area ratios (Grathoff and Moore, 1996). The illite ratios of I/S mixed-layers were calculated based on "% illite = 183.41 x ln (Δ°2θ) - 297.48 (R2=0.9896)" equation (Moore and Reynolds, 1997).

3.3.1. Gavurpınarı Quarry K-bentonites

KI values of illites range from 0.69 to 0.77 (an average of 0.72 Δ°2θ) for Gavurpınarı quarry K-bentonites. The Ir changes between 1.26-1.53 (an average of 1.42). Illite polytype ratios ($2M_1/(2M_1+1M_d$%)) range between 25-45% (an average of 37%). Based on (060) reflections (1.49-1.50Å) and also $(I_{002})/(I_{001})$ ratios (0.38-0.40), the calculated Mg/Fe contents of K-bentonites are between 0.27-0.36 (an average of 0.3) for the Gavurpınarı quarry samples. The calculated b-cell dimensions (b_0) of Gavurpınarı K-bentonites range between 8.9946-9.0090. Comparison of the d-spacings for the (Ir = $I(001/003)_{random}$ / $I(001)/(003)_{glycolated}$) illite peaks suggests at most 5% expandability (Table 1).

Table 1. The Crystal-Chemical Characteristics of Representative K-Bentonite Samples From Gavurpınarı Quarry.

Sample No	KI Δ°2θ	I_{002}/I_{001}	Ir*	d_{060} Å	b_0	$1M_d$	$2M_1$	Mg/Fe
Gavurpınarı Quarry K-bentonites								
OCB2-B	0.77	0.40	1.48	1.4991	8.9946	75	25	0.27
OCB2-A	0.69	0.38	1.26	1.5000	8.9990	60	40	0.27
OCB1-S	0.69	0.38	1.53	1.5015	9.0090	55	45	0.36

* $[(I_{003}/I_{001})$air-dried$/(I_{003}/I_{001})$glycol-saturated]

3.3.2. Yılanlı Burnu Quarry K-bentonites

KI values of Yılanlı Burnu illites range between 0.47 and 0.93 (an average of 0.71 Δ°2θ). The Ir values are between 1.13-2.21 (an average of 1.47). Illite polytype ratios ($2M_1/(2M_1+1M_d\%)$) change between 20-50% (an average of 36%). Based on (060) reflections (1.49-1.50Å) and also $(I_{002})/(I_{001})$ ratios (0.32-0.48), the calculated Mg/Fe contents of K-bentonites are ranging between 0.10-0.51 (an average of 0.36). The calculated b-cell dimensions (b_0) of Yılanlı Burnu K-bentonites display values ranging between 8.9474-9.0234. And, Yılanlı Burnu K-bentonites reveal a 5% mixed-layer I/S composition similar to those of Gavurpınarı quarry (Table 2).

Table 2. The Crystal-Chemical Characteristics of Representative K-Bentonite Samples From Yılanlı Burnu Quarry.

Sample No	KI Δ°2θ	I_{002}/I_{001}	Ir*	d_{060} Å	b_0	$1M_d$	$2M_1$	Mg/Fe
Yılanlı Burnu Quarry								
YBA-19A	0.69	0.32	2.21	1.5033	9.0198	60	40	0.48
YB-1	0.47	0.37	1.43	1.5013	9.0078	60	40	0.38
YB-2	0.78	0.41	1.13	1.4995	8.9970	80	20	0.30
YBA-10	0.84	0.40	1.38	1.5013	9.0078	55	45	0.38
YBA-8	0.93	0.48	1.44	1.4912	8.9474	80	20	0.10
YBA-5	0.53	0.43	1.20	1.5039	9.0234	50	50	0.51

* $[(I_{003}/I_{001})$air-dried$/(I_{003}/I_{001})$glycol-saturated]

The KI reflects progressive reactions such as the depletion in smectite layers, a decrease in compositional heterogeneity of series members and polytypic transformations during illitization process. Three very low-grade metapelitic zones: high-grade diagenetic zone (KI > 0.42); anchizone (0.42 > KI > 0.25); and epizone (KI < 0.25) can be distinguished by interpretation of KI values values (e.g., Merriman and Frey, 1999). Therefore, KI of both Gavurpınarı (0.69-0.77 with an average of 0.72 Δ°2θ) and Yılanlı Burnu (0.47-0.93 with an average of 0.71 Δ°2θ) present similar values and indicate a high-grade diagenetic zone for that illite formation.

In the comparison with Gavurpınarı quarry illites, the Ir of Yılanlı Burnu illites (1.13-2.21; with an average of 1.47) display an increase. This can be explained by lower diagenetic conditions for Yılanlı Burnu K-bentonites, since a higher Ir value indicate a lower crystallinity degree.

In Figure 3.7., the comparison of KI and Ir of Gavurpınarı and Yılanlı Burnu illites exhibits that the contents (max. 5%) of swelling component (smectite %) and crystallite size values (N=10-20 nm) of illites indicate that those K-bentonites were affected by high-grade diagenetic conditions.

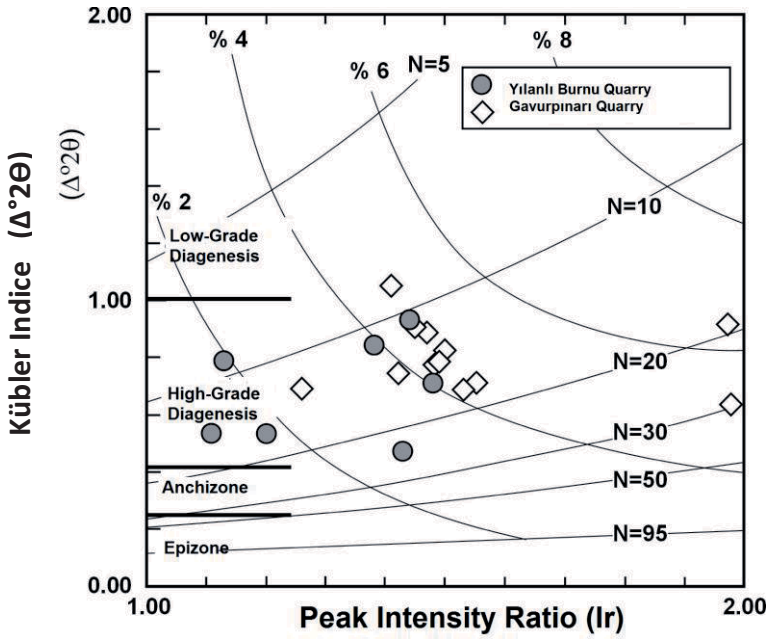


Figure 3.7. The KI versus Ir diagram of illites within K-bentonites collected from Yılanlı Burnu and Gavurpınarı quarries.

The determined polytypes in K-bentonites are $2M_1$ and $1M_d$ (Figure 3.8). Illite polytype ratios ($2M_1/(2M_1+1M_d\%)$) range between 25-45% (an average of 37%) for Gavurpınarı quarry K-bentonites, whereas 20-50% (an average of 36%) for the Yılanlı Burnu quarry samples. In both locations, the polytypes ratios are close to each other. And, this suggests that there is not a significant variation in diagenetic conditions of these two locations.

The polytype distributions of different sized particles (> 2 µm; 2-1 µm; 1-0.5 µm; 0.5-0.25 µm; <0.25 µm) for only two representative K-bentonite samples of OCB-2A (Gavurpınarı quarry) and YBA-19A (Yılanlı Burnu quarry) also examined on the basis of seperation by high-speed (6000 circuit/min.) and cooling controlling centrifuges at Laboratory of Geological Engineering Department, University of Georgia (Athens, Georgia, USA). The data obtained from these two samples present similar results (Figure 3.9). With increasing crystal sizes, 1*M* polytype ratios decrease whereas $2M_1$ polytype ratios increase. This finding indicates a progressive diagenetic maturation and supports interpretations mentioned above.

The asymmetric patterns of illite peaks obtained from oriented fractions suggest different crystallinity degrees of illites WCI (well-crystallized illite), PCI (poorly-crystallized illite) and the presence of I/S (Meunier and Velde 2004). The deconvolution of asymmetric peaks was performed by WINFIT program (by Prof. Dr. Ömer Bozkaya); and the crystallinity degrees of illites were determined such as WCI and PCI, and lesser amounts of I/S (Figure 3.10). Associated with increasing crystal sizes, the PCI and WCI peaks relatively sharpen and become narrower. And, this increase is suitable with a progressive diagenetic process. During diagenesis, the percentage of the mixed-layer I/S sub-population decreases, while the abundance PCI and especially WCI sub-population increases (e.g., Lanson et al., 1998; Bozkaya et al. 2011).

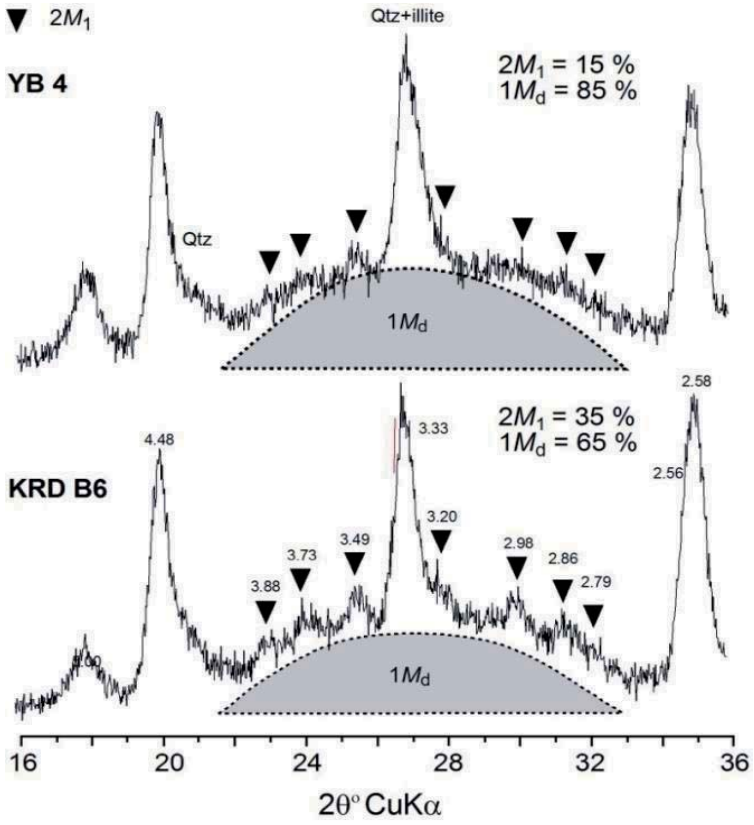


Figure 3.8. Unoriented powder diffraction patterns of the illite polytypes from samples of YB4 (Yılanlı Burnu quarry) and KRDB6 (Gavurpınarı quarry).

The smallest sized clay fraction of illite (<0.25 µm) presents the lowest crystalline representing diagenetic and incipient metamorphism on the basis of Kübler index (Whittington, 2010). And, from (0.25-1 µm) sized clay fractions to the (1-2 µm), the crytallinity degree increases (Figure 3.10) suggesting a progressive diagenetic process. The size increase in clay fraction suggests that the crystallinity of larger-sized clay fraction is greater than the smaller-sized clay fraction. Decrease in relative abundence and peak variabilities suggests that the crystallinity of coarser clay fraction is greater than small clay fraction. By decreasing in grain size, the peak width increases. This variation supports a progressive diagenetic process developed as gradual type.

a)

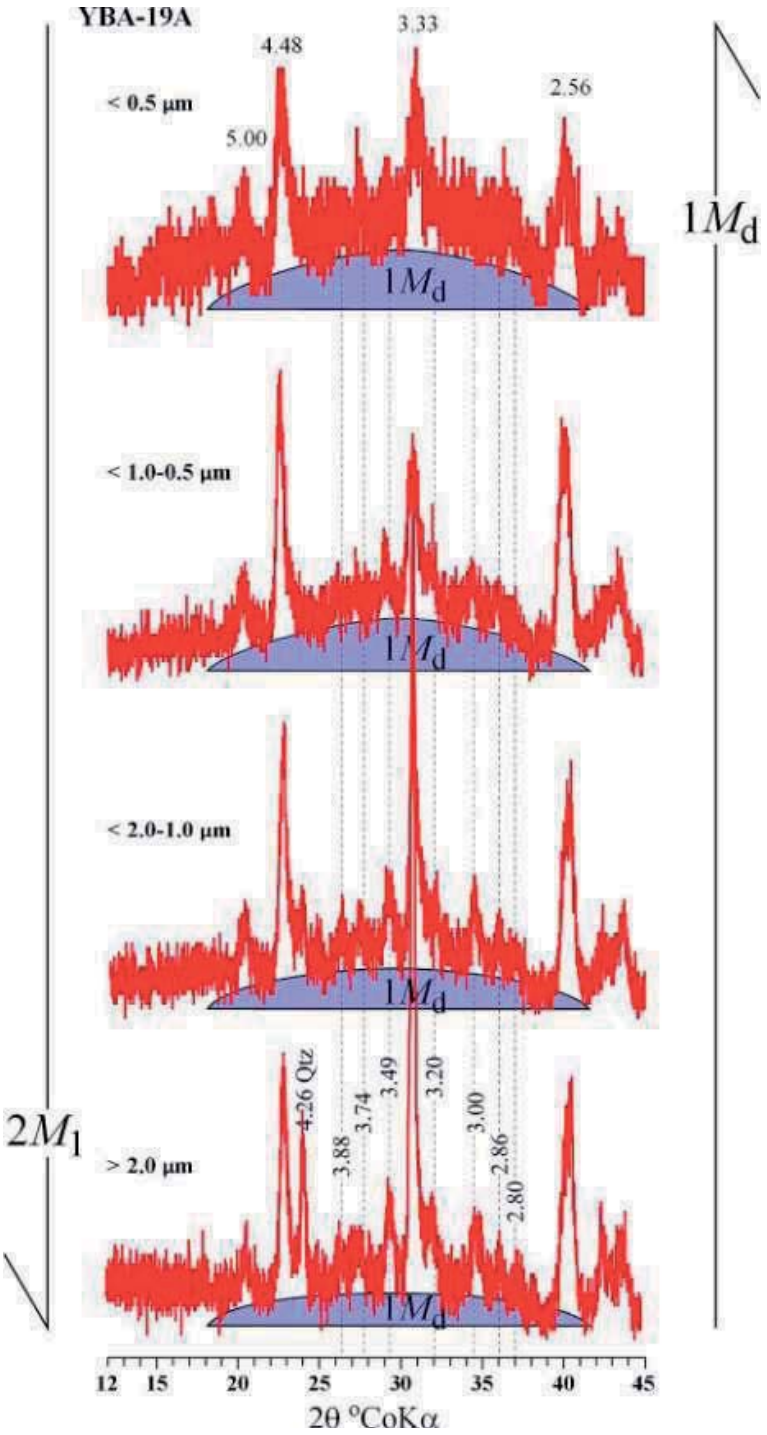


Figure 3.9. Unoriented powder diffraction patterns of the illite polytypes for different sized fractions a) YBA-19A K-bentonite sample from Yılanlı Burnu quarry b) OCB-2A K-bentonite sample from Gavurpınarı quarry.

b)

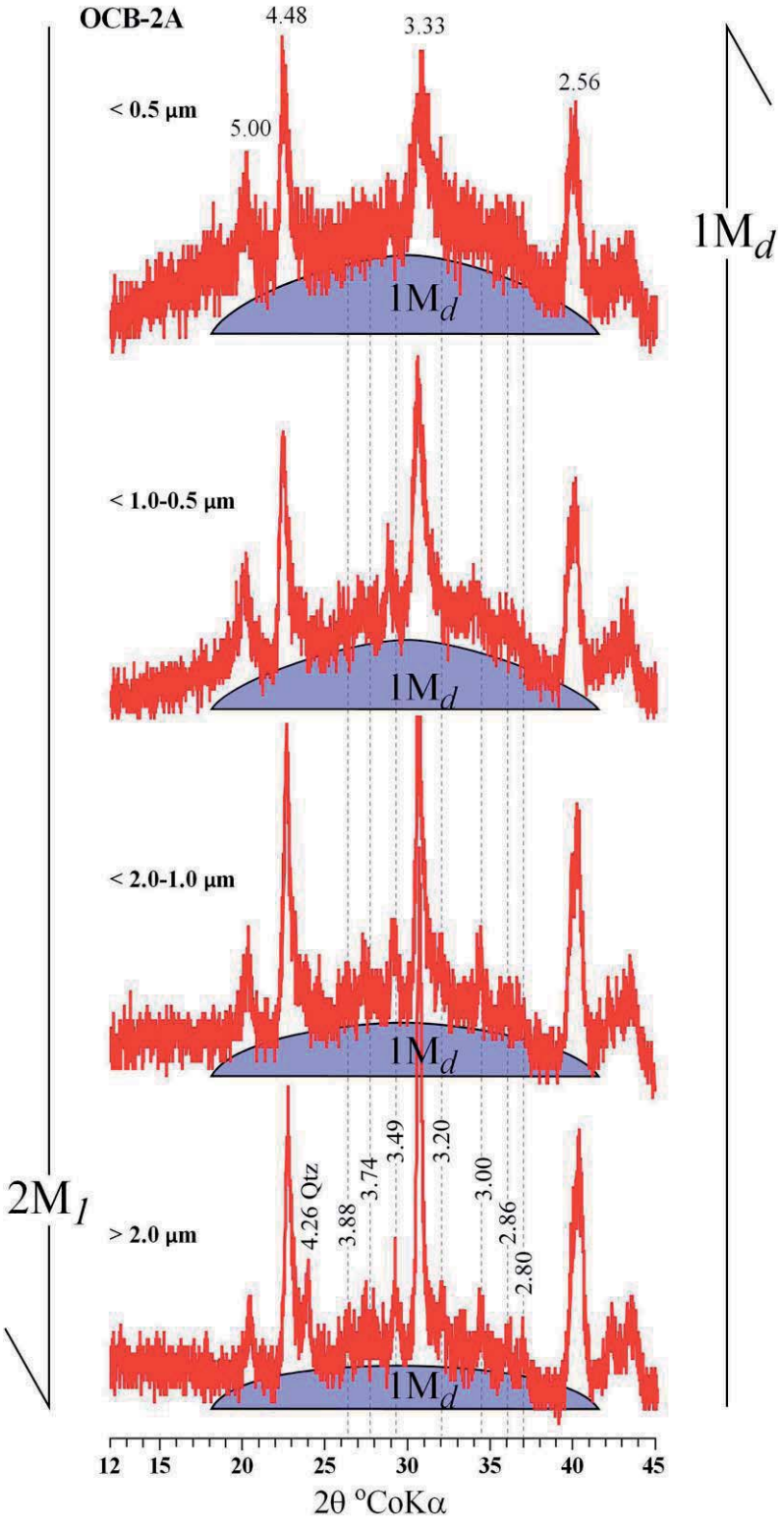


Figure 3.9. Unoriented powder diffraction patterns of the illite polytypes for different sized fractions a) YBA-19A K-bentonite sample from Yılanlı Burnu quarry b) OCB-2A K-bentonite sample from Gavurpınarı quarry (continued).

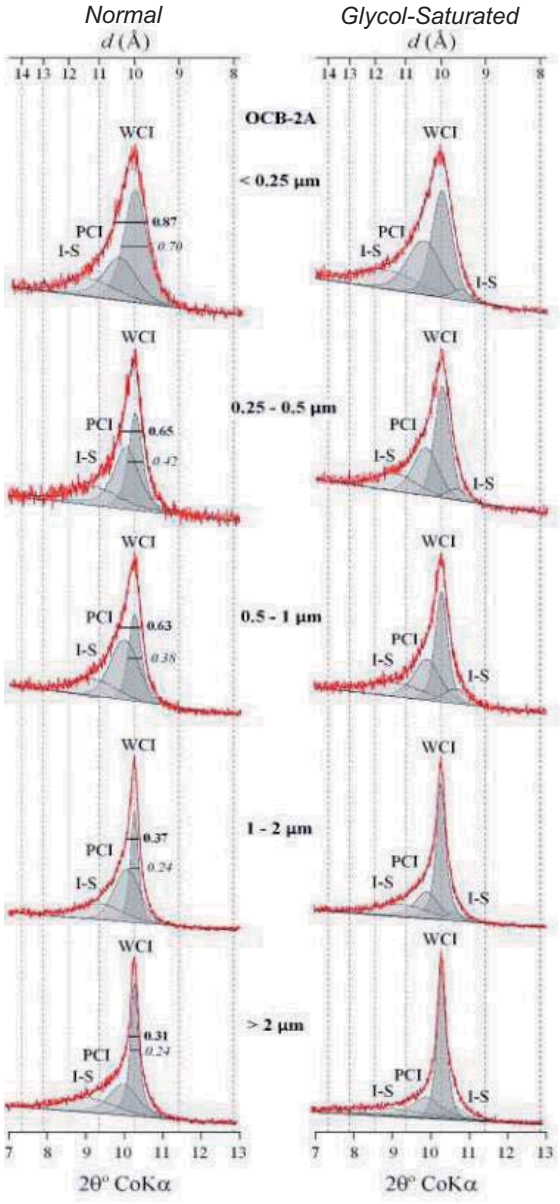
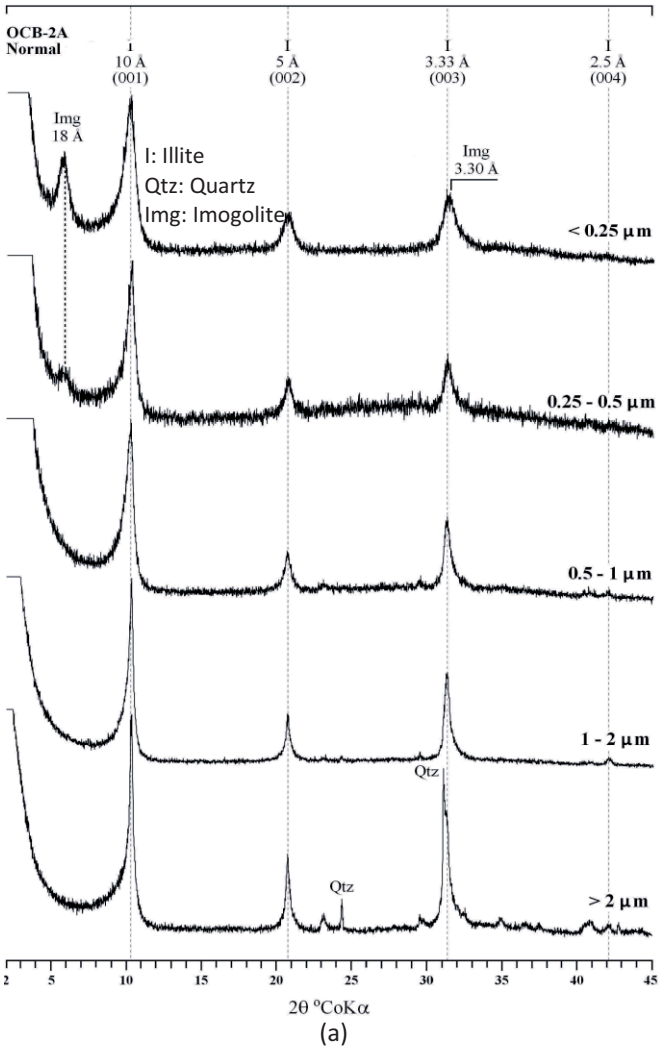


Figure 3.10. The polytype distribution of different sized fractions and variations in peak widths according to the increasing crystal size.

The characteristic peak of 'imogolite' mineral in 0.5-0.25 µm and < 0.25 µm sized clay fractions has been determined (Figure 3.11-3.12). Imogolite is an aluminium-silicate mineral ($Al_2O_3SiOH(OH)_3$) which indicates a volcanic source. The term 'imogo' means "volcanic ash" in Japanese (Yoshinaga and Aomine, 1962; Wada and Yoshinaga, 1969). The characteristic d-spacing of immogolite is at 17-18 Å. The presence of only two peaks near 18 Å and 3.3 Å caused from oriented sample preparation rather than unoriented powder diffraction data. Another result obtained from different particle sizes is that similarity of Yılanlı Burnu and Gavurpınarı quarry illites suggests that these illite occurences are both K-bentonites and have similar origins.

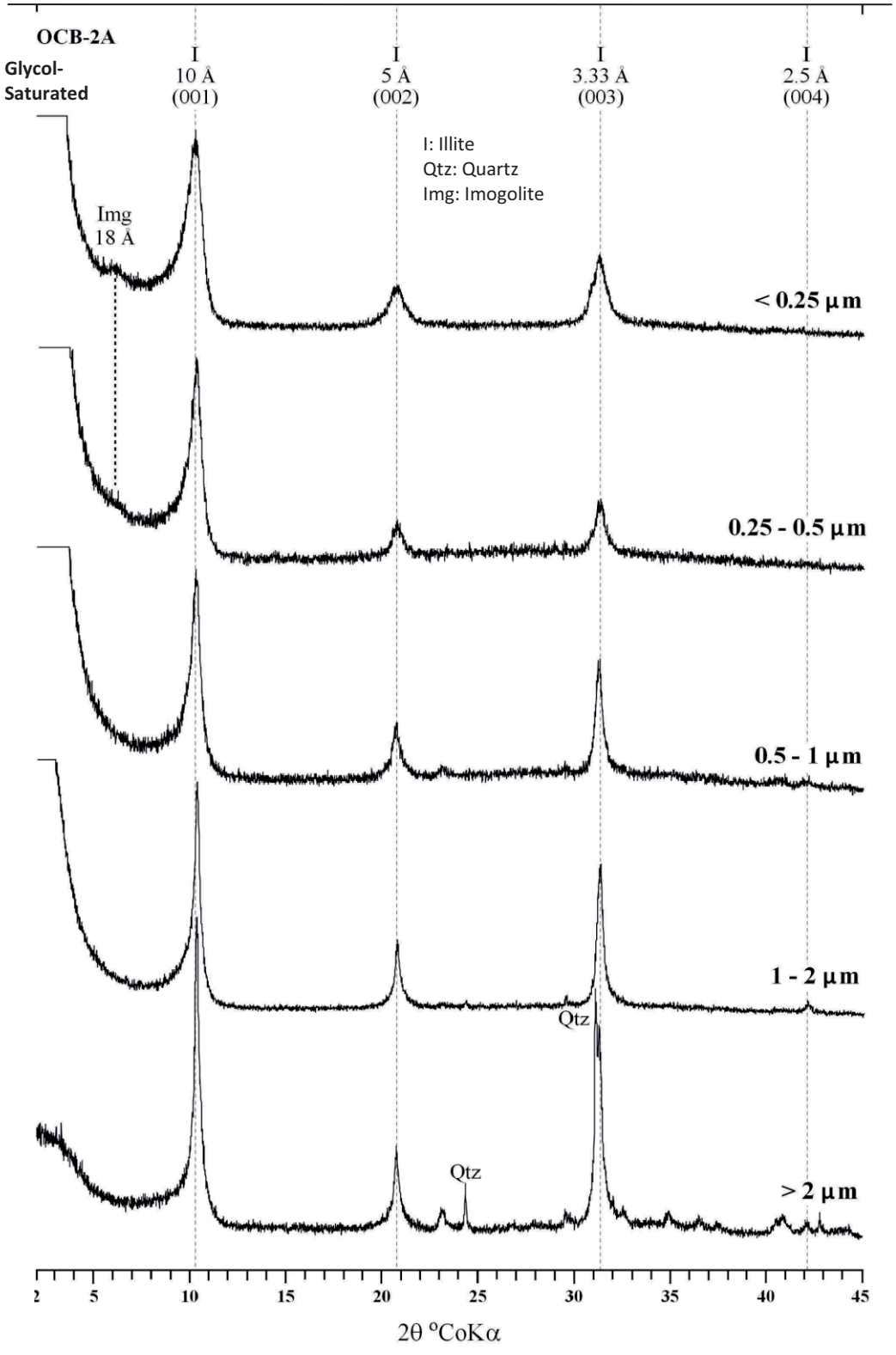
Based on illite (060) reflections data, for Gavurpınarı and Yılanlı Burnu quarry illites, the Mg+Fe contents range respectively between 0.27-0.36 (an average of 0.30) and 0.10-0.51 (an average of 0.36) displaying a dioctahedral composition for illites. The I_{002}/I_{001} results for Yılanlı formation K-bentonites, which are above 0.3, supports a dioctahedral composition. Eventhough it is still contentious, Larsen and Chilingar (1983) stated that the $I_{002(5Å)}/I_{001(10Å)}$ below 0.3 represents a high Fe+Mg content and a trioctahedral illite. And, Esquevin (1969) also stated that when the intensity ratio $I_{002(5Å)}/I_{001(10Å)}$ is above 0.3, indicating a high Al / (Mg + Fe) ratio, the 10 peak width can be used as a reliable indicator of the grade of metamorphism. In the octahedral layers, the substitution of Fe^{2+} and/or Mg^{2+} for Al^{3+} takes place during low-grade metamorphism, thus the relative low abundance of Fe and/or Mg contents of illites indicates a high-grade diagenetic origin for illite (Esquevin, 1969, Gingele, 1996; cited in Whittington, 2010). The illites in the studied K-bentonites are Al-rich suggesting a diagenetic origin which increases the accuracy when used as an indicator of thermal maturation (Esquevin, 1969).

The average of calculated b_0 values of both Gavurpınarı and Yılanlı Burnu illites is about 9,000 Å and represents an evolution process under low to moderate pressure conditions (Sassi & Scolari, 1974; Guidotti & Sassi, 1986).



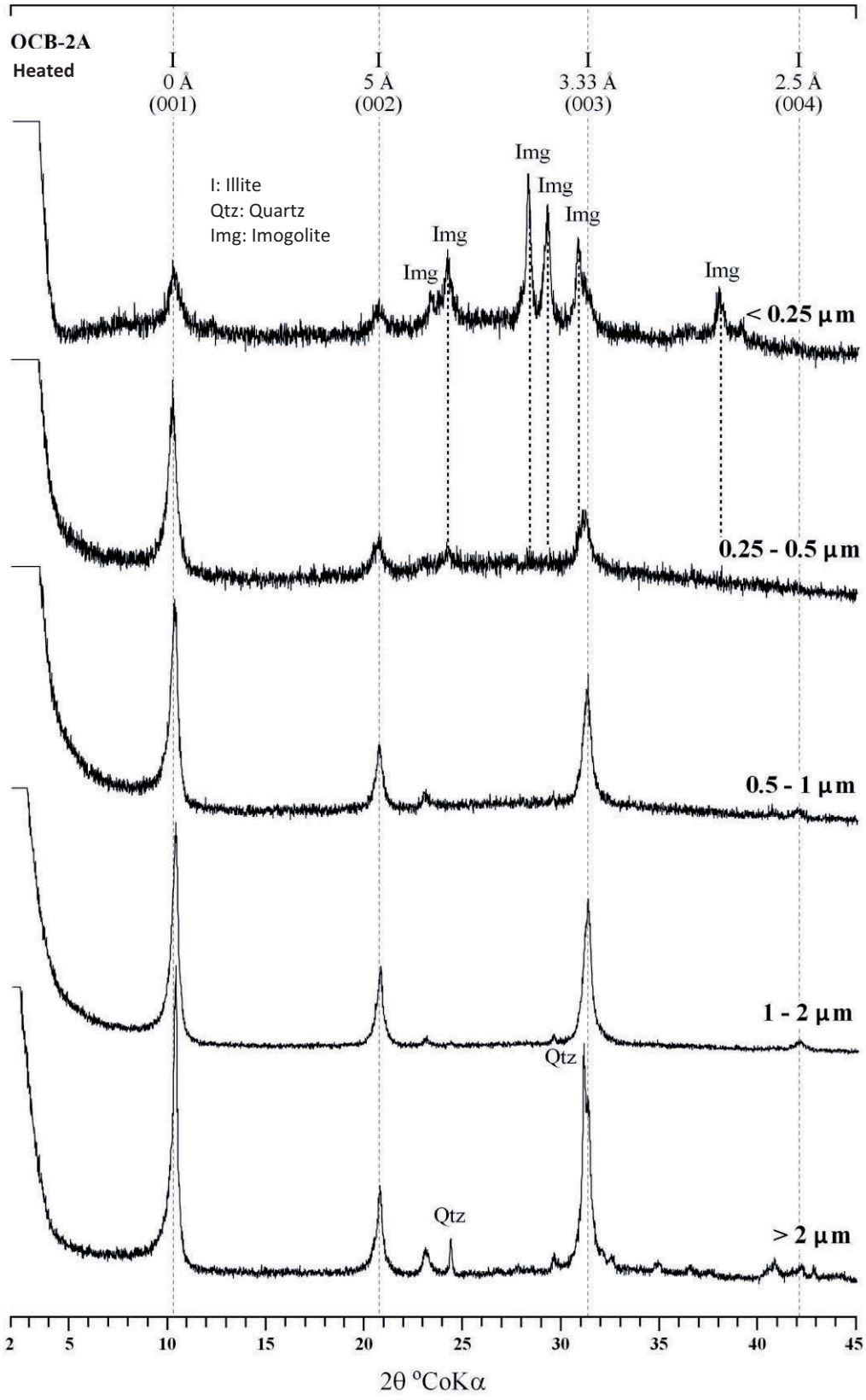
(a)

Figure 3.11. The XRD patterns of oriented different-sized clay fractions of sample OCB-2A a) Normal, b) Ethylene-Glycolated, c) Heated.



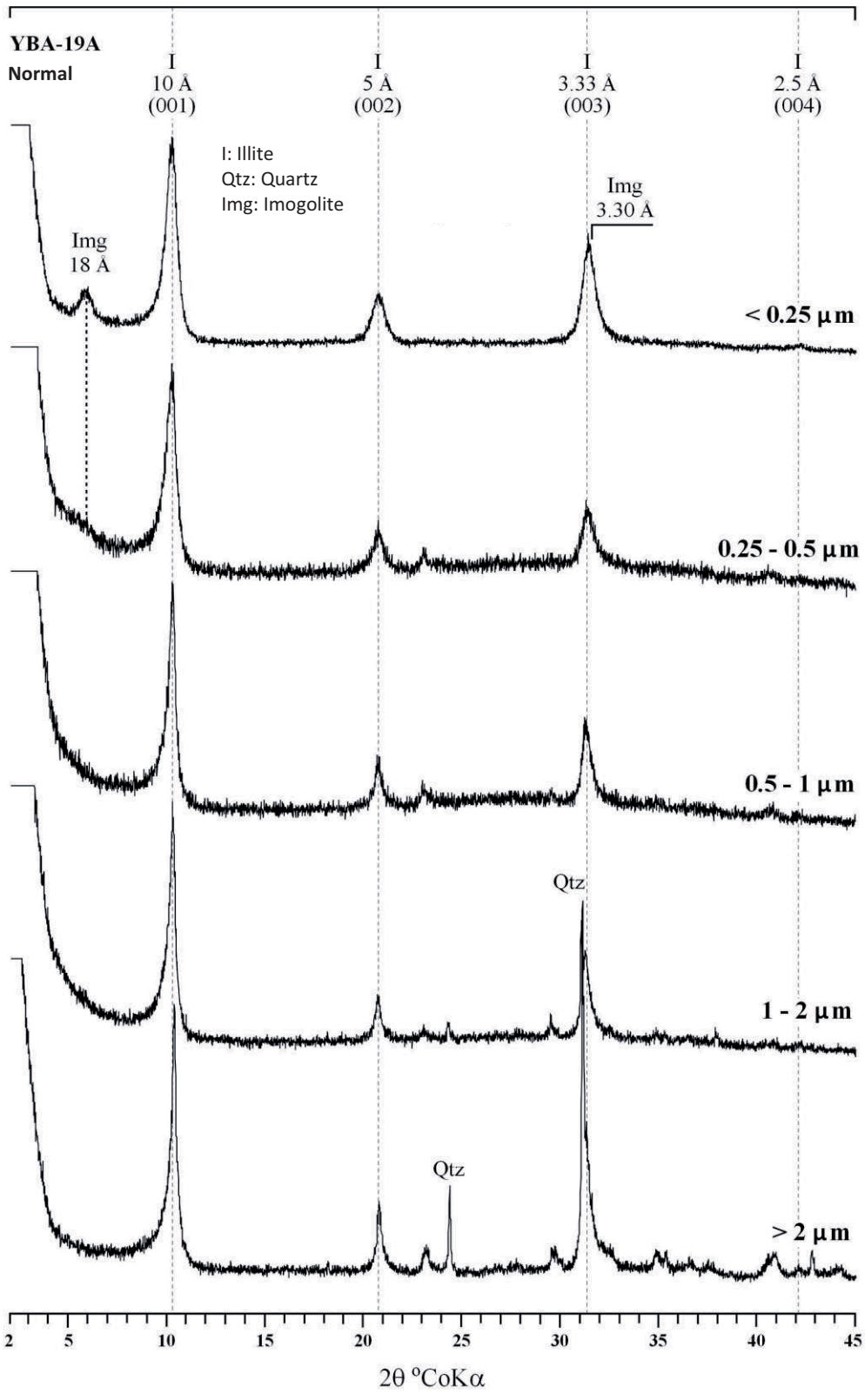
(b)

Figure 3.11. The XRD patterns of oriented different-sized clay fractions of sample OCB-2A a) Normal, b) Ethylene-Glycolated, c) Heated (continued).



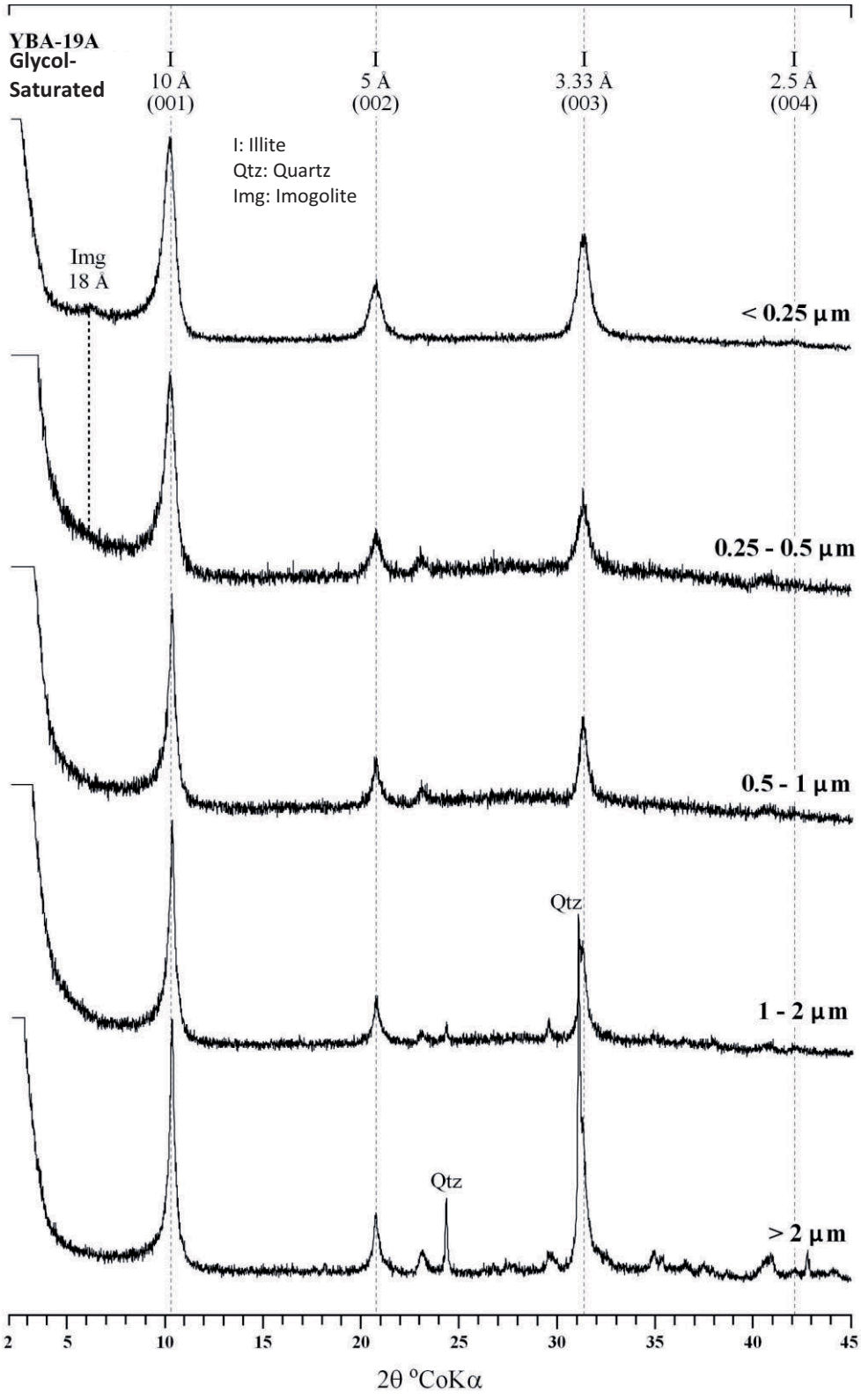
(c)

Figure 3.11. The XRD patterns of oriented different-sized clay fractions of sample OCB-2A a) Normal, b) Ethylene-Glycolated, c) Heated (continued).



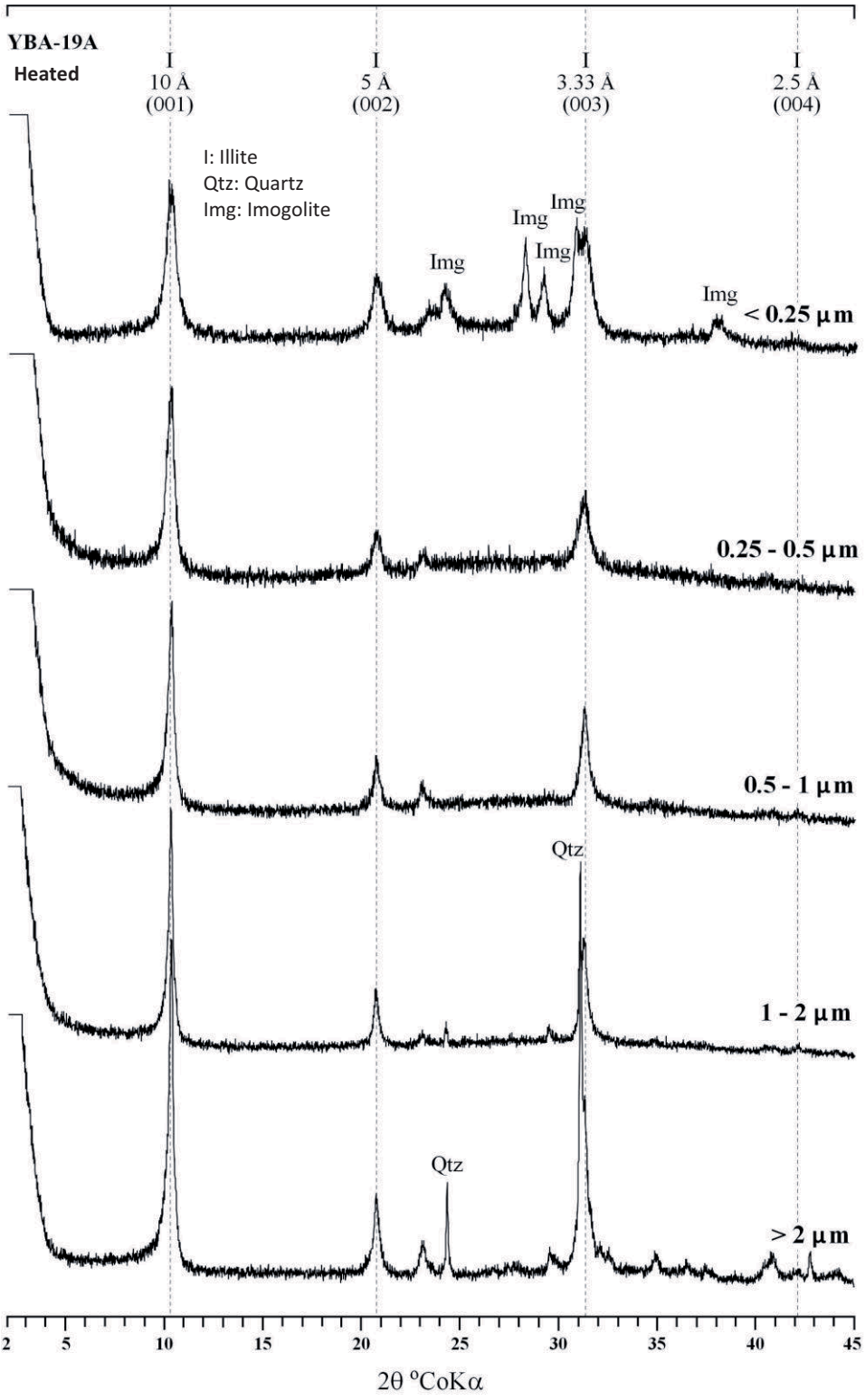
(a)

Figure 3.12. The XRD patterns of oriented different-sized clay fractions of sample YBA-19A a) Normal, b) Ethylene-Glycolated, c) Heated.



(b)

Figure 3.12. The XRD patterns of oriented different-sized clay fractions of sample YBA-19A a) Normal, b) Ethylene-Glycolated, c) Heated (continued).



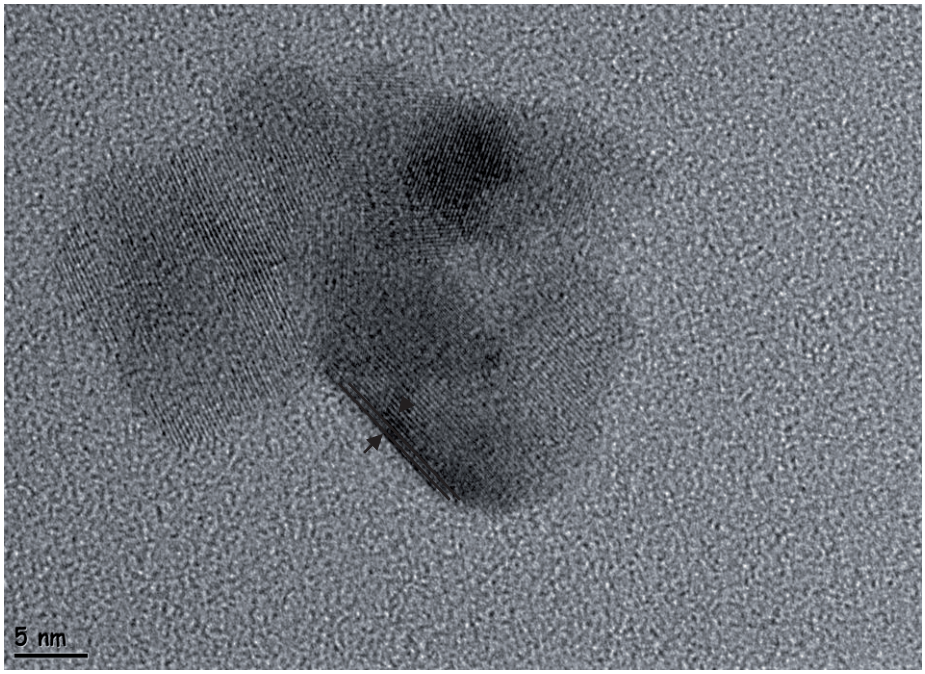
(c)

Figure 3.12. The XRD patterns of oriented different-sized clay fractions of sample YBA-19A a) Normal, b) Ethylene-Glycolated, c) Heated (continued).

3.4. Crystal Structure of Illites Based on HR-TEM Analyses

For two representative and separated < 0.1 µm clay fractions of illite-rich K-bentonite samples from two different locations (OCB-2A from Gavurpınarı quarry and YBA-19A from Yılanlı Burnu quarry), the high-resolution transmission electron microscopy analyses were carried out. On HR-TEM observations (Figure 3.13) regular stacking sequence of illites could be observed. It suggests that the illite mineral can be a long-range ordered (≥R3) mixed-layer illite-smectite on the basis of change from random (R0) to short-range (R1) ordered, and then to long-range (R3) ordered I/S during progressive illitization of smectite (Bethke et al. 1986; Lindgreen and Hansen 1991).

a)



b)

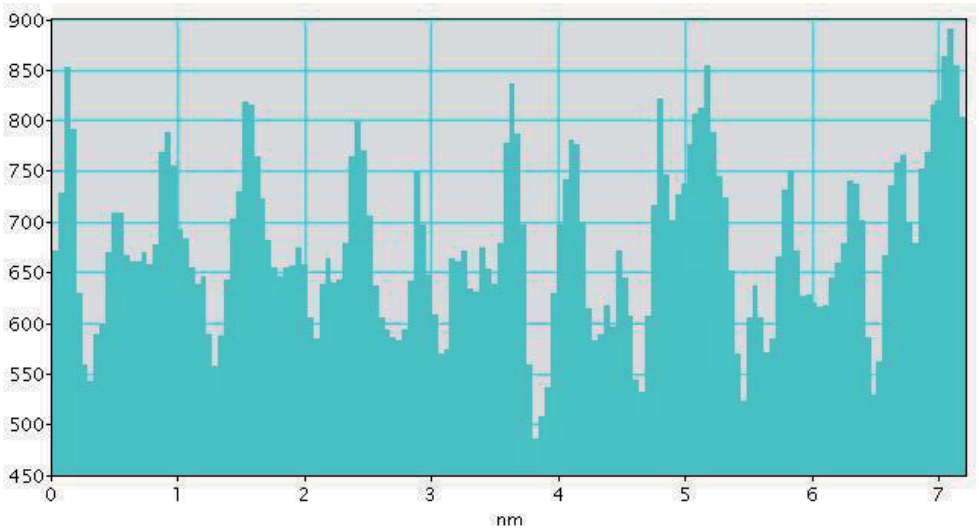


Figure 3.13. a) HR-TEM microphotograph shows regular stacking sequence of illites (10Å) within Sample YBA-19A. b) The profile obtained perpendicularly to atomic planes.

3.5. Micromorphology and Crystal Habit of Illites Based on SEM-EDX Analyses

Representative SEM microphotographs from the Gavurpınarı and Yılanlı Burnu K-bentonites reveal a platy morphology with anhedral flakes which is common in bentonites (Nadaeu et al. 1985; Inoue et al. 1990; Altaner and Ylagan 1997). Illite minerals exhibit the typical platy habit of illite also with curved flakes in some samples (Figure 3.14). By increasing proportion of illite layers in mixed-layer I/S, the morphology of illite changes from sponge-like or cellular to platy or ribbon-like as a result of change in layer stacking from turbostratic (randomly distributed layers in any direction) to rotational ordering of the $1M_d$ type during burial diagenesis. This rotational ordered structure results in a plate- or sheet-like crystal habit by means of a contiguity of quasihexagonal oxygen surfaces from adjacent layers which allows more crystalline regularity in the direction of *a-b* plane (Keller et al. 1986).

OCB-2A and OCB-2B samples display a platy-juxtaposed crystal habit in their SEM microphotographs (Figure 3.14-3.15a). In the SEM examination of sample YBA-19A from Yılanlı Burnu quarry, illite minerals display a morphology of irregular mats of coalesced flakes (Figure 3.17a). The EDX pattern of the sample reveals an illitic composition (Figure 3.17b). Illites in yellow-coloured OCB1G (Figure 3.16a) and gray-coloured OCB-1S (Figure 3.18a) samples reveal a platy morphology. The rhombohedral structure and chemical composition of dolomites in sample YBA-19C is seen in SEM-EDX analyses results (Figure 3.19-3.20). The platy and juxtaposed morphology of illites within sample OC1(B3) K-bentonite can be observed in SEM microphoto (Figure 3.21a); and the EDX data of the same sample is compatible with illite composition (Figure 3.21b). In Figure 3.22, the association of platy illite with quartz and calcite crystals in sample OC1(B3) can be seen.

a)

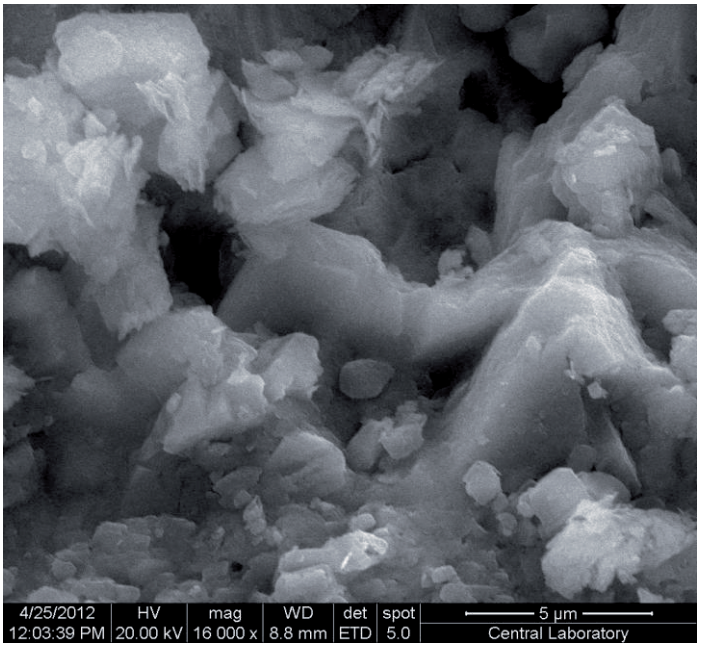


Figure 3.14. a-b) The irregular platy and juxtaposed morphology of illite crystals within the sample OCB-2A from Gavurpınarı quarry.

b)

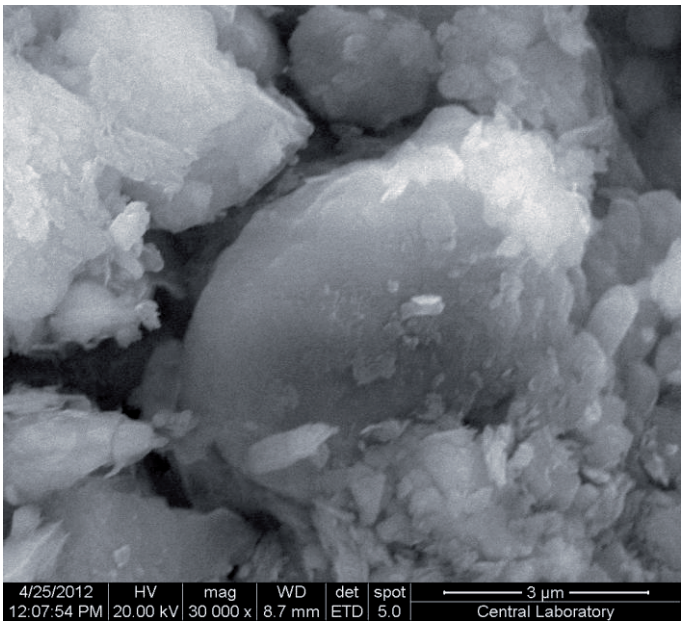


Figure 3.14. a-b) The irregular platy and juxtaposed morphology of illite crystals within the sample OCB-2A from Gavurpınarı quarry (continued).

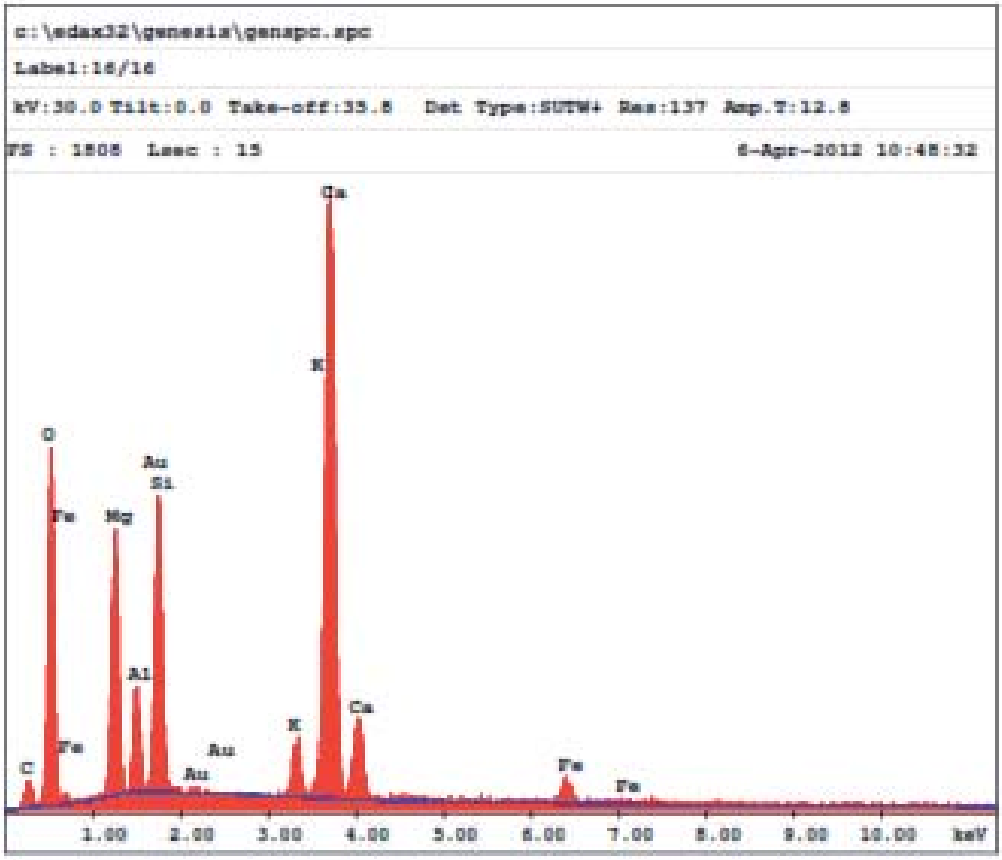
a)



(*The red plot represents the area which was analyzed by SEM-EDX)

Figure 3.15. a) The platy habit of illites with curved flakes and surrounding calcite minerals b) The EDX pattern of sample OCB-2B (carbonate minerals result in a carbonate-rich chemical composition in EDX data).

b)



EDAX ZAF Quantification (Standardless)
Element Normalized
SEC Table : Default

Element	Wt %	At %	K-Ratio	Z	A	F
C K	10.30	16.56	0.0216	1.0335	0.3026	1.0007
O K	47.56	57.38	0.0864	1.0189	0.1781	1.0004
MgK	10.54	8.36	0.0365	0.9823	0.3518	1.0036
AlK	3.91	2.80	0.0145	0.9546	0.3852	1.0049
SiK	8.92	6.13	0.0421	0.9832	0.4786	1.0030
AuM	0.29	0.03	0.0023	0.7795	1.0268	1.0009
K K	1.28	0.63	0.0110	0.9319	0.8596	1.0369
CaK	15.94	7.68	0.1407	0.9536	0.9245	1.0009
FeK	1.25	0.43	0.0108	0.8822	0.9785	1.0004
Total	100.00	100.00				

Figure 3.15. a) The platy habit of illites with curved flakes and surrounding calcite minerals b) The EDX pattern of sample OCB-2B (carbonate minerals result in a carbonate-rich chemical composition in EDX data) (continued).

a)

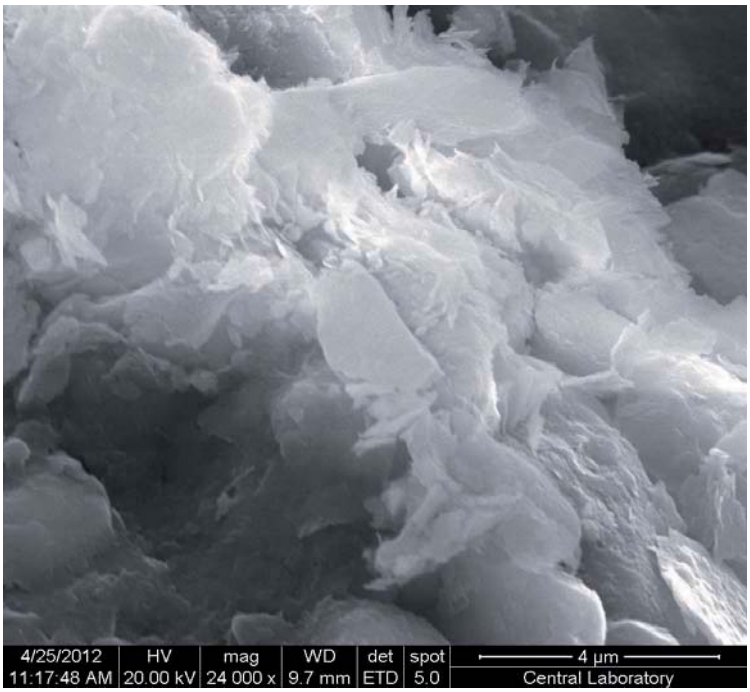


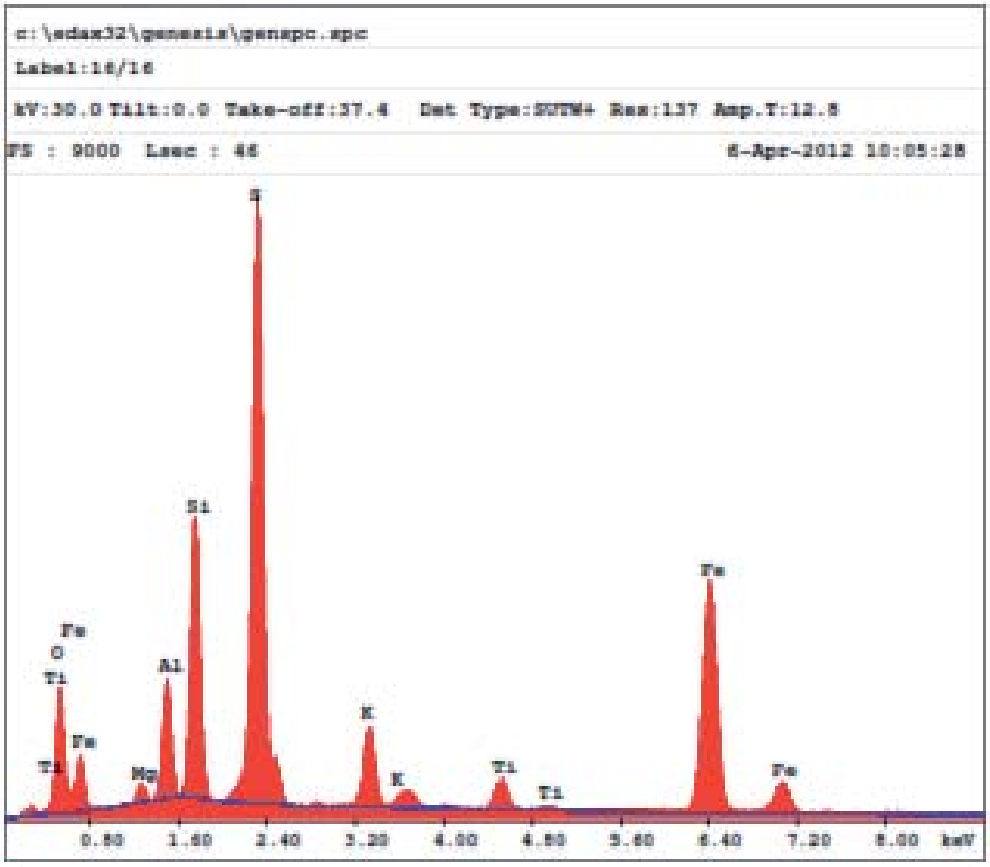
Figure 3.16. Lamellar-platy morphology of illites in the OCB1G sample from Gavurpınarı quarry.

a)



(*The red plot represents the area which was analyzed by SEM-EDX)
Figure 3.17. (a) The platy and coalesced morphology of illites within sample YBA-19A from Yılanlı Burnu quarry (b) The EDX pattern of YBA-19A presents the illitic composition (high S and Fe contents indicate pyritization)

b)



EDAX ZAF Quantification (Standardless)
Element Normalized
SEC Table : Default

Element	Wt %	At %	K-Ratio	Z	A	F
O K	24.80	42.05	0.0477	1.0534	0.1828	1.0009
MgK	1.21	1.35	0.0037	1.0153	0.3011	1.0074
AlK	6.44	6.48	0.0265	0.9864	0.4118	1.0113
SiK	13.45	12.99	0.0664	1.0161	0.4800	1.0114
S K	27.34	23.13	0.1651	1.0096	0.5958	1.0037
K K	4.14	2.87	0.0276	0.9692	0.6809	1.0081
TiK	1.74	0.99	0.0138	0.9091	0.8521	1.0255
FeK	20.87	10.14	0.1836	0.9145	0.9638	1.0000
Total	100.00	100.00				

Figure 3.17. (a) The platy and coalesced morphology of illites within sample YBA-19A from Yılanlı Burnu quarry (b) The EDX pattern of YBA-19A presents the illitic composition (high S and Fe contents indicate pyritization) (continued).

a)

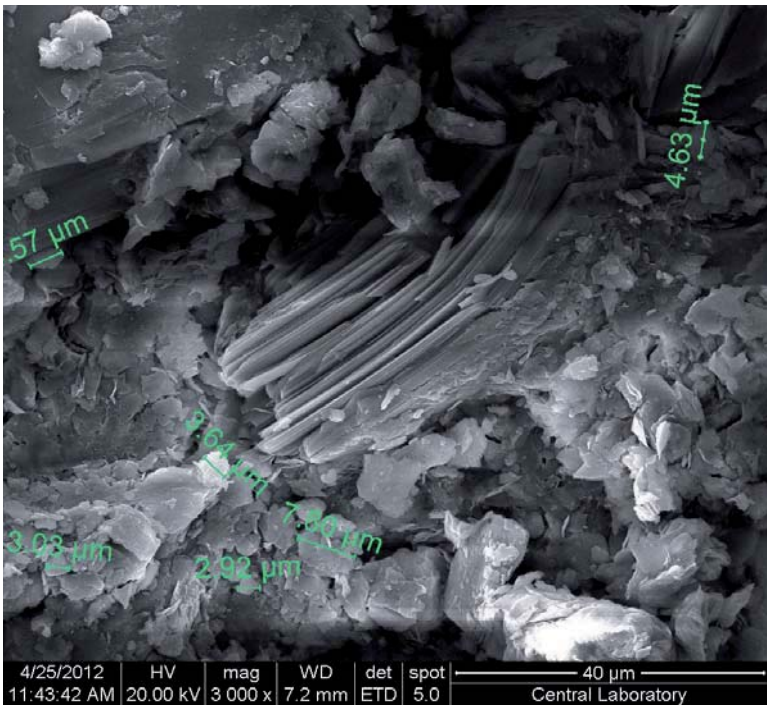
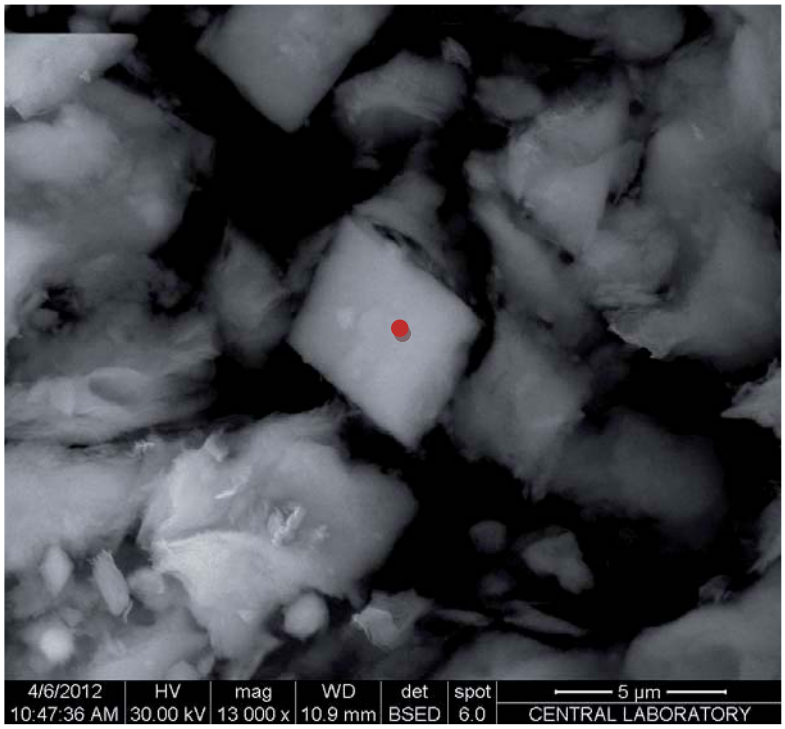


Figure 3.18. Lamellar gypsum crystal seen in OCB1S sample from Gavurpınarı quarry.

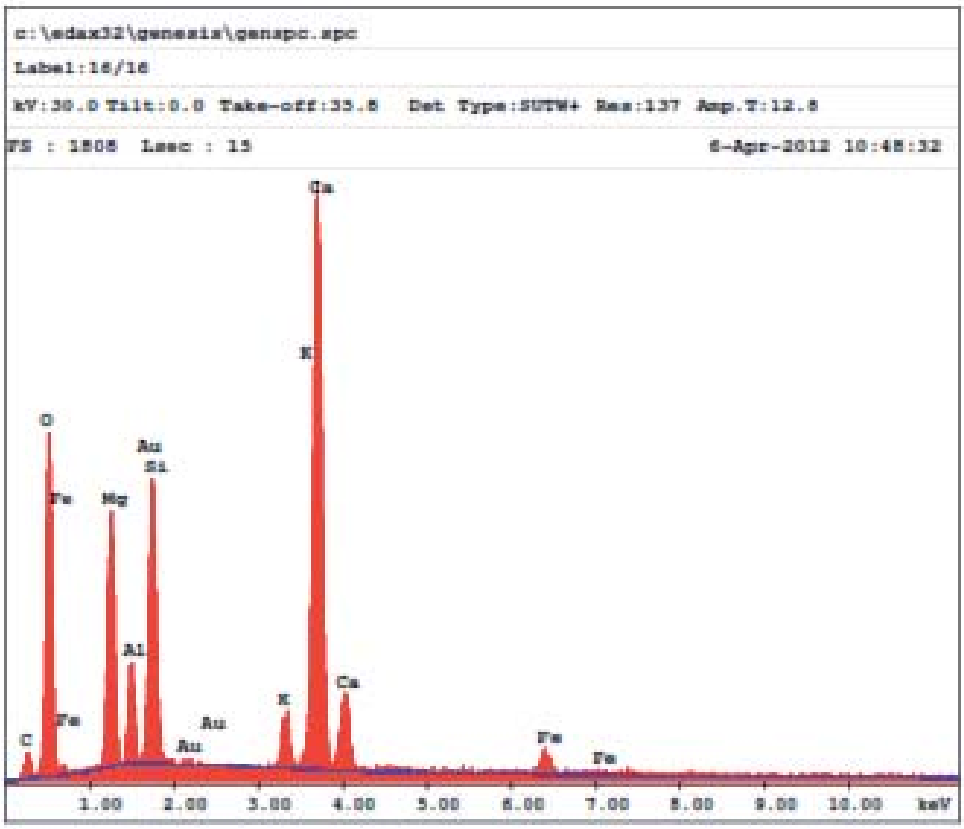
a)



(*The red plot represents the area which was analyzed by SEM-EDX)

Figure 3.19. (a) In SEM microphotograph of sample YBA-19C, rhombohedral dolomite crystals can be seen and (b) The EDX pattern of the sample reveals illite and dolomite composition.

b)



EDAX ZAF Quantification (Standardless)
Element Normalized
SEC Table : Default

Element	Wt %	At %	K-Ratio	Z	A	F
C K	10.30	16.56	0.0216	1.0335	0.2026	1.0007
O K	47.56	57.38	0.0864	1.0169	0.1781	1.0004
MgK	10.54	8.36	0.0365	0.9823	0.3518	1.0038
AlK	3.91	2.80	0.0145	0.9546	0.3852	1.0049
SiK	8.92	6.13	0.0421	0.9832	0.4786	1.0030
AuM	0.29	0.03	0.0023	0.7795	1.0268	1.0009
K K	1.28	0.63	0.0110	0.9319	0.8596	1.0369
CaK	15.94	7.68	0.1407	0.9536	0.9245	1.0009
FeK	1.25	0.43	0.0108	0.8822	0.9785	1.0004
Total	100.00	100.00				

Figure 3.19. (a) In SEM microphotograph of sample YBA-19C, rhombohedral dolomite crystals can be seen and (b) The EDX pattern of the sample reveals illite and dolomite composition (continued).

a)

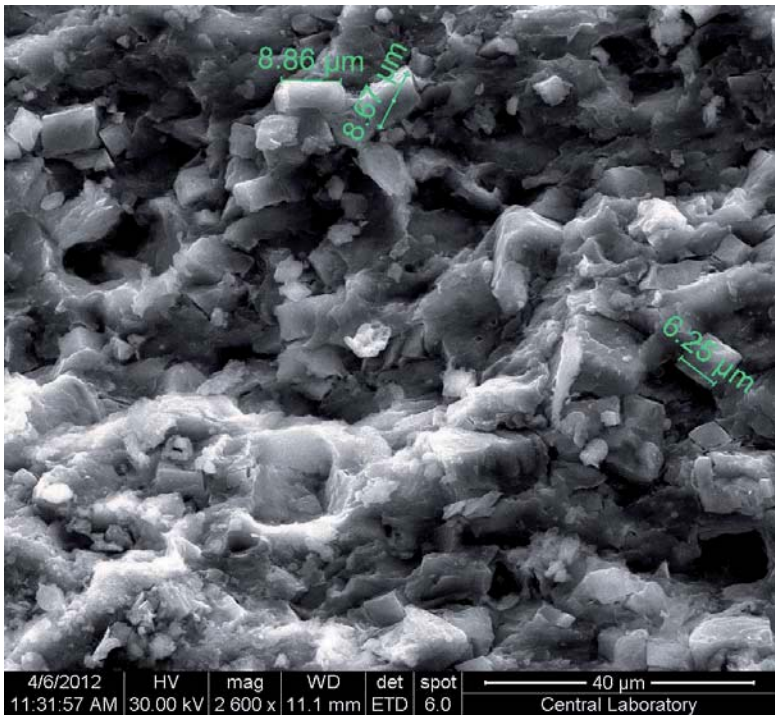


Figure 3.20. The irregular distribution of platy illites and rhombohedral dolomites in sample YBA-19C.

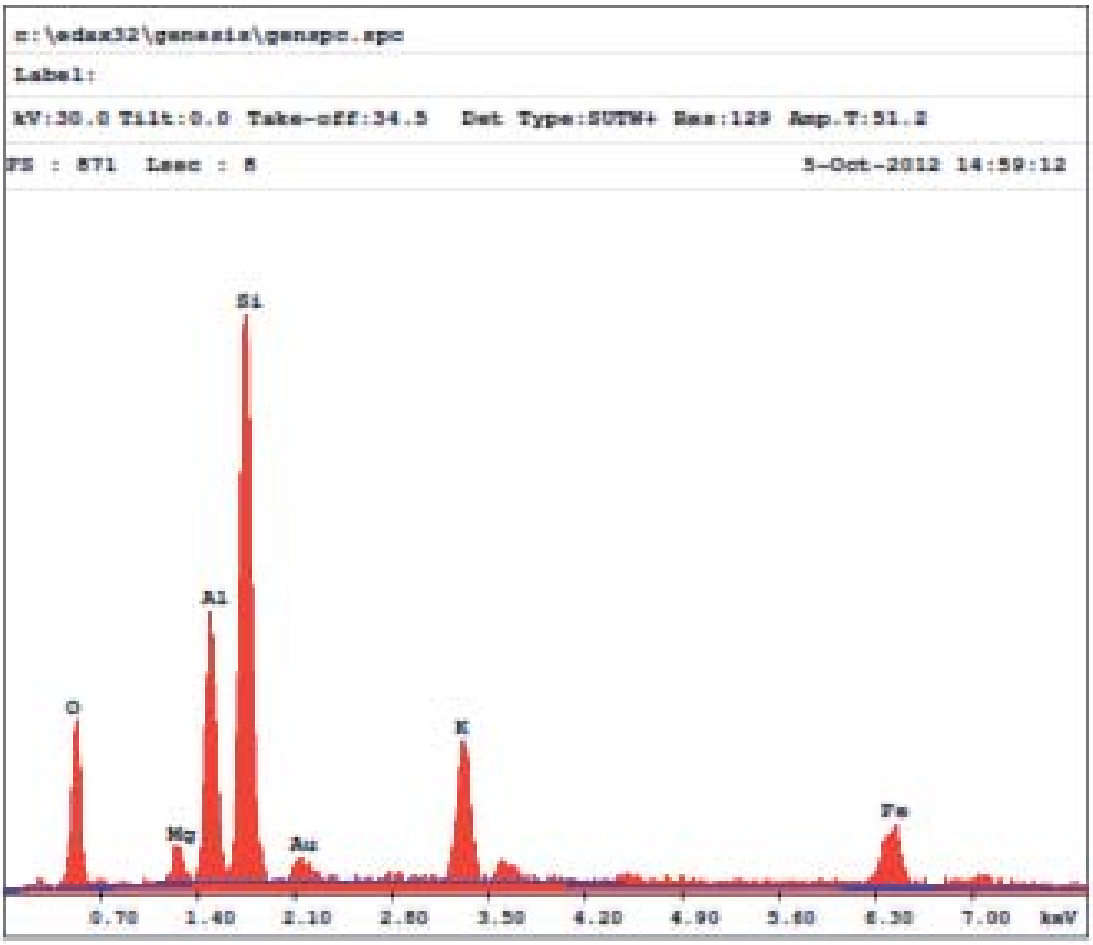
a)



(*The red plot represents the area which was analyzed by SEM-EDX)

Figure 3.21. (a) The SEM microphotograph displays platy and juxtaposed structure of illites and (b) EDX pattern of OC1(B3) sample indicates the illitic composition of the sample.

b)

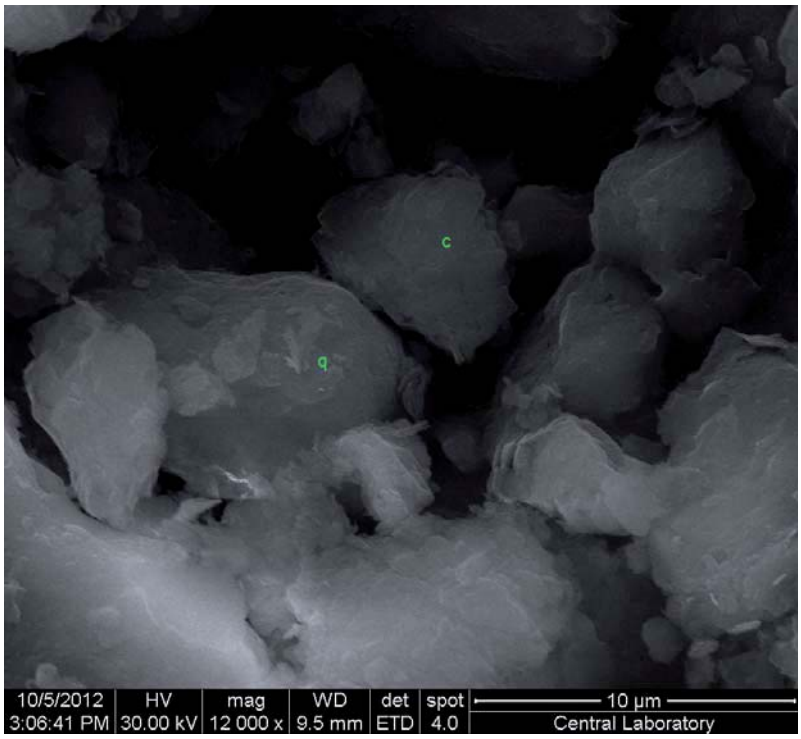


EDAX ZAF Quantification (Standardless)
Element Normalized
SEC Table : Default

Element	Wt %	At %	K-Ratio	Z	A	F
O K	30.79	47.30	0.0645	1.0456	0.2002	1.0007
MgK	2.38	2.41	0.0092	1.0078	0.3767	1.0112
AlK	13.41	12.22	0.0665	0.9792	0.4650	1.0134
SiK	33.50	29.32	0.1573	1.0087	0.4649	1.0014
AuM	5.05	0.63	0.0281	0.7998	0.8958	1.0003
K K	8.38	5.27	0.0558	0.9616	0.8915	1.0021
FeK	6.50	2.86	0.0589	0.9074	0.9601	1.0054
Total	100.00	100.00				

Figure 3.21. (a) The SEM microphotograph displays platy and juxtaposed structure of illites and (b) EDX pattern of OC1(B3) sample indicates the illitic composition of the sample (continued).

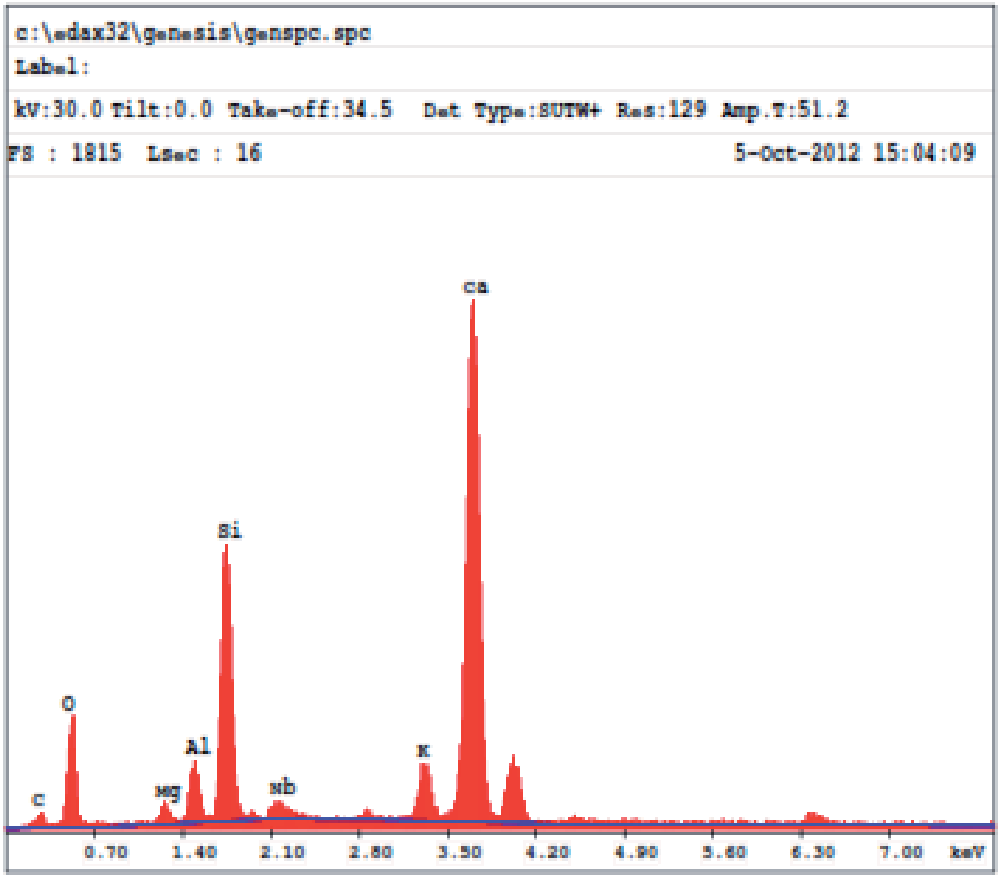
a)



(*The letters c and q represents respectively the analyzed calcite and quartz crystals in sample OC1(B3)).

Figure 3.22. (a) The quartz and calcite crystals surrounded by thin illite flakes in sample OC1(B3) From Gavurpınarı quarry and (b) The EDX pattern of calcite and (c) quartz minerals in sample OC1(B3).

b)

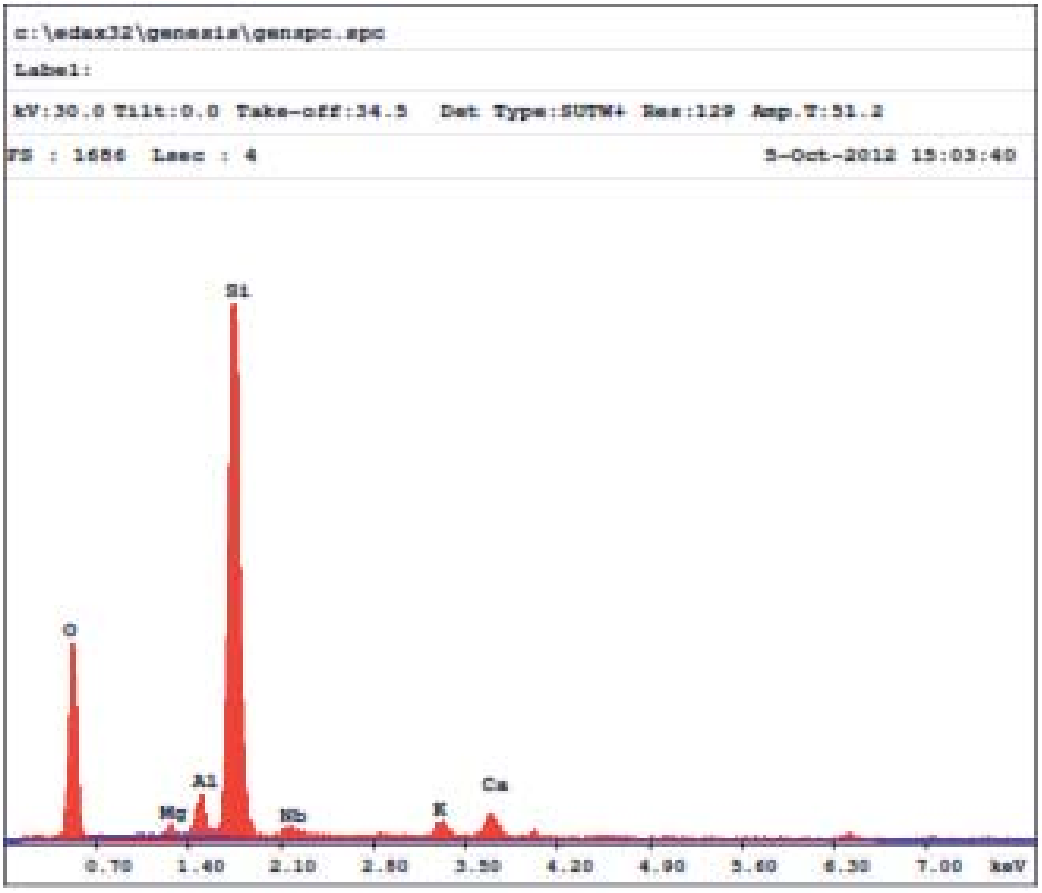


EDAX ZAF Quantification (Standardless)
Element Normalized
Spc Table : Default

Element	Wt %	At %	K-Ratio	Z	A	F
C K	10.08	17.93	0.0208	1.0409	0.1986	1.0006
O K	37.45	50.03	0.0478	1.0262	0.1243	1.0003
MgK	1.49	1.31	0.0050	0.9892	0.3349	1.0058
AlK	3.38	2.67	0.0148	0.9611	0.4532	1.0094
SiK	14.22	10.82	0.0784	0.9901	0.5532	1.0061
NbL	1.96	0.45	0.0140	0.8432	0.8345	1.0121
K K	2.53	1.38	0.0220	0.9409	0.8702	1.0598
CaK	28.89	15.40	0.2495	0.9627	0.8972	1.0000
Total	100.00	100.00				

Figure 3.22. (a) The quartz and calcite crystals surrounded by thin illite flakes in sample OC1(B3) From Gavurpınarı quarry and (b) The EDX pattern of calcite and (c) quartz minerals in sample OC1(B3) (continued).

c)



EDAX ZAF Quantification (Standardless)
Element Normalised
SEC Table : Default

Element	Wt %	At %	K-Ratio	Z	A	F
O K	50.45	65.51	0.1264	1.0329	0.2409	1.0005
MgK	0.94	0.80	0.0036	0.9561	0.3856	1.0115
AlK	3.16	2.44	0.0161	0.9582	0.5198	1.0198
SiK	38.63	28.58	0.2362	0.9671	0.6183	1.0015
NbL	2.98	0.67	0.0151	0.8406	0.8029	1.0012
K K	1.47	0.78	0.0103	0.9362	0.7407	1.0036
CaK	2.36	1.22	0.0181	0.9581	0.8014	1.0000
Total	100.00	100.00				

Figure 3.22. (a) The quartz and calcite crystals surrounded by thin illite flakes in sample OC1(B3) From Gavurpınarı quarry and (b) The EDX pattern of calcite and (c) quartz minerals in sample OC1(B3) (continued).

CHAPTER 4

GEOCHEMICAL CHARACTERISTICS OF K-BENTONITES

4.1. Introduction

14 representative whole rock K-bentonite samples with some carbonate rocks from two different localities (Gavurpınarı and Yılanlı Burnu quarries) within the Devonian Yılanlı Formation successions were examined in order to reveal their geochemical characteristics (Appendix A). Depending on the composition of the precurser volcanic material and the water/rock ratio in a marine system, the chemical composition of the initial volcanic ash is modified through gains and losses of elements with respect to the altering solutions (Christidis, 1998). By homogenization of tephra with marine water, precurser material (volcanic glass) transforms into smectite, then mixed-layer illite/smectite, and then finally illite progressively. Thus, the usage of major elements is eliminated in determination of original volcanic ash chemistry due to modification of relative proportions of most elements by alteration processes; and only immobile elements such as Ti, Zr, Y and Nb (Winchester and Floyd, 1977) in bulk samples of K-bentonites are used in this research. Hereby, K-bentonites were characterized in the light of this geochemical research in order to determine possible tectonic environments from which they derived.

4.2. Major Element Composition of the Investigated K-bentonites

The Gavurpınarı K-bentonites and clayey limestones are described by SiO_2 (wt. %) contents ranging from 23.35 to 58.64, while the Yılanlı Burnu samples are represented by lower SiO_2 (wt. %) with the contents ranging from 6.82 to 44.26 (geochemical data is given in Appendix A). The K_2O (wt. %) content of Gavurpınarı samples changes from 2.66 to 6.01, while the Yılanlı Burnu samples present a K_2O content (wt. %) ranging between 0.73-5.91. The Gavurpınarı samples have MgO contents between 0.9-5.06, whereas the Yılanlı Burnu samples are characterized by MgO (wt. %) contents ranging from 8.12 to 18.56. The Al_2O_3 and Fe_2O_3 (wt. %) contents of Gavurpınarı samples are respectively ranging between 8.93-21.5 and 2.45-8.76, while Yılanlı Burnu samples have respectively (wt. %) 2.04-15 and 0.92-4.79 Al_2O_3 and Fe_2O_3 contents. The variability of SiO_2 and alkali values of samples from two localities is probably caused by the alteration. Additionally, the investigated samples from Gavurpınarı and Yılanlı Burnu quarries display similar "Loss On Ignition" (LOI) values changing between 8.4 and 43.3 (wt. %). And, this relatively high LOI values can be interpreted as the result of chemical mobility of elements during burial diagenesis in marine environment. Due to the unreliability of major elements of altered K-bentonites, these result will not be interpretted and not used in geochemical discrimination.

4.3. Geochemical Classification of K-Bentonites

To determine original composition of K-bentonites, the method of Floyd and Winchester (1978) by plotting the Zr/Ti and Nb/Y ratios of 8 bulk K-bentonite samples against one another was performed. The results shown in Figure 4.1 indicate an alkali-basaltic character for the possible volcanic source originated the tephra (Chalot-Prat, 2007).

The samples from both Gavurpınarı and Yılanlı Burnu quarries reveal similar geochemical characteristics on the basis of chondrite-normalized trace and REE diagrams (Figure 4.2 and 4.3). The lack of negative anomalies of Ta and Nb elements and REE diagram indicates a possible mantle source for tephras. The relative negative anomaly of Sr could be explained by alteration of the bentonite deposit. The negative Eu anomaly is commonly attributed to the removal of Eu by

plagioclase feldspar during fractionation of the melt. This anomaly is typical of evolved magmas (Calarge et al., 2005). K content of illites could be originated from K-bearing primary minerals such as feldspars or micas. But, for the original composition of volcanic material generating those studied K-bentonites (tephras), the geochemical discrimination analyses suggest an alkali-basaltic magma source (Figure 4.1); and an anorthite-rich feldspar composition will be expected for this magma composition. Thus, the possible source of high K content of illites remains as a question.

Late Devonian volcanism presenting similar geochemical characteristics have been observed in northern Caucasia, Donbas Basin in Schytian Platform and Eastern Europe. Based on acquired data, for now tephras could be considered as derived by rifting tectonism in Late Devonian. In future studies, this similarity will be investigated by geochemical fingerprinting and geochronological analyses.

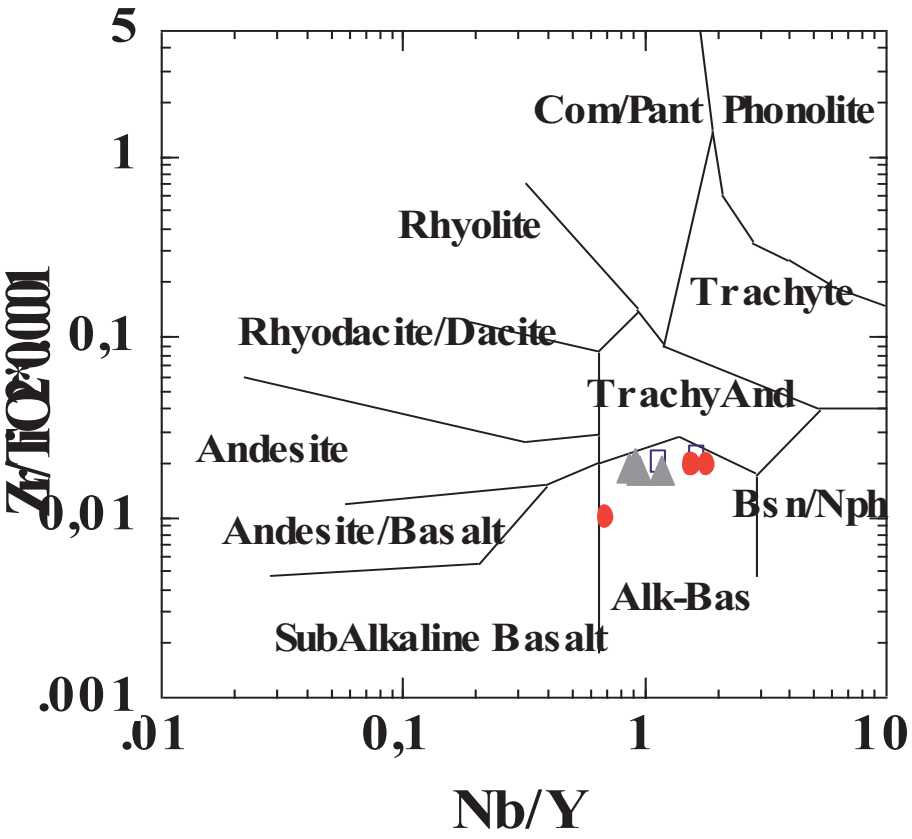


Figure 4.1. Geochemical characteristics of K-bentonites. a) Zr/TiO2-Nb/Y diagram (Floyd & Winchester, 1978) (The triangles and blue squares represent K-bentonite samples from Gavurpınarı quarry, while the circles are representative of K-bentonite samples from Yılanlı Burnu quarry).

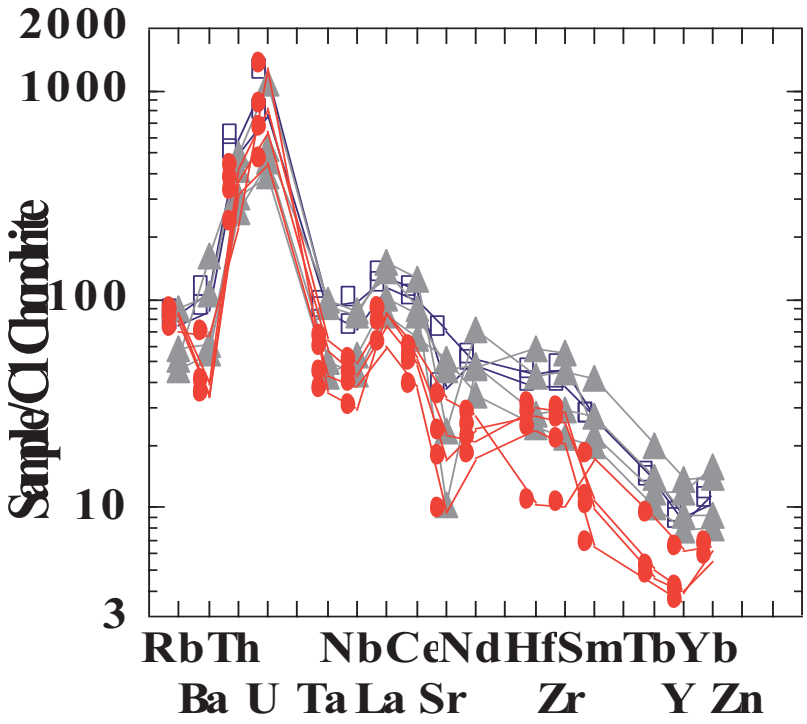


Figure 4.2. The chondrite-based normalized trace element diagram of K-bentonites.

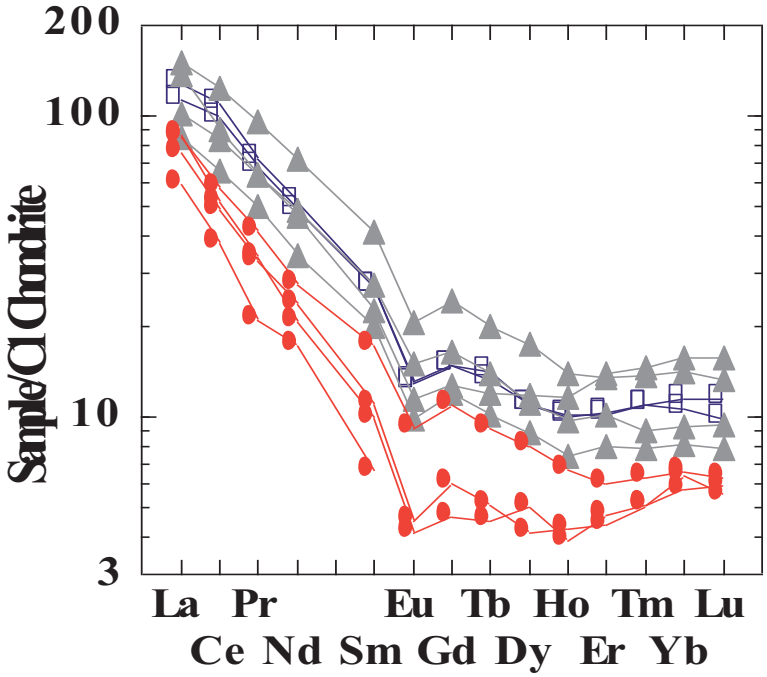


Figure 4.3. The chondrite-based normalized REE diagram of K-bentonites.

CHAPTER 5

DISCUSSION AND CONCLUSION

5.1. Discussion

The following topics can be discussed based on the results obtained by this study.

5.1.1. Mineralogy of Devonian K-Bentonites and Their Environment of Deposition

Mineralogical analysis of the samples collected fron Gavurpınarı and Yılanlı Burnu quarries by using the methods of optical microscope, XRD, SEM-EDX it is revealed that the major clay mineral of K-bentonites is illite, although few amounts of kaolinite and mixed-layer illite-smectite are also identified. In the fine clay fraction (< 0.25μm) imogolite was identified. The non-clay minerals of primary origin are quartz, feldspar, biotite, zircon, amphibole and apatite. This suit of non-clay minerals represent that the studied K-bentonites were originated from volcanic ashes (tephra) which are probably from a distal volcanic source as suggested by the small grain size (around 100μm) of especially the zircon crystals. Also the presence of imogolite in the fine clay fraction supports volcanic origin of K-bentonites.

New minerals which are foreign to the original tephras are the clay minerals illite, kaolinite and mixed-layer I-S. They should owe their origin to the diagenetic processes. Pyrite, calcite, dolomite and gypsum on the other hand are the new non-clay minerals which formed also due to diagenetic processes. Pyrite is present abundantly in some of the K-bentonite samples. They were oxidized when exposed to air so that the grayish-greenish original colors of K-bentonite beds were replaced by brownish color. This property provides a quick identification of Devonian K-bentonites beds in the field.

The petrographic examination of carbonate rocks, mainly limestones and dolomitic limestones, from the studied quarries indicated that original volcanic ashes were settled in a shallow intra-platform sedimentation environment. Intercalating mudstone and marn with limestone and dolostone lithologies in the studied quarries defines an “epieric” platform character for the sedimentary depositional environment. In such an environment interaction with the deposited ash and seawater should cause very early diagenesis of ash (halmyrolysis) on the sea bottom and should cause elemental gains and losses especially in the major elemental compositions of the original tephras. The origin of potassiumn (K) is still not known for the studied K-bentonites, but one possible source of K, might be the sea water.

5.1.2. Illitization Process of Tephra and Degree of Diagenesis

According to optical microscopy studies, XRD-based crysto-chemical analyses (KI, Ir, $I_{002(5Å)}/I_{001(10Å)}$, d_{060}, Al/Mg+Fe, b_0), SEM observations and EDX data, HR-TEM images both Gavurpınarı and Yılanlı Burnu quarry K-bentonites reveal similar mineralogies, crysto-chemical characteristics, and texture and structures. The polytype ratios, the Mg+Fe content of dioctahedral layers, the crystal morphology observed on SEM microphotographs (platy morphology), thin section observations (phenocrysts of zircons and biotites), and the layer structure observed on HR-TEM microphotographs (regular stacking sequence) of illites support the suggestion that these K-bentonites formed as a consequence of illitization of tephras under high-grade diagenetic conditions (at 100-150 °C). Even though in low contents, the 5% expandable layer (smectite) content of clay mineral fraction of Yılanlı

Formation K-bentonites may indicate an initial smectite in tephra-originated K-bentonites from which illite derived as a result of a possible progressive diagenetic alteration. In the lights of previous studies, it is possible to say that progressively increasing temperature during diagenesis may cause smectite to mixed-layer I/S and then illite transformation gradually. And, the data obtained from $I_{002(5Å)}/I_{001(10Å)}$, d_{060}, b_0 analyses reveal a high-grade diagenetic environment in which those illites formed. KI versus Ir diagram also supports those conditions with the crystallite thickness of (*N*=10-20 nm). In TEM photos, any signatures of smectite-mixed layer illite/smectite-illite transformation stages can not be observed, but it can be explained by a progressive transformation of smectite largely to illite (95%) with a low content of mixed-layer illite/smectite (5%).

Polytype identification of the illites from Gavurpınarı and Yılanlı burnu K-bentonites indicated that no significant difference exists between them, so that the diagenetic conditions are similar. The evidences obtained based on the polytype identifications from different size fraction of illites showed that K-bentonites formed by progressive diagenetic maturation: with increasing crystallite size of illites 1*M* polytypes were replaced by $2M_1$ polytype due to increasing degree of metamorphism.

5.1.3. Chemical Composition of Original Volcanic Ash and Source of Volcanism

Since the major elemental compositions of the studied K-bentonite samples from studied locations, are not reliable for the determination of the original parent ash composition, trace and REE data were analysed by means of chemical discrimination diagrams. The significant results obtained from this part of the study indicated that the original ashes had alkali basaltic compositions, close to the field of trachy andesite in the Zr/TiO_2-Nb/Y diagram of Floyd & Winchester (1978). This may partly explain the origin of K for illitization process took place during diagenesis of tephras as it is provided by the original K content of the volcanic ashes. However, this as a source of K is still remains to be unproven. In the REE diagrams, lack of Ta and Nb negative anomalies are characteristic for a mantle origin of the original volcanic ashes of Middle-Late Devonian age tephras forming K-bentonites by diagenetic evolution.

5.2. Conclusions

The analyses results suggest that those illitic bentonites are most probably K-bentonites which were derived from tephras (volcanic ashes) in a shallow marine environment by chemical modification and progressive illitization of smectite during late diagenesis.

The following conclusions were obtained at the end of the study;

1- K-bentonites of Devonian age are outcropped in the Yılanlı Formation exposed in the nearby area around Zonguldak-Bartın. Based on volcanogenic non-clay minerals, especially zircon, biotite, feldspar and quartz, those K-bentonites are derived from tephra as a result of diagenesis. These primary non-clay minerals are accepted as indicators of a volcanic origin (tephra or volcanic ash).

2- The presence of imogolite by XRD analyses of finer clay fractions also supports the volcanic origin for K-bentonites.

3- K-bentonites contain mainly (min 95%) illite as a clay mineral, however in few of them kaolinite and mixed-layer illite/smectites are also identified.

4- The illite formed during diagenesis by fixation of K into interlayer positions of illite/smectites. Based on crysto-chemical analyses (KI, Ir, $I_{002(5Å)}/I_{001(10Å)}$, d_{060}, b_0) the degree of diagenesis has been determined as late-diagenesis.

5- Crystal thicknesses (*N*) of illites has been determined as 10-20 nm, and polytypes identified are $2M_1$ and $1M_d$.

6- SEM observations reveal a lamellar-platy and juxtaposed morphology for illites from both quarries which indicates high-grade diagenetic conditions. And, EDX data for studied samples support the illitic composition.

7- TEM images present a regular stacking sequences (*R*>3) for illite crystals as a result of illitization under high diagenetic conditions.

8- The geochemical analyses reveal a similar chemical composition for the studied K-bentonites, and indicate an alkali-basaltic character for the possible original tephra. REE element composition points out that source tephras had a mantle source.

9- Based on the limited literature survey on Late Devonian volcanism having similar geochemical characteristics, the source volcano of K-bentontes found in Zonguldak-Bartın area might be located in northern Caucasia, Donbas Basin in Schytian Platform and Eastern Europe.

Suggestions for further studies:

1- The detailed study on the progressive illitization mechanism of clay minerals should provide significant data about thermal maturation and also subsidence history of the sedimentary basin of the study area.

2- The field studies to identify other Devonian aged K-bentonites outcrops should be performed, and the potential of these K-bentonite horizons for long-distance stratigraphic correlations and tectonomagmatic setting should be investigated.

REFERENCES

Ahn, J. H., and Peacor, D. R., 1986. Transmission and analytical electron microscopy of the smectite-to-illite transition. Clays and Clay Minerals, 34, 165-179.

Ahn, J. H., and Peacor, D. R., 1987. Kaolinitization of biotite: TEM data and implications for an alteration mechanism. American Mineralogists, 72, 353-356.

Ahn, J. H., and Peacor, D. R., 1989. Illite/smectite from Gulf Coast shales: A reappraisal of transmission electron microscope images. Clays & Clay Miner., 37: 542-546.

Allen, V. T., 1932. Ordovician altered volcanic material in Iowa, Wisconsin, and Missouri: J. Geol., 40, 259-269.

Artyushkova, O. V. and Maslov, V. A., 2008. Detailed correlation of the Devonian deposits in the South Urals and some aspects of their formation. Bulletin of Geosciences, 83(4), 391–399.

Aydın, M., Serdar, H. S., Şahintürk, Ö., Yazman, M., Çokuğra, R., Demir, O., and Özçelik, Y., 1987. Geology of the Çamdağ (Sakarya)-Sünnicedağ (Bolu) Region. Bull. Geol. Soc. Turkey 30/1, 1-4 (in Turkish).

Bailey, S., Hurley, P., Fairbairn, H., and Pinson, W., 1962. K/Ar dating of sedimentary illite polytypes: Geological Society of America Bulletin, 73, 1167-1170.

Batchelor, R. A. and Clarkson, E. N. K., 1993. Geochemistry of a Silurian metabentonite and associated apatite from the North Esk Inlier, Pentland Hills. Scottish Journal of Geology, 29, 123-130.

Batchelor, R. A. and Weir, J. A., 1988. Metabentonite geochemistry: magmatic cycles and graptolite extinctions at Dob's Linn, southern Scotland. Transactions of the Royal Society of Edinburgh: Earth Sciences, 79, 19-41.

Benedict, L. J. and Ver Straeten, C. A., 2005. Geochemical and physical evidence indicating complex depositional and eruptive histories for Devonian K-bentonites of the Appalachian foreland basin. Northeastern Section, 40th annual meeting, Abstracts with Programs - Geological Society of America, 37, 73.

Benedict, L., 2004. Complexity of Devonian K-bentonites in the Appalachian foreland basin: Geochemical and physical evidence supporting multi-layered K-bentonite horizons. Master Thesis. State University of New York at Albany, 258 p.

Berg, G., 1910. Geologische Beobachtungen in Kleinasien. Z. Dtsch.Geol. Gesell., Abh. Bd. 62.

Bergström, S. M., Huff, W. D., Kolata, D. R. and Bauert, H., 1995. Nomenclature, stratigraphy, chemical fingerprinting and areal distribution of some Middle Ordovician K-bentonites in Baltoscandia. Geologiska Foreningens i Stockholm Forhandlingar, 117, 1-13.

Bergström, S. M., Huff, W. D., Kolata, D. R. and Kaljo, D., 1992. Silurian K-bentonites in the Iapetus region: a preliminary event-stratigraphic and tectonomagmatic assessment. Geologiska Foreningens i Stockholm Forhandlingar, 114, 327-334.

Bergström, S. M., Huff, W. D., Kolata, D. R. and Melchin, M. J., 1997. Occurrence and significance of Silurian K-bentonite bedds at Arisaig, Nova Scotia, Eastern Canada. Canadian Journal of Earth Sciences, 34, 1630-1643.

Berkley, J. L. and Baird, G. C., 2002. Calcareous K-bentonite deposits in the Urica Shale and Trenton Group (Middle Ordovician) of the Mohawk Valley, New York State. Physics and Chemistry of the Earth, 27, 265-278.

Bethke, C. M., Vergo, N. & Altaner, S. P., 1986. Pathways of smectite illitization. Clays and Clay Minerals, 34, 125–35.

Boles, J. R. and Franks S. G., 1979. Clay diagenesis in Wilcox sandstones of Southwest Texas: Implications of smectite diagenesis on sandstone cementation. Sed. Petr., 49 (1), 55-70.

Boncheva, I., Göncüoğlu M. C., Leslie, S. A., Lakova, I., Sachanski, V., Saydam, G., Gedik, I. and Königshof, P., 2009. New Conodont and palynological data from the Lower Paleozoic in Northern Çamda^g, NW Anatolia, Turkey. Acta Geol. Pol., 59, 2, 157—171.

Bozkaya, Ö. and Yalcin, H., 2004. Diagenetic to low-grade metamorphic evolution of clay mineral assemblages in Paleozoic to early Mesozoic rocks of the Eastern Taurides, Turkey. Clay Minerals, 39, 481–500.

Bozkaya, Ö. and Yalçın, H., 2009. Kil diyajenezi/metamorfizması ve jeotektonik konum. 14. Ulusal Kil Sempozyumu, Karadeniz Teknik Üniversitesi, Trabzon, 1-3 Ekim, Bildiriler Kitabı, s. 46-70.

Bozkaya, Ö., and Yalçın, H., 2004. New mineralogic data and implications for the tectono-metamorphic evolution of the Alanya Nappes, Central Tauride Belt, Turkey. International Geology Review, 46, 347-365.

Bozkaya, Ö., Yalçın, H. & Kozlu, H., 2011. Clay Mineralogy of the Paleozoic-Lower Mesozoic sedimentary sequence from the Northern Part of the Arabian Platform, Hazro (Diyarbakır), Southeast Anatolia. Geologica Carpathica, 62, 6, 489-500.

Bozkaya, Ö., Yalçın, H., Göncüoğlu, M. C., 2002. Mineralogic and organic responses to stratigraphic irregularities: an example from the Lower Paleozoic very low-grade metamorphic units of the Eastern Taurus Autochthon, Turkey. Schweizerische Mineralogische und Petrographische Mitteilungen, 82, 355-373.

Bozkaya, Ö., Yalçın, H., Göncüoğlu, M.C., 2012. Mineralogic evidences of a mid-Paleozoic tectono-thermal event in the Zonguldak terrane, NW Turkey: implications for the dynamics of some Gondwana-derived terranes during the closure of the Rheic Ocean. Canadian Journal of Earth Sciences, 49, 559-575.

Buatier, M. D., Peacor, D. R., O'Neil, J. R., 1992. Smectite-illite transition in Barbados Accretionary wedge sediments: TEM and AEM evidence for dissolution/crystallization at low temperature: Clays and Clay Minerals, 40, no. 1, 65–80.

Buggisch, W., 1991. The global Frasnian–Famennian "Kellwasser Event". Geologische Rundschau, 80, 49–72.

Burst, J. F., 1969. Diagenesis of Gulf Coast clayey sediments and its possible relation to petroleum migration. Bull. Am. Ass. Petrol. Geol., 53, 73-93.

Calarge, L., Meunier, A., Lanson, B., and Formoso, M., 2006. Chemical signature of two Permian volcanic ash deposits within a bentonite bed from Melo, Uruguay. Anais da Academica Brasileira de Ciências, 78, 525-541.

Chalot-Prat, F., Tikhomirov P., and Saintot, A., 2007. Late Devonian and Triassic basalts from the southern continental margin of the East European Platform, tracer of a single heterogeneous lithospheric mantle source. J. Earth Syst. Sci. 116, 469–495.

Chen, F., Siebel, W., Satır, M., Terzioğlu, M.N., and Saka, K., 2002. Geochronology of the Karadere basement (NW Turkey) and implications for the geological evolution of the Istanbul zone. International Journal of Earth Sciences, 91(3), 469–481.

Christidis, G. E., 1998. Comparative Study of The Mobility of Major and Trace Elements During Alteration of an Andesite and a Rhyolite to Bentonite, in Island of Milos and Kimolos, Aegean, Greece, Clays and Clay Minerals, 46, 379-399.

Clayton, C. R. I., 1983. The influence of diagenesis on some index properties of chalk in England. Geotechnique, 33, 225-241.

Compton, J. S., Conrad, M. E., and Vennemann, T. W., 1999. Stable isotope evolution of volcanic ash layers during diagenesis of the Miocene Monterey Formation, California. Clays and Clay Minerals, **47,** 84-95.

Copper, P., 1986. Frasnian/Famennian mass extinction and cold-water oceans. Geology, 14, 835-839.

Copper, P., 1998. Evaluating the Frasnian-Famennian mass extinction: Comparing brachiopod faunas. Acta Palaeontologica Polonica, 43, 137-54.

Copper, P., 2002. Reef development at the Frasnian/Famennian mass extinction boundary: Palaeogeography, Palaeoclimatology, Palaeoecology, 181, 27-65.

Cronin, S., Hedley, M. and Neall, V., 1996. Impact of October 1995 Ruapehu ash fall on soil fertility. Estimates of elemental deposition rates and impact on soil and pasture chemical composition. Department of Soil Science and Fertilizer and Lime Research Centre, Massey University.

Dean, W. T., Martin, F., Monod, O., Demir, O., Rickards, R. B., Bultynck, P,. and Bozdoğan, N. 1997. Lower Paleozoic stratigraphy, Karadere-Zirze area, central Pontides, northern Turkey. In: Göncüoğlu M. C. and Derman A. S. (Eds.): Early Paleozoic evolution in NW Gondwana. IGCP Project No. 351, II. International Meeting, November 5-11, 1995, Ankara, Turkey. Spec. Publ. Turkish Assoc. Petrol. Geol., Ankara, 3, 32-38.

Dean, W. T., Monod, O., Rickards, R. B., Demir, O., and Bultynck, P. 2000. Lower Palaeozoic stratigraphy and palaeontology, Karadere-Zirze area. Pontus Mountains, northern Turkey. Geol. Mag., 137, 555-582.

Eberl, D. D., 1984. Clay mineral formation and transformation in rocks and soils: Philosophical Transactions of The Royal Society of London A, 311, 241-257.

Elliott, W. C. and Aronson, J. L. 1987. Alleghanian episode of K-bentonite illitization in the southern Appalachian Basin: Geology, 15, 735-739.

Eslinger, E. and Pevear D., 1988. Clay Minerals for Petroleum Geologists and Engineers. Society of Economic Paleontolgists and Mineralogists, Tulsa, OK.

Esquevin, J. 1969. Influence de la composition chimique des illites sur leur cristallinite: Bull. Centre de Recherches de Pau Soc. National des Petroles d'Aquitaine, 3, 147-153.

Floyd, P. A., and Winchester, J. A.,1978. Identification and discrimination of altered and metamorphosed volcanic rocks using immobile elements. Chemical Geology, 21, 291-306.

Fortey, N. J., Merriman, R. J. and Huff, W. D., 1996. Silurian and Late-Ordovician K-bentonites as a record of late Caledonian volcanism in the British Isles. Transactions of the Royal Society of Edinburgh: Earth Sciences, 86, 167-180.

Freed, R. L., and Peacor, D. R., 1989a. TEM lattice fringe images with R1 ordering of illite/smectite in Gulf Coast pelitic rocks (abstract). G. S. A. Abstr. with Prog., 21, A16.

Gedik, I. and Önalan, M., 2001. A new approach to the Paleozoic stratigraphy of the Çamdağ (Sakarya province). Istanbul Univ. Engineering Faculty's Earth Sci. Rev., Istanbul, 14, 61-76 (in Turkish).

Gedik, I., Pehlivan, Ş., Timur, E., and Duru, M., 2005. Geological maps of Turkey, 1 : 50,000 scaled, No. 12, Istanbul F23d sheet. MTA Publ., Ankara (in Turkish).

Göncüoğlu, M. C., 1997. Distribution of Lower Paleozoic units in the Alpine Terranes of Turkey. Paleogeographic constrains. In:Göncüoğlu, M. C. and Derman, A. S. (Eds.): Lower Paleozoic evolution in northwest Gondwana. Turkish Assoc. Petrol. Geol., Spec. Publ., Ankara 3, 13—24.

Göncüoğlu, M. C., 2010. Introduction to the Geology of Turkey: Geodynamic Evolution of the Pre-Alpine and Alpine Terranes. General Dictorate and Mineral Research and Exploration, MTA, 66 p.

Göncüoğlu, M. C., Boncheva, I., Gedik, I., Lakova, I., Sachanski, V., Saydam, G., Okuyucu, C., Özgül, N. and Yanev, S. 2005b: Perigondwanan versus Laurussian Origin of the NW Anatolian Paleozoic Terranes: A correlation of Mid-Paleozoic Events in Istanbul and Zonguldak. International Workshop Depositional Environments of the Gondwanan and Laurasian Devonian. Abstracts and field trip guidebooks. 15—16.

Görür, N., Monod, O., Okay, A. I., Sengör, A. M. C., Tüysüz, O., Yigitbas, E., Sakinc, M. and Akkök, R., 1997. Paleogeographic and tectonic position of the Carboniferous rocks of the western Pontides (Turkey) in the frame of the Varican belt. Bull. Soc.Géol. France 168, 197-205.

Grim, R. E. 1962 Clay mineralogy: Science, 13S, No. 3507, pp. 890-898.

Guggenheim, S., Bain, D. C., Bergaya, F., Brigatti, M. F., Drits, V., Eberl, D. D., Formoso, M., Galán, E., Merriman, R. J., Peacor, D. R., Stanjek, H., and Watanabe, T., 2002. Report of the Association Internationale pour L'etude des Argiles (AIPEA) Nomenclature Committee for 2001: Order, disorder, and crystallinity in phyllosilicates and the use of the "crystallinity" index. Clays and Clay Minerals, 50, 406-409, and Clay Minerals, 37, 389-393.

Guidotti, C., and Sassi, F., 1986. Classification and correlation of metamorphic facies series by means of muscovite b0 data from Low-grade metapelites. Neus Jahrbuch fur Mineralogie Abhandlungen, 157, 363–380.

Hallam, A. and Wignall, P. B., 1997. Mass extinctions and their aftermath. Oxford, Oxford University Press, 330 pp.

Histon, K., Klein, P., and Schonlaub, H. P., 2007. Lower Palaeozoic K-bentonites from the Carnic Alps, Austria. Austrian Journal of Earth Sciences, 100, 26-42.

Hoffman, J. and Hower, J., 1979. Clay mineral assemblages as low grade metamorphic geothermometers: application to the thrust-faulted disturbed belt of Montana, U.S.A. Aspects of Diagenesis (P. A. Scholle & la. R. Schluger, editors). S.E.P.M. Spec. laubl., 26, 55-80.

Hoffman, J. and Hower, J., 1979. Clay mineral assemblages as low grade metamorphic geothermometers: Application to the thrust faulted disturbed belt of Montana, USA: in Aspects of Diagenesis, P. A. Scholle and P. R. Schluger, eds., Soc. Econ. Paleontol. Mineral. Spc. Publ. 26, 55-79.

House, M. R., Menner, V. V., Becker, R. T., Klapper, G., Ovnatanova, N. S., and Kuzmin, V., 2000. Reef episodes, anoxia and sea-level changes in the Frasnian of the southern Timan (NE Russian platform). In: Carbonate platform systems: components and interactions (ed. Insalaco, E., Skelton, P.W., and Palmer, T.J.). The Geological Society of London. London, England, 147-176.

Hower, J. F., 1981. X-ray diffraction of mixed layered clay minerals, in: "Clays and the Resource Geologist", Longstaffe, F. J., ed. Mineral. Soc. Canada Short Course, 7, 39–59.

Hower, J., Eslinger, E. V., Hower, M. E., and Perry, E. A., 1976. Mechanism of burial metamorphism of argillaceous sediments, 1. Mineralogical and chemical evidence: Geol. Soc. Amer. Bull., 87, 725-737.

Hower, J., Hurley, P. M., Pinson, W. H., and Fairbahirn H. W., 1963. The dependence of K-Ar age on the mineralogy of various particle size ranges in a shale. Geochim. Cosmochim. Acta, 27, 405 410.

Huff W. D., and Morgan, D. J., 1990. Stratigraphy, mineralogy and tectonic setting of Silurian K-bentonites in Southern England and Wales. In: V.C. Farmer & Y. Tardy (eds.) Proceedings of the 9th International Clay Conference, Strasbourg. 33-42.

Huff, W. D. and Türkmenoğlu, A. G., 1981. Chemical characteristics and origin of Ordovician K-bentonites along the Cincinnati Arch. Clays and Clay Minerals, 29, 113-123.

Huff, W. D., Anderson, T. B., Rundle, C. C. and Odin, G. S., 1991. Chemostratigraphy, K-Ar ages and illitization of Silurian K-bentonites from the Central Belt of the Southern Uplands- Down Longford Terrane, British Isles. Journal of the Geological Society of London, 148, 861-868.

Huff, W. D., Astini, R. A., and Bergstrom, S. M., 1998. Ordovician K-bentonites in the Argentine Precordillera: relations to Gondwana margin evolution. Geological Society of America Special Publication, 142, 107-126.

Huff, W. D., Bergström, S. M. and Kolata, D. R., 1992. Gigantic Ordovician volcanic ash fall in North America and Europe: biological, tectonomagmatic and event-stratigraphic significance. Geology, 20, 875-878.

Huff, W. D., Bergström, S. M. and Kolata, D. R., 2000. Silurian K-bentonites of the Dnestr Basin, Podolia, Ukraine. Journal of the Geological Society, London, 157, 493-504.

Hunziker, J. C., Frey M., Clauer N., Dallmeyer, R. D., Frıedrichsen A., Flehmig W., Hochstrasser K., Roggwiler, P. and Schwander, H., 1986. The evolution of illite to muscovite: Mineralogical and isotopic data from the Glarus Alps, Switzerland. Contrib. Min. Pet. 92, 157-180.

Inanli, F. Ö., Huff, W. D. and Bergström, S. M., 2009. The Lower Silurian (Llandovery) Osmundsberg K-bentonite in Baltoscandia and the British Isles: chemical fingerprinting and regional correlation. GFF, 131, 269-279.

Inoue, A., and Kitagawa, R., 1994. Morphological characteristics of illitic clay minerals from a hydrothermal system. American Mineralogists, 79, 700-711.

Inoue, A., 1986. Morphological change in a continuous smectite-to-illite conversion series by scanning and transmission electron microscopies: J. Coll. Arts & Sci., Chiba Univ., B-19, 23-33.

Inoue, A., Kohyama, N., Kitagawa, R., Watanabe, T., 1987. Chemical and morphological evidence for the conversion of smectite to illite. Clays and Clay Mineralogy, 35, 111-120.

Inoue, A., Watanabe, T., Kohyama, A. and Brusewitz, A. M., 1990. Characterization of illitization of smectite in bentonite beds at Kinnekulle, Sweden. Clays & Clay Miner., 38, 241-249.

Jeans, C. V., Merriman, R. J., Mitchell, J. G., and Bland, D. J., 1982. Volcanic clays in the Cretaceous of southern England and northern Ireland. Clay Miner., 17, 105-156.

Kay, G. M., 1944. Middle Ordovician of central Pennsylvania; Part 1, Chazyan and earlier Mohawkian (Black River) formations; Part 2, Later Mohawkian (Trenton) formations: J. Geol., 52, l-23, 97-116.

Kaya, O. and Birkenheide, R., 1988. Contributions to the stratigraphy of Middle Devonian in the Surroundings of Adapazarô, Northwest Turkey. Bull. Min. Res. Exp., 108, 118-124.

Keller, G., 1986. Stepwise mass extinctions and impact events; late Eocene to early Oligocene. Marine Micropaleontology 10, 267 – 293.

Keller, G., 2005. Impacts, volcanism and mass extinctions: random coincidence or cause and effect? Australian J Earth Sci., 52, 725–757.

Kiipli, T., Kallaste, T., Nestor, V. and Loydell, D. K., 2010b. Integrated Telychian (Silurian) K-bentonite chemostratigraphy and biostratigraphy in Estonia and Latvia. Lethaia, 43, 32-44.

Kipman, E., 1974, Geology of the marine iron deposits of Sakarya Çamdağ (Kestanepınar-Yassıgeçit villages). Istanbul Üniversitesi Fen Fakültesi Monografi Serisi, 25, 72 (in Turkish).

Kisch, H. J., 1991. Illite crystallinity: recommendations on sample preparation X-ray diffraction settings and inter-laboratory samples. J. Met. Geol., 9, 665-670.

Kleinsorge, H. and Wijkerslooth, P., 1940. Devonian oolitic iron deposits in Çamdağ around Adapazarı (Kocaeli province). Bull. Min. Res. Exp., 20, 319-334.

Knox, R. W. O'B., 1983. Volcanic ash in the Oldhaven Beds of southeast England, and its stratigraphical significance. Proceedings of the Geologists' Association, 94, 245-250.

Kolata, D. R., Frost. J. K. and Huff, W. D., 1987. Chemical correlation of K-bentonite beds in the Middle Ordovician Decorah subgroup, Upper Mississippi Valley. Geology, 15, 208-211.

Kolata, D. R., Huff, W. D. and Bergstrom, S. M., 1996. Ordovician K-bentonites of eastern North America. Geological Society of America Special Paper, 313, 1-84.

Kolata, D. R., Huff, W. D., and Bergstrom, S. M., 1998. Nature and regional significance of unconformities associated with the Middle Ordovician Hagan K-bentonite complex in the North American midcontinent. Bulletin of the Geological Society of America, 110, 723-739.

Kozur, H. and Göncüoğlu M. C., 1998. Main feaures of the preVariscan development in Turkey. Acta Univ. Carol. Geol., 42, 3-4, 459-464.

Krumm, S., 1996. WINFIT 1.2: version of November 1996 (The Erlangen geological and mineralogical software collection) of WINFIT 1.0: a public domain program for interactive profile analysis under WINDOWS. XIII Conference on Clay Mineralogy and Petrology, Praha, 1994, Acta Universitatis Carolinae Geologica, 38, 253-261.

Kübler, B., 1967. La cristallinite de l'illite et les zones tout a fait superieures du metamorphisme. Etages Tectoniques (Colloque de Neuchâtel). Collegue de Neuchatel, pp. 105-121.

Kübler, B., 1968. Evaluation quantitative du metamorphisme par la cristallinite de l'illite. Bull. Centre Rech. Pau-SNPA, 2, 385-397.

Lakova, I., Sachanski, V., and Göncüoglu, M.C., 2006. Earliest cryptospore record in NW Anatolia dated by graptolites and acritarchs, Lower Ordovician Bakacak Formation, Zonguldak Terrane, NW

Anatolia. GCP 503 Ordovician Paleogeography Ann. Meeting, 30 Aug–1 Sept., Glasgow-UK, Abstracts and Field Excursion Guide, 30–31.

Lanson, B., Velde, B., Meunier, A., 1998. Late stage diagenesis of illitic clay minerals as seen by decomposition of X-ray diffraction patterns: contrasted behaviors of sedimentary basins with different burial histories. Clays and Clay Minerals,46,1,69-78.

Larsen, L. If., and Poldervaart, A, 1957. Measurement and distribution of zircons in some granitic rocks of magmatic origin. Min. Mag., 31, 544-564.

Larsen, G., and Chilingar, G. V., 1983. Diagenesis in sediments and sedimentary rocks. Elsevier, Dev. Sediment., pp. 352-355.

Lindgreen, H., and Hansen, P. L., 1991. Ordering of illite-smectite in Upper Jurassic claystones from the North Sea. Clay Miner., 26, 105-125.

Lounsbury, R. W. and Melhorn, W. N., 1964. Clay mineralogy of paleozoic K-bentonites of the eastern United States (Part 1). Clays and Clay Minerals, Proc. 12th Nat. Conf., N.Y., Pergamon, 557-565.

Ma, X. P., and Bai, S. L., 2002. Biological, depositional, microspherule, and geochemical records of the platformal Frasnian–Famennian boundary beds, Hunan, China. Palaeogeography, Palaeoclimatology, Palaeoecology, 181, 325–346.

Marker, P. G., and Huff, W. D., 2005. What is a K-bentonite?: Abstracts with Programs - Geological Society of America, 37, 143.

Maxwell, D. T., and Hower, J., 1967. High-grade diagenesis and low-grade metamorphism of illite in the Precambrian Belt Series. American Mineralogists, 52, 843-857.

McGhee, G. R., Jr., 2005. Modelling Late Devonian extinction hypotheses, in Over, D. J., Morrow, J. R., and Wignall, P. B., eds., Understanding Late Devonian and Permian-Triassic Biotic and Climatic Events: Towards an Integrated Approach: Amsterdam, Elsevier, 37–50.

Merriman, R. J. and Roberts, B., 1990. Metabentonites in the Moffat Shale Group, Southern Uplands of Scotland: geochemical evidence of ensialic marginal basin volcanism. Geological Magazine, 127, 259-271.

Meunier, A., and Velde, B., 2004. Illite: Origin, Evolution and Metamorphism. Springer, New York.

Millot, G., 1970. Geology of Clays, Springer, New York. Swindale, L. O. and Fan, P. F. 1967 Transformation of gibbsite to chlorite in ocean-bottom sediments. Science, 157, 799-800.

Min, K., Renne, P. R. and Huff, W. D., 2001. $^{40}Ar/^{39}Ar$ dating of Ordovician K-bentonites in Laurentia and Baltoscandia. Earth & Planetary Science Letters, 185, 121-134.

Moore, D. M. and Reynolds, R. C., Jr., 1997. X-Ray Diffraction and the Identification and Analysis of Clay Minerals, 2nd edition, Oxford, New York: Oxford University Press, 378 pp.

Nadeau, P. H., Wilson, M. J., Mchardy W. J., and Tait, J. M., 1985. The nature of some illitic clays from bentonites and sandstones: implications for the conversion of smectite to illite during diagenesis. Mineral. Mag., 49, 393-400.

Nadeau, P. H., Wilson, M. J., McHardy, W. J. and Tait, J. M., 1985. The conversion of smectite to illite during diagenesis: evidence from some illitic clays from bentonites and sandstones. Mineralogical Magazine, 49, 393-400.

Nelson, B. W., 1959. Clay mineral assemblages from the Rappahannock River: in Program and Abstracts, Seventh National Clay Conference, Washington, D.C. (Abstract).

Nelson, W. A., 1921. Notes on a volcanic ash bed in the Ordovician of Middle Tennessee. Tennessee Division of Geology Bulletin, 25, 46-48.

Nelson, W. A., 1922. Volcanic ash bed in the Ordovician of Tennessee. Geological Society of America Bulletin, 33, 605-616.

Okay, A. I., Sengör, A. M. C. and Görür, N., 1994. The Black Sea: a kinematic history of opening and its effect on the surrounding regions. Geology, 22, 267—270.

Okuyucu, C., Djenchuraeva, A. V., Neyevin A. V., Saydam, G. D., Çakırsoy, Ö. B., Vorabiev, T., Çörekçioçlu, E. and Ekmekçi, E., 2005. The biostratigraphic correlation of Paleozoic successions in Krygzhistan and Turkey. MTA Report 10746, 1-94.

Peacor, D. R., 1992a. Diagenesis and low-grade metamorphism of shales and slates. In: Buseck, P. R., editor. Minerals and reactions at the atomic scale. Reviews in Mineralogy and Geochemistry, 27, 335-380.

Perry, E. and Hower, J., 1970. Burial diagenesis in Gulf Coast pelitic sediments: Clays and Clay Minerals, 18, 165-177.

Peterhänsel, A. and Pratt, B. R., 2001. Nutrient-triggered bioerosion on a giant carbonate platform masking the postextinction Famennian benthic community: Geology, 29, 1079–1082.

Pevear, D. R., 1999. Illite and hydrocarbon exploration. Proceedings of the National Academy of Sciences, 96, 3440-3446.

Powers, M. C., 1959. Adjustment of clays to chemical changes and the concept of the equivalent level. Clays and Clay Minerals, 6, 309-326.

Powers, M. C., 1967. Fluid release mechanisms in compacting marine mudrocks and their importance in oil exploration. American Association of Petroleum Geologists Bulletin, 51, 1240-1254.

Price, K. L., and McDowell, S. D., 1993. Illite/smectite geothermometry of the Proterozoic Oronto Group, Midcontinent Rift System. Clays Clay Miner, 41, 134-147.

Pytte, A. M., and Reynolds, R. C., 1989. The thermal transformation of smectite to illite. In Naeser, N. D., and McCulloh, T. H., Eds., Thermal history of sedimentary basins, p. 133-140. Springer-Verlag, Berlin.

Racki, G., 1999a. Silica−secreting biota and mass extinctions: survival patterns and processes. Palaeogeography, Palaeoclimatology, Palaeoecology, 154, 107–132.

Racki, G., Racka, M., Matyja, H., and Devleeschouwer, X., 2002. The Frasnian/Famennian boundary interval in the South Polish−Moravian shelf basins: integrated event−stratigraphical approach. Palaeogeography, Palaeoclimatology, Palaeoecology, 181: 251–297.

Reynolds, R. C., 1980. Interstratified clay minerals. Pp. 249-303 in: Crystal Structures of Clay Minerals and their X-ray Identification (G. Brindley & G. Brown, editors). Mineralogical Society, London.

Reynolds, R. C., Jr., 1993. Three dimensional X-ray powder diffraction from disordered illite: Simulation and interpretation of the diffraction patterns. In Reynolds, R.C., Jr, and Walker, J. R.,

editors. Computer applications to X-ray powder diffraction analysis of clay minerals, CMS Workshop Lectures 5. Boulder, CO: Clay Minerals Soc., 43-78.

Rosenkrans, R. R., 1934. Correlation studies of the central and south-central Pennsylvania bentonite occurrences. American Journal of Science, 17, 113-134.

Sassi, F., and Scolari, A., 1974. The b_0 of the potassic white micas as a barometric indicator in low-grade metamorphism of pelitic schist. Contribution to Mineralogy and Petrology, 45, 143–152.

Sell, B. K., and Samson, S. D., 2011a. Apatite phenocryst compositions demonstrate a miscorrelation between the Millbrig and Kinnekulle K-bentonites of North America and Scandinavia: Geology, 39, 303–306.

Srodon, J., 1984. X-ray powder diffraction identification of illitic materials. Clays and Clay Minerals, 32 (5), 337-349.

Şengör, A. M. C. and Yılmaz, Y., 1981. Tethyan evolution of Turkey: a plate tectonic approach, Tectonophysics, 75, 181-241.

Thompson, R., Bradshaw, R. H. W., and Whitley, J. E., 1986. The distribution of ash in Icelandic lake sediments and the relative importance of mixing and erosion processes. Journal of Quaternary Science, 1, 3-11.

Trapp, E., Kaufmann, B., Mezger, K., Korn, D. and Weyer, D., 2004. Numerical calibration of the Devonian-Carboniferous boundary: Two new U-Pb isotope dilution-thermal ionization mass spectrometry single-zircon ages from Hasselbachtal (Sauerland, Germany). Geology, 32, 857-860.

Tribovillard, N., Averbuch, O., Devleeschouver, X., Racki, G., and Riboulleau, A., 2004. Deep-water anoxia during the Frasnian-Famennian boundary events (La Serre, France): an echo of a tectonically-induced Late Devonian oceanic anoxic event? Terra nova, 16, 288-295.

Turkmenoğlu, A. G., 2001. A Paleozoic K-bentonite occurence in Turkey, Mid-European Clay Conference' 01, MECC, September 9-14, Stara Leusa, Slovakia. Book of Abstracts, p. 108.

Turkmenoğlu, A. G., Goncüoğlu, M. C., and Bayraktaroğlu, Ş., 2009. Early Carboniferous K-bentonite formation around Bartın: geological implications. "2nd International Symposium on the Geology of the Black Sea Region", p.209.

Ustaömer, P. A., 1999. Pre-Early Ordovician Cadomian arc-type granitoids, the Bolu Massif, West Pontides, northern Turkey: geochemical evidence. International Journal of Earth Sciences, 88, no. 1, 2-12.

Ustaömer, P.A., and Rogers, G., 1999. The Bolu Massif: remnant of a pre-Early Ordovician active margin in the west Pontides, northern Turkey. Geological Magazine, 136(5), 579–592.

Velde, B. and Hower, J., 1963. Petrological significance of illite polymorphism in Paleozoic sedimentary rocks. American Mineralogists, 48, 1239-1254.

Ver Straeten, C. A., 2004. Sprout Brook K-bentonites: New interval of Devonian (Early Emsian?) K-bentonites in eastern North America: Northeastern Geology and Environmental Science, 26, 298-305.

Ver Straeten, C. A., 2007a. Basinwide Stratigraphic Synthesis and Sequence Stratigraphy, Upper Pragian, Emsian and Eifelian Stages (Lower to Middle Devonian), Appalachian Basin: in Becker, R. T., and Kirchgasser, W. T., eds., Devonian Events and Correlations: Geological Society of London, Special Publications, 278, 39-81.

Wada, K. and Yoshinaga, N., 1969. The structure of imogolite. Am. Mineral., 54, 50-71.

Walliser, O. H., 1996a. Global Events in the Devonian and Carboniferous; p. 225-250 in Walliser, Otto H. (ed.), Global Events & Event Stratigraphy in the Phanerozoic. Springer-Verlag, Berlin Heidelberg, 333 p.

Wang, H., Frey, M., Stern, W. B., 1996. Diagenesis and metamorphism of clay minerals in the Helvetic Alps of Eastern Switzerland. Clays and Clay Minerals, 44, 96-112.

Warr, L. N. and Rice, A. H. N., 1994. Interlaboratory standardisation and calibration of clay mineral crystallinity and crystallite size data. Journal of Metamorphic Geology, 12, 141-152.

Weaver, C. E. and Bates, T. E., 1952. Clay Minerals Bulletin, 1, 258.

Weaver, C. E., 1953. Mineralogy and petrology of some Ordovician K-bentonites and related limestones. Geological Society of America Bulletin, 64, 921-944.

Weaver, C. E., 1956. Distribution and identification of mixed-layer clays in sedimentary rocks.

Weaver, C. E., 1959. The clay petrology of sediments. In: Swineford, A. Edi., Clays and Clay Minerals, Proceedings of the Sixth National Conference on Clays and Clay Minerals, Pergamon, New York, 154-187.

Weaver, C. E., 1961. Clay minerals of the Ouachita structural belt and adjacent foreland: University of Texas, Bur. Economics, Geology Publ., 6120, 147-162.

Wehrmann, A., Yılmaz, İ., Wilde V., Yalçın, M. N., and Schindler, E., 2010. The Devonian Coastline of Northern Gondwana: Sedimentary Signatures of Depositional Environments at the Land-Sea Transition (Taurides, Turkey). 7th International Symposium on Eastern Mediterranenan Geology, 18-20 October, Univercity of Çukurova, Adana-Turkey, 55.

Whittington, R. A., 2010. Clay Mineralogy and Illite Crystallinity in the Late Devonian to Early Mississippian Woodford Shale in the Arbuckle Mountains, Oklahoma, USA. Master Thesis. Georgia State University, USA.

Wilson, M., and Lyashkevich Z. M., 1996. Magmatism and the geodynamics of rifting of the Pripyat-DnieprDonets rift, East European Platform; Tectonophys., 268, 65–81.

Winchester, J. A. and Floyd, P. A., 1977. Geochemical discrimination of different magma series and their differentiation products using immobile elements. Chemical Geology, 20, 325–344.

Wray, D. S., 1999. Identification and long-range correlation of bentonites in Turonian - Coniacian (Upper Cretaceous) chalks of northwest Europe. Geological Magazine, 136, 361-371.

Yalçın, M. N., Bozdoğan, N., Brocke, R., Gedik, I., Janssen, U., Karsıoğlu, Ö., Königshof, P., Nazik, A., Nalcioğlu G., Saydam, G., Uguz, M. F. and Yılmaz, I., 2007. Stratigraphy and facies development of the Devonian of northwestern Turkey. Devonian land-sea interaction: evolution of ecosystems and climate. Field Meeting IGCP 499, 84-86, May, 2007, San Juan, Argentina.

Yalçın, M. N., Yılmaz, İ., 2010. "Devonian in Turkey - a review" Geologica Carpathica, 61, number 3, 235-253.

Yanev, S., Göncüoğlu M. C., Gedik, I., Lakova, I., Boncheva, I., Sachanski, V., Okuyucu, C., Özgül, N., Timur, E., Maliakov, Y. and Saydam, G., 2006. Stratigraphy, correlations and palaeogeography of Palaeozoic terranes of Bulgaria and NW Turkey: a review of recent data. In: Robertson, A. H. F. and

Mountrakis, D. (Eds.): Tectonic development of the Eastern Mediterranean Region. Geol. Soc. London, Spec. Publ., 260, 51—67.

Yoshinaga, N. and Aomine, S., 1962b. Immogolite in some Ando Soils. Soil Sci. Pl. Nutr. Tokyo 8 (3), 22-29.

APPENDIX A

GEOCHEMICAL DATA OF 14 REPRESENTATIVE K-BENTONITE SAMPLES

Gavurpınarı Limestone Quarry									
ELEMENT	OC1	OCB2A	OCB2B	OCB1G	OCB1S	OCB3	OC2	KRDB6	KRDB7
SiO_2	58,64	23,35	25,93	42,18	52,85	32,33	28,65	47,75	35,91
Al_2O_3	21,5	8,93	9,76	13,71	18,53	12,27	10,93	17,99	15,26
Fe_2O_3	2,45	3,22	3,89	5,61	8,76	5,43	2,83	3,74	4,69
MgO	0,9	1,43	1,57	2	2,65	1,72	1,69	5,06	2,18
CaO	0,83	31,23	28,33	14,76	1,28	21,51	27,1	5,27	16,83
Na_2O	0,11	0,05	0,05	0,08	0,1	0,06	0,05	0,10	0,08
K_2O	2,66	2,96	3,2	4,47	6,01	3,82	3,54	5,74	4,88
TiO_2	1,2	0,45	0,5	0,68	0,94	0,57	0,57	0,88	0,78
P_2O_5	0,05	0,09	0,09	0,17	0,28	0,22	0,13	0,23	0,20
MnO	<0.01	0,01	0,01	0,01	<0.01	<0.01	<0.01	<0,01	<0,01
Cr_2O_3	0,021	0,008	0,009	0,011	0,016	0,011	0,01	0,016	0,014
Ni	26	30	23	122	50	35	23	30	45
Sc	20	8	8	12	16	9	10	15	14
LOI	11,5	28,1	26,6	16,2	8,4	21,9	24,4	13,0	19,0
SUM	99,86	99,87	99,88	99,85	99,82	99,82	99,87	99,76	99,81
Ba	385	133	143	214	258	164	148	265	210
Be	5	2	4	4	4	2	<1	3	3
Co	2,7	9,1	4	40,4	10,8	10,1	4,3	8,2	8,2
Cs	23,1	6,6	6,6	10,4	13	6,9	7,5	12,1	17,6
Ga	24,9	9,7	11,6	16,2	23,4	13,8	13,3	22,5	17,3
Hf	6,2	2,6	2,7	3	4,6	2,3	3	4,7	4,1
Nb	21,8	10,7	12	14,8	20,6	11,8	13,2	23,8	17,5
Rb	120,2	107,2	129,5	153,3	210,1	127,7	134,7	193,5	173,2
Sn	4	2	2	2	3	2	2	3	5
Sr	75,4	377,3	267,6	197,5	171,5	733,3	330,6	268,8	502,1
Ta	1,4	0,7	0,8	0,9	1,3	0,7	0,6	1,3	1,2
Th	12,2	7,7	8,5	10,9	14,2	8,6	8,9	17,0	14,3
U	4,2	3,7	2,4	24,5	8,8	5,1	3,1	9,6	6,1
V	198	68	78	94	148	136	82	152,0	173,0
W	3,2	1,5	2,2	2,2	3,2	2,7	3,6	5,4	5,0

Gavurpınarı Limestone Quarry (continued)									
ELEMENT	OC1	OCB2A	OCB2B	OCB1G	OCB1S	OCB3	OC2	KRDB6	KRDB7
Zr	216,5	84,3	95,4	117,5	172,8	94,6	113,9	177,1	148,1
Y	18,7	12,4	11,3	15,4	21,6	8,1	14,5	13,3	14
La	32,3	20,1	19,2	27,1	35,6	20,4	24,1	30,3	26,8
Ce	55,2	40	40,9	56,8	76,1	39	51	66,5	60,4
Pr	6,03	4,74	4,53	6,92	9,1	4,35	6,07	6,85	6,45
Nd	21,8	16,1	15,8	25,5	33,3	15,3	22,7	24,1	22,7
Sm	3,43	3,05	2,8	4,74	6,34	2,56	4,22	4,15	4,13
Eu	0,67	0,57	0,52	0,93	1,19	0,46	0,87	0,75	0,76
Gd	2,61	2,46	2,19	3,65	5,01	1,72	3,36	3,03	3,03
Tb	0,45	0,38	0,35	0,55	0,75	0,28	0,52	0.50	0,53
Dy	3,01	2,24	2,09	2,83	4,42	1,58	2,82	2,79	2,79
Ho	0,66	0,42	0,41	0,58	0,79	0,33	0,55	0,58	0,57
Er	2,32	1,32	1,24	1,67	2,24	0,98	1,68	1,68	1,71
Tm	0,37	0,2	0,21	0,25	0,35	0,15	0,23	0,28	0,28
Yb	2,66	1,37	1,39	1,72	2,39	1,12	1,58	1,96	1,80
Lu	0,4	0,2	0,2	0,23	0,34	0,16	0,24	0,29	0,25

Yılanlı Burnu Quarry					
ELEMENT	YB4	YBA5	YBA19A	YB1	YB2
SiO_2	42,4	12,41	38,74	6,82	44,26
Al_2O_3	14,32	4,09	14,35	2,04	15
Fe_2O_3	3,6	1,44	4,79	0,92	3,95
MgO	9,16	16,51	8,53	18,56	8,12
CaO	6,93	23,42	8,62	27,01	6,05
Na_2O	0,05	0,04	0,08	0,04	0,06
K_2O	5,8	1,81	5,91	0,73	5,81
TiO_2	0,44	0,19	0,42	0,11	0,62
P_2O_5	0,04	0,04	0,1	0,13	0,06
MnO	0,02	0,01	0,02	0,01	0,01
Cr_2O_3	0,01	0,004	0,011	0,003	0,012
Ni	28	<20	41	<20	29
Sc	10	4	13	2	10
LOI	17	39,7	18,2	43,3	15,8
SUM	99,8	99,69	99,77	99,64	99,79
Ba	81	64	159	44	93
Be	3	<1	<1	<1	2
Co	8,9	2,8	10,9	2,2	6
Cs	11,5	1,8	8,5	0,8	12,6
Ga	18	4,7	17,9	2,1	21,9
Hf	2,5	1,1	1,1	0,7	3,2
Nb	9,4	3,1	7,3	1,7	12
Rb	197,2	43,6	163,8	16,8	198,7
Sn	2	<1	2	<1	3
Sr	68,1	104,6	241,6	299,7	162,6
Ta	0,6	0,2	0,5	0,2	0,9
Th	9,3	2,9	6,5	1,5	12,3
U	3,6	3,7	10,3	3,6	6,6
V	90	31	97	22	98
W	1,2	0,5	1	0,8	1,6
Zr	79,5	32,1	38,8	22,2	112,5
Y	5,4	4,2	9,7	3,9	6,1
La	14,2	6,8	20,2	4,2	20,4
Ce	23,1	14	35	8	31,8
Pr	2,46	1,62	3,94	1,01	3,24
Nd	8,4	6,1	12,9	3,6	9,7
Sm	1,28	1,23	2,64	0,71	1,52
Eu	0,2	0,23	0,53	0,14	0,24
Gd	0,87	0,91	2,25	0,61	0,95
Tb	0,14	0,15	0,34	0,1	0,17
Dy	0,82	0,81	2,04	0,66	1,27
Ho	0,2	0,16	0,38	0,12	0,22
Er	0,61	0,5	0,99	0,33	0,78
Tm	0,1	0,07	0,16	0,05	0,13
Yb	0,69	0,46	1,11	0,38	1,08
Lu	0,11	0,07	0,16	0,05	0,14